Journal of Medicinal Chemistry



Article

# Discovery of a Series of Efficient, Centrally Efficacious BACE1 Inhibitors through Structure-Based Drug Design

Christopher R. Butler, Michael A. Brodney, Elizabeth M. Beck, Gabriela Barreiro, Charles E. Nolan, Feng Pan, Felix F. Vajdos, Kevin Parris, Alison H. Varghese, Christopher J. Helal, Ricardo Lira, Shawn D. Doran, David Riddell, Leanne M. Buzon, Jason K. Dutra, Luis A. Martinez-Alsina, Kevin Ogilvie, John C Murray, Joseph M. Young, Kevin Atchison, Ashley Robshaw, Cathleen Gonzales, Jinlong Wang, Yong Zhang, and Brian T. O'Neill

*J. Med. Chem.*, **Just Accepted Manuscript** • DOI: 10.1021/jm501833t • Publication Date (Web): 19 Feb 2015





Journal of Medicinal Chemistry is published by the American Chemical Society. 1155 Sixteenth Street N.W., Washington, DC 20036

# Discovery of a Series of Efficient, Centrally Efficacious BACE1 Inhibitors through Structure-Based Drug Design

Christopher R. Butler*[a], Michael A. Brodney[a], Elizabeth M. Beck[a], Gabriela Barreiro[e], Charles E. Nolan[b], Feng Pan[b], Felix Vajdos[d], Kevin Parris[d], Alison H. Varghese[d], Christopher J. Helal[c], Ricardo Lira[c], Shawn Doran[e], David Riddell[b], Leanne Buzon[c], Jason Dutra[c], Luis Martinez-Alsina[c], Kevin Ogilvie[c], John C. Murray[c], Joseph Young[c], Kevin Atchison[b], Ashley Robshaw[b], Cathleen Gonzales[b], Jinlong Wang[f], Yong Zhang[f] and Brian T. O'Neill[c]

[a]Neuroscience Worldwide Medicinal Chemistry, [b]Neuroscience Research Unit, Pfizer Worldwide Research and Development, 610 Main St, Cambridge, MA, 02139, United States; [c]Neuroscience Worldwide Medicinal Chemistry, [d]Center of Chemistry Innovation and Excellence, [d]Pharmacokinetics, Dynamics, and Metabolism, Pfizer Worldwide Research and Development, 445 Eastern Point Road, Groton, CT, 06340, United States; [e]Eurofarma Laboratorios S.A., Departamento de Inovação, Av. Vereador José Diniz, 3465, Campo Belo, São Paulo, Brasil, [f]WuXi AppTec 288 Fute Zhong Road Waigaoqiao Free Trade Zone Shanghai 200131, China

RECEIVED DATE (to be automatically inserted after your manuscript is accepted if required

ABSTRACT

The identification of centrally efficacious β-secretase (BACE1) inhibitors for the treatment of Alzheimer's disease (AD) has historically been thwarted by an inability to maintain

alignment of potency, brain availability, and desired ADME properties. In this paper, we describe a series of truncated, fused thioamidines that are efficiently selective in garnering BACE1 activity without simultaneously inhibiting the closely related Cathepsin D or negatively impacting brain penetration and ADME alignment, as exemplified by **36**. Oral administration of these inhibitors exhibit robust brain availability and are efficacious in lowering central Aβ levels in mouse and dog. In addition, chronic treatment in aged PS1/APP mice effects a decrease in the number and size of Aβ-derived plaques. Most importantly, evaluation of **36** in a two-week exploratory toxicology study revealed no accumulation of autofluorescent material in retinal pigment epithelium or histology findings in the eye, issues observed with earlier BACE1 inhibitors.

## Introduction

Alzheimer's disease (AD) is a devastating neurological disorder that brings about a slow progression of cognitive decline, dementia, and ultimately death. Amyloid β (Aβ)-derived plaques in the hippocampal and cortical regions of the brain are hallmarks of this disease. The amyloid hypothesis suggests that an increase in Aβ, engendered either through its increased production or decreased clearance, initiates a molecular cascade that eventually leads to neurodegeneration and AD.[1,2] Aβ production occurs by the consecutive degradation of amyloid precursor protein (APP) by β and γ-secretases.[3] The initial proteolytic event occurs via β-site APP cleaving enzyme (BACE1) within the endosome, to afford a soluble N-terminal ectodomain of APP (sAPPβ) and the C-terminal fragment C99.[4] The membrane-bound C99 is subsequently cleaved by γ-secretase to release the Aβ isoforms, including Aβx-40 and Aβx-42.[5] Recently, an

APP mutation has been reported that has been shown to have protective effects against AD; this mutant protein is cleaved more slowly by BACE1.[6] The ability to safely, but effectively, inhibit BACE1 (and thus modulate the Aβ cascade) has therefore been a target of great interest for a number of groups over the last two decades.[7]

One of the consistent challenges in the effective inhibition of BACE1 in vivo has been overcoming significantly impaired CNS penetration.[8] There has been a myriad of inhibitor classes that exhibit excellent BACE1 potency but struggle to achieve in vivo efficacy at clinically viable doses because they fail to adequately cross the blood-brain barrier (BBB). A key factor underlying this common problem is the strategy that has been employed to engage the two aspartates in the catalytic site of BACE1 has generally been to design inhibitors that contain a basic amine, which engages these residues either directly, or through a water-mediated hydrogen bond interaction.[9,10] This amine can be deleterious to brain penetration, as it often contains two hydrogen bond donors, and its impact can be further exacerbated by a basic $pK_a$, as both of these characteristics contribute to recognition by P-glycoprotein (P-gp) efflux transporters.[11] In this light, the recent report of compound **1** (Figure 1) advancing to the clinic as an efficacious BACE1 inhibitor with a well-balanced ADME profile is quite notable.[12] Unfortunately, clinical examination of **1** has been discontinued due to retinal toxicity observed in preclinical species.[12] We and others postulated that such ocular toxicity was potentially due to the off-target inhibition of Cathepsin D (CatD), a related aspartyl protease that has significant regulatory function in the eye.[13,13b] In its initial disclosure, **1** was described to have ~100x selectivity between BACE1 and CatD inhibition (250 nM and 25 μM $IC_{50}$, respectively).[12] In similarly run cell-free fluorescence polarization (FP) assays for BACE1 and CatD, however, **1** exhibited only a 6-fold selectivity for BACE1 over CatD (Figure 1).

In contrast, there is a plethora of BACE inhibitors reported to have significant CatD selectivity, including thioamidine **2** (Figure 1).[14] This class of inhibitors is characterized by the presence of an amide moiety that occupies the S1/S3 pockets of BACE1 and engages Gly-230 (Figure 2a), which has been a successful strategy to significantly increase BACE1 potency and improve selectivity over CatD. However, this structural motif imparts a significant P-gp-mediated efflux liability (MDR efflux ratio (MDR) = 5.3), presumably due to the third hydrogen bond donor and increased molecular weight (320 → 369) of **2**. This efflux liability translates to substantially impaired brain penetration observed in rodents ($C_{u,b}/C_{u,p}$ = 0.07).[15] Such impairment requires a significantly increased body burden of inhibitor in order to achieve the same degree of central efficacy, resulting in lower safety therapeutic indices relative to an equivalent inhibitor with good CNS penetration.

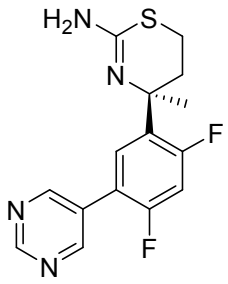

**1**

BACE1 FP $IC_{50}$: 0.9 uM
LipE: 5.01
BACE1 WCA $IC_{50}$: 50 nM
CatD FP $IC_{50}$: 5.3 uM
HLM: < 8.8
MDR: 1.5
RRCK: 24
$C_{u,b}/C_{u,p}$ = 1

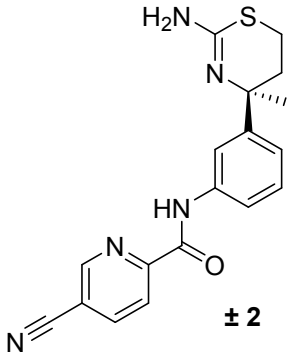

**± 2**

BACE1 FP $IC_{50}$: 0.08 uM
LipE: 6.42
BACE1 WCA $IC_{50}$: 3 nM
CatD FP $IC_{50}$: >92 uM
HLM: 21.4
MDR: 5.3
RRCK: 15
$C_{u,b}/C_{u,p}$ = 0.07

**Figure 1**. Literature thioamidine-derived BACE1 inhibitors and properties

Thus, our objective herein was to efficiently improve CatD selectivity without simultaneously impacting CNS penetration. We have adopted a reductionist approach to this challenge, truncating back to a minimally required pharmacophore within this series, and evaluating opportunities to improve selectivity using structure-based drug design. It was

recognized that paring back in this fragment-like approach would generate a significant loss in BACE1 potency that would need to be addressed. Although this strategy allows for selective reconstruction in an efficient manner, it requires a committed investment to build inhibitors back into reasonable potency space without disruption of the balanced ADME properties. This approach is particularly attractive when considering the observed interplay between molecular weight (MW), $pK_a$, the number of hydrogen bond donors (HBDs), and their coordinated impact on P-gp-mediated efflux liabilities.[16] As the thioamidine inherently contains two hydrogen bond donors, diligence in design is required throughout to introduce additional molecular weight only where necessary, at the same time remaining cognizant of any impact on $pK_a$, in order to mitigate efflux concerns.

## Results and Discussion

We initiated our design strategy by truncating the pyrimidine of **1** that occupies the S3 pocket to prepare fragment-like **6**[17], synthesis of which can be quickly accomplished via simple acid-catalyzed cyclization of intermediate **5** (Scheme 1).[18]

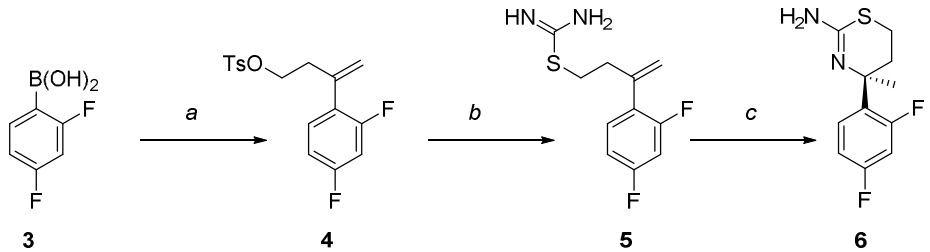


**Scheme 1**. Preparation of compound **6**

Reagents and conditions: (a) 3-bromobut-3-en-1-yl 4-methylbenzenesulfonate, $(Ph_3P)_4Pd$, CsF, THF, 70 °C, 90%; (b) thiourea, $CH_3CN$, 75 °C, 83%; (c) 6 N HCl, 95 °C, 17% then chiral separation.

As expected, **6** is only weakly potent at BACE1 ($IC_{50}$, 36 μM) and has no measurable activity at CatD (up to 100 μM). A co-crystal structure of **6** bound to BACE1 was obtained and the binding of **6** to CatD was modeled, in an effort to identify opportunities to impart selectivity (Figure 2). The BACE1 structure reveals that the amidine group engages in hydrogen bonds with the catalytic aspartic acid residues 228 and 32, with the difluorophenyl ring occupying the S1 pocket. Analyses of the BACE1 crystal structure and CatD-bound model of **6** afford three potential points of differentiation that could be exploited to gain selectivity (Figure 2a). First, an Arg – Asp salt bridge is present in CatD in the S3 pocket, but absent in BACE1 (Region I). Thus molecules that fit deeply into the S3 pocket are likely to disrupt the salt bridge, explaining the selectivity of molecules similar to **2**. Secondly, the fold of Phe-108 loop of BACE1 is significantly different from the corresponding region of CatD (Region II). In particular, the residues that correspond to Phe-108 and Phe-109 of BACE1 are Ile and Thr, respectively, in CatD. More importantly, the residue that would correspond to the backbone carbonyl acceptor Phe-108 in BACE1 does not present its carbonyl to the S1 pocket in CatD. This is consistent with the structure and activity relationship of previous spiropiperidine series, where engagement with the Phe-108 backbone carbonyl significantly improved selectivity over CatD.[10] Third, although the flap loop conformation represented by BACE1 Tyr-71 and Trp-76 is similar to that in CatD, the substitution of Trp-76 by Leu (CatD) in the flap loop prevents hydrogen bond formation to Tyr-78 (by Trp). Instead, Tyr-78 engages Trp-40, which is not within the flap loop, likely rigidifying this region in CatD (Region III). Thus, it was anticipated that building towards the flap in BACE1 would be better tolerated than the corresponding perturbation to the CatD flap region. This analysis suggested three subtle, but key structural differences that could potentially be exploited to design in selectivity over CatD.

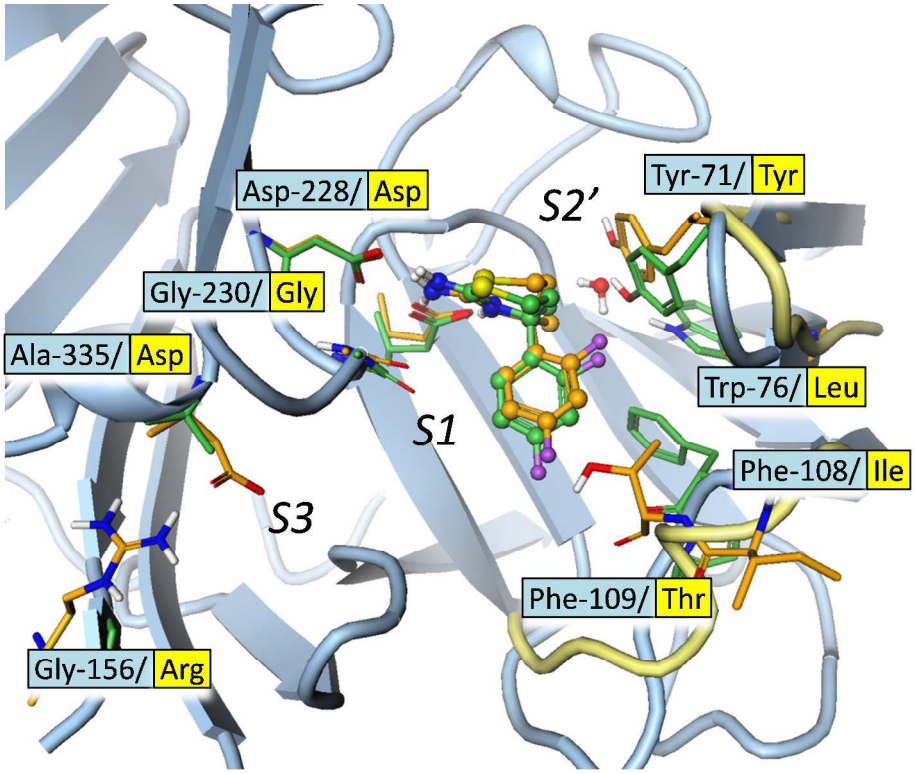
Asp-228/ Asp
Tyr-71/ Tyr
S2'
Gly-230/ Gly
Ala-335/ Asp
Trp-76/ Leu
S1
Phe-108/ Ile
S3
Phe-109/ Thr
Gly-156/ Arg

(a)

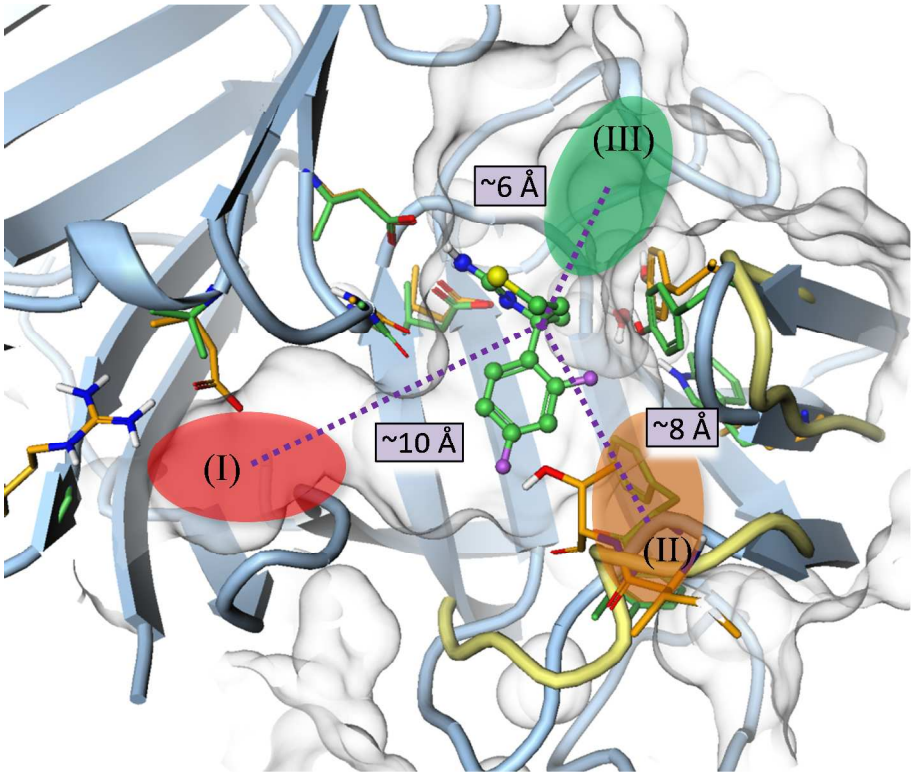
(III)
~6 Å
~10 Å
~8 Å
(I)
(II)

(b)

(c)

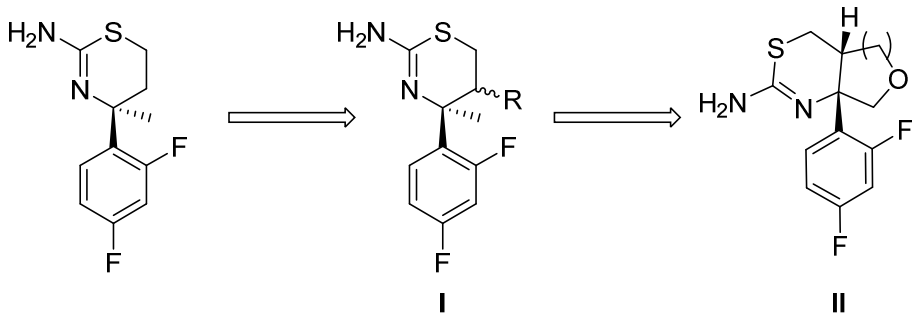


**Figure 2**. a) X-ray crystal structure of **6** with BACE1 (green ball & stick/light blue ribbon) with a model of **6** in Cathepsin D (orange ball & stick/yellow ribbon). Residues in the area of interests are labeled with BACE1 residue names and numbers (light blue) following by the corresponding CatD residue names (yellow). b) Potential regions to exploit for BACE1 vs. Cathepsin D selectivity. c) Strategic construction to explore S2'.

Investigation of each of these key regions of differentiation delineated three potential strategies (Regions I-III, Figure 2b) for series progression. In an effort to rank the efficiency of these strategies, the distances between the center of **6** to the corresponding key residues for each of the regions outlined above that are expected to impart selectivity were measured (Figure 2b). Of these, the S2' pocket (Region III) clearly provides the closest opportunity, suggesting that filling this pocket would be preferred from an "efficient selectivity" perspective. In contrast, disruption of the S3 salt bridge (Region I) would require a substantial molecular weight increase; additionally, the most efficient method in the literature for building in this direction introduced the aforementioned third HBD, significantly increasing the risk of impaired brain penetration. Building toward Region II can be deprioritized as well, given that optimal interactions with the Phe-108 carbonyl would also require a 3$^{rd}$ HBD. Thus, the strategy of building efficiently towards the S2' pocket was selected as our preferred approach to enhance selectivity for BACE1 over CatD.

The crystal structure of **6** and BACE1 suggested that access to the S2' pocket could be achieved by building from the C-5 position of the thioamidine ring in I, as outlined in Figure 2c. A methoxymethyl group in this position was initially selected, to target the desired region without a dramatic increase in lipophilicity. We chose a strategy that could broaden the potential range of SAR and simplify the initial synthesis. We used Ellman imine technology to control the absolute stereochemistry of the quaternary carbon at pro-C-4 but left the eventual C-5 substituent stereochemistry unrestrained, providing both diastereomers in the P2' region.[19] We expected that separation would be straightforward at a late stage in the synthesis and a more selective synthesis was not necessary at this point. The key late steps of the synthesis are depicted in Scheme 2. Thioamidine ring formation stemmed from the differentially protected propanediol **7** (supporting information) equipped with (*S*)-2-methylpropane-2-sulfinimine functionality. Lewis acid-mediated addition of lithio-5-bromo-2,4-difluorophenyl anion provided **8** with the (*S*) configuration at pro-C4 and as a 1:1 mixture of diastereomers at pro-C-5. Concomitant hydrolysis of the sulfinamide and removal of the silyl protecting group revealed the amino alcohol **9** as a mixture of optically active diastereomers, which was easily acylated by benzoyl isothiocyanate. The thiourea **10** was cyclized to the thioamidine **11** as a 1:1 mixture at C-5 by selective activation of the alcohol with triflic anhydride at -20 $^{o}$C. The protecting group was exchanged for *t*-BOC and the diastereomers **13a** and **13b** were chromatographically separated at this point. Incorporation of the versatile bromide offered a viable route to SAR extension. For our initial two targets, the bromide was removed through halogen-metal exchange and protonation, followed by acidic removal of the BOC group. The sequence provides compounds **14a** and **14b** in a 1:3 ratio.

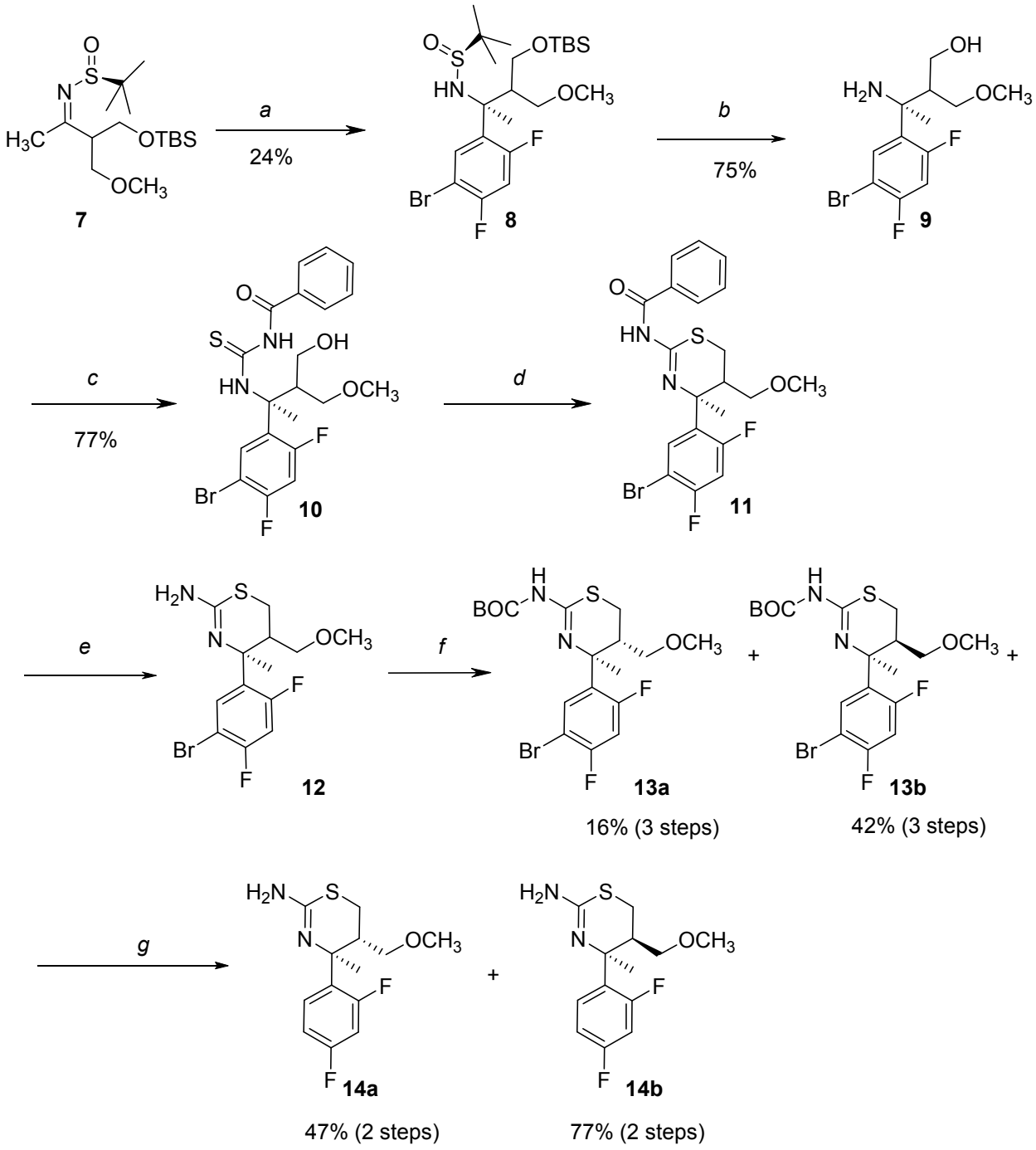


**Scheme 2**. Reagents and conditions: (a) 1,5-dibromo-2,4-difluorobenzene, *n*-BuLi, $AlMe_3$, -70°C, tol; (b) HCl in dioxane, rt; (c) PhC(O)NCS, THF, rt; (d) $Tf_2O$, pyridine, -20°C, $CH_2Cl_2$; (e) DBU, MeOH, 80°C; (f) *t*-$BOC_2O$, aq $NaHCO_3$-THF,rt, then chromatography; (g) **13a** and **13b** separately: *n*-BuLi, -78°C, THF then TFA, $CH_2Cl_2$, rt.

As shown in Table 1, analog **14a,** which has a *trans*-relationship between the methoxymethyl and difluorophenyl substituents, maintains some potency in both the FP and whole-cell (WCA) BACE1 assays, but remains inactive at CatD and thus indicates a productive direction for further exploration. The diminished activity observed for **14b** reinforces the relevance of stereochemistry in this series. Although clearly some benefit accrued from growing in this direction, the multiple degrees of freedom retained by the simple methoxy substituent in **14a** may be problematic. First, this relatively small substituent lacks sufficient bulk to enforce a ring conformation placing the aryl group in the crucial axial position, which is required for binding. It was supposed that a significant population exists in the inactive ring conformation, leading to the observed suboptimal potency. Second, the methoxymethyl group itself has no conformational bias to orient specifically towards S2', again limiting the population of the most active conformation

**Table 1**. In Vitro Data for **14a**/**14b**

| Cpd | BACE1 FP $IC_{50}$ (μM)[a] | CatD FP $IC_{50}$ (μM)[b] (fold) | BACE1 WCA $IC_{50}$ (nM)[c] | MDR Er[d] | HLM[e] (mL/min /kg) | LipE | LE |
|---|---|---|---|---|---|---|---|
| **14a** | 21 | >100 (5.5x) | 850 | 1.95 | 33 | 3.8 | 0.34 |
| **14b** | 88 | >100 | 3,940 | 1.71 | <8 | 2.7 | 0.30 |

[a]$IC_{50}$ values obtained from BACE1 FP Assay. [b]$IC_{50}$ values obtained from CatD FP Assay. [c]$IC_{50}$ values obtained from BACE1 Whole-Cell Assay (WCA). [d]Ratio from the MS-based quantification of apical/basal and basal/apical transfer rates of a test compound at 2 μM across contiguous monolayers from MDR1-transfected MDCK cells. [e]Hepatic clearance predicted from in vitro human microsomal stability study.

It was envisaged that the two conformational challenges identified above could be overcome by fashioning the two alkyl substituents into a THF or THP ring, as fused bicyclic variants of thioamidine **6** (**II** in Figure 2c).[20] This would necessarily lock the aryl group into

an axial orientation with respect to the thioamidine ring and provide a template for further precise elaboration towards S2' from the newly constructed ring; this was anticipated to exploit the flap differences outlined above. We settled on a synthetic strategy that would accommodate an examination of ring size, as well as facile control of multiple $Csp^3$ stereocenters, in order to further probe the S2' regions of the protein. An approach that performed well for this class of inhibitor involved early ring construction via an intramolecular [3+2] cycloaddition to form a [3.3.0] or [4.3.0] fused ring system whose constraints enforce stereocontrol along the ring fusion (Scheme 3). In these early cases, we also decided to use chiral chromatography to separate enantiomers for testing in biological screens. Introduction of the aryl function occurs predominantly on the convex face, with excellent stereocontrol; this was followed by ring expansion to the thioamidine. In the forward sense, allylic or homoallylic alcohols are elaborated to the oxime **18a,b**, one of several possible precursors to a nitrile oxide. Nitrile oxide cycloaddition occurs in a straightforward fashion for either the fused tetrahydrofuran or tetrahydropyran ring, with a small amount of accompanying nitrile oxide dimer or intermolecular isoxazoline formation. Subsequent addition of the (2,4-difluoro)phenyl anion was very sensitive to the conditions employed: at a minimum, the process required imine activation with $BF_3$-$OEt_2$ and low temperature to avoid benzyne formation from the (2,4-difluoro)phenyl anion. We also noticed that variable quantities of unreacted isoxazoline often remained following the addition, presumably due to deprotonation of the isoxazoline ring. The optimal conditions involved formation of the anion at -78 $^{o}$C, followed by drop-wise addition of $BF_3$-$OEt_2$ and the isoxazoline while maintaining the reaction temperature below -73 $^{o}$C. As expected, these reactions were highly stereoselective for the *cis*-ring fusion, with no detectable formation of the *trans*-isomer. The thioamidine ring formation

was initiated after reductive cleavage of the N-O bond of **20a,b** with zinc metal and acylation with a suitable isothiocyanate. The resulting thiourea **22a,b** could be cyclized to the thioamidine by the novel use of the Ghosez reagent,[21] which selectively activated the primary alcohol, or by treatment with aqueous acid, with loss of water. The FMOC or benzoyl protecting groups were removed by standard methods to afford the target compounds **24a** and **24b**.

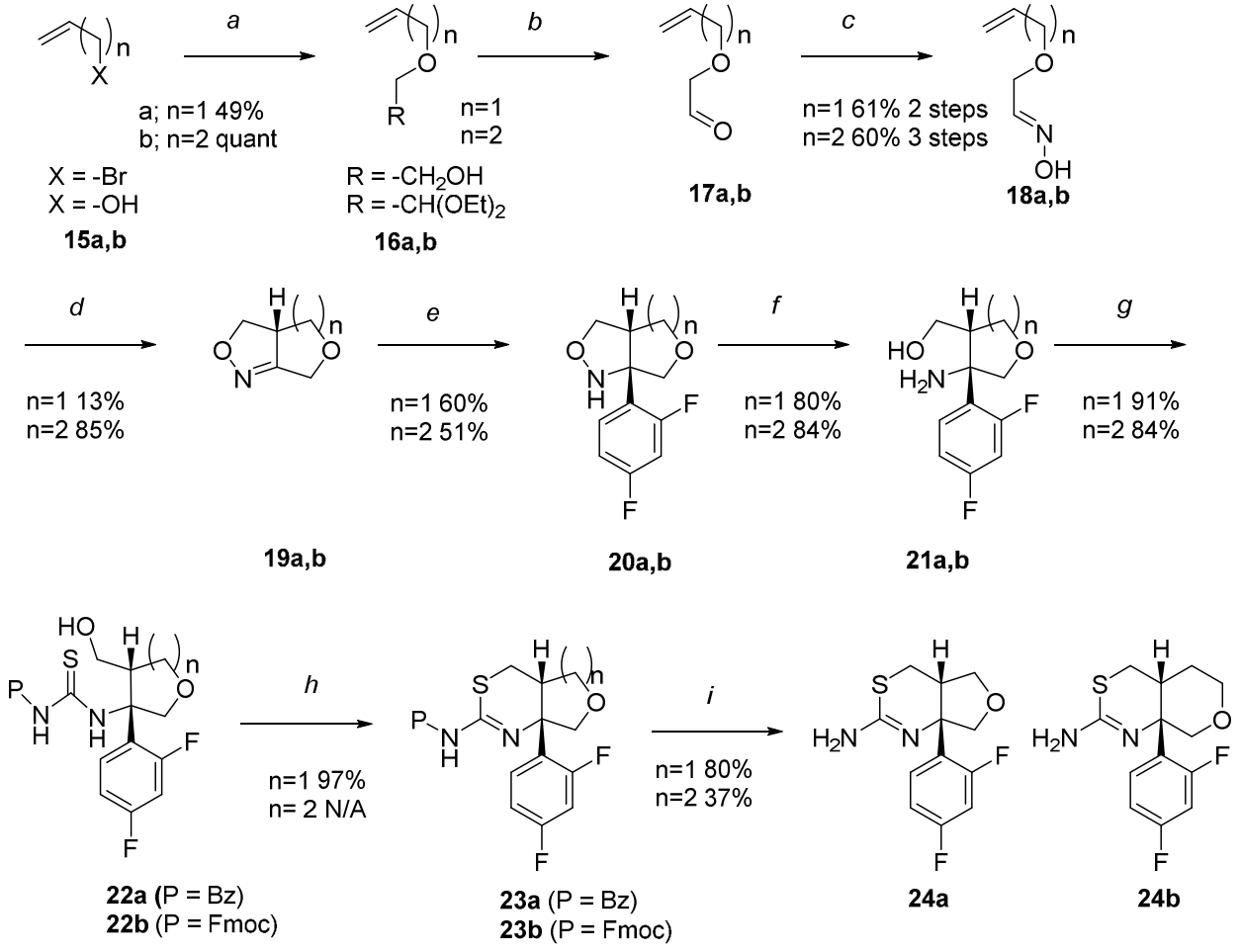


**Scheme 3**. Reagents and conditions: (a) n=1[22]: $HOCH_2CH_2OH$, KOH, THF, 60 °C; n=2: $BrCH_2CH(OEt)_2$, NaH, THF, 0 °C then 68 °C; (b) n=1: $(COCl)_2$, DMSO, $CH_2Cl_2$, -78 °C; n=2: aq HCl, THF, 70 °C; (c) n=1, 2: $NH_2OH$-HCl, NaOAc, EtOH-$H_2O$, 60 °C; (d) n=1,2: NaOCl, $Et_3N$, $CH_2Cl_2$, rt; n=2: then chiral HPLC; (e) n=1, 2: *n*-BuLi, 1-bromo-2,4-difluorobenzene, THF-tol 1:3, -78 °C then $BF_3$-$OEt_2$, **19a,b**, toluene, -78 °C – rt; (f) n=1,2: Zn, AcOH, rt; (g) n=1:

BzNCS, $CH_2Cl_2$, rt; n=2: FMOC-isothiocyanate, $CH_2Cl_2$, rt; (h) n=1: Ghosez reagent, tol, 70 $^oC$; n=2: concd HCl (aq), MeOH, 70 $^oC$; (i) n=1: DBU, MeOH, 60$^oC$, then chiral HPLC; n=2: MeCN, piperidine, rt.

As shown in Table 2, these compounds indeed show improved selectivity over CatD. The tetrahydrofuran derivative **24a** exhibits only modest improvements in BACE1 potency to 17.2 μM, whereas the pyran-containing **24b** is >20x selective for BACE1 over CatD, driven by a significant increase in BACE potency. Moreover, **24b** exhibits a lipophilic efficiency (LipE) improvement over **14a,** suggesting that building in this direction is indeed a productive direction, rather than a simple improvement in potency due to increased lipophilicity. A modest increase in ligand efficiency hinted that the substituent may partially be influencing the population of active conformations for **24b**, relative to the unsubstituted **14a**. Additionally, the compounds maintain preferred ADME properties (MDR Er < 2.5, HLM <10), reaffirming our strategy and providing an excellent starting point for further functionalization.

**Table 2**. In Vitro Data for **24a**/**24b**

| Cpd | BACE1 FP $IC_{50}$ (μM)[a] | CatD FP $IC_{50}$ (μM)[b] (fold) | BACE1 WCA $IC_{50}$ (nM)[c] | MDR Er[d] | HLM[e] (mL/min/kg) | LipE | LE |
|---|---|---|---|---|---|---|---|
| **24a** | 17.2 | >100 (>7x) | 375 | 1.48 | < 8 | 3.9 | 0.36 |
| **24b** | 5.8 | >100 (>20x) | 290 | 1.23 | < 8 | 4.4 | 0.38 |

[a]$IC_{50}$ values obtained from BACE1 FP Assay. [b]$IC_{50}$ values obtained from CatD FP Assay. [c]$IC_{50}$ values obtained from BACE1 Whole-Cell Assay (WCA). [d]Ratio from the MS-based quantification of apical/basal and basal/apical transfer rates of a test compound at 2 μM across contiguous monolayers from MDR1-transfected MDCK cells. [e]Hepatic clearance predicted from in vitro human microsomal stability study.

An X-ray crystal structure of **24b** bound in the BACE1 active site reveals a significant difference compared to what had been observed previously with **6** (Figure 3). In this structure,

Tyr-71 has rotated, forced into a lower energy conformation by the addition of the fused ring system. The hydrogen bond that had existed between Tyr-71 and Trp-76 is now replaced by a water-mediated hydrogen bond from Trp-76 to the THP oxygen (red water, Figure 3). In addition, this significant conformational change reveals a pocket adjacent to the space occupied by the THP ring. Analysis using HydroSite[23] suggests that there is a high-energy, unstable water exposed in this pocket (cyan water). It was proposed that the introduction of small alkyl substituents into this lipophilic pocket should displace this calculated water, likely enhancing BACE1 potency.

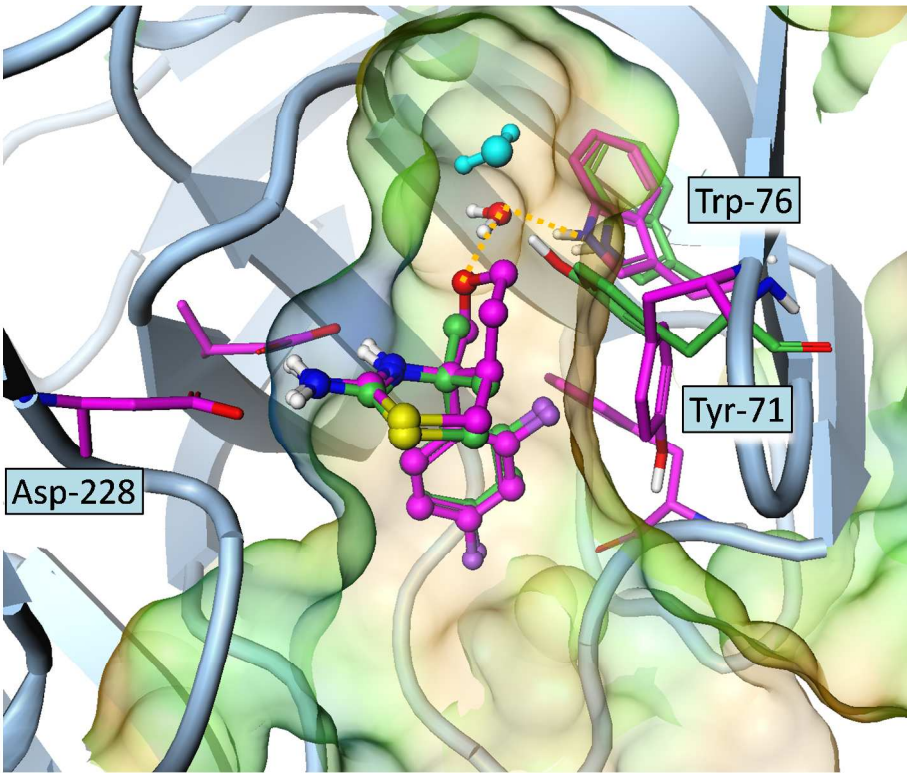


**Figure 3**. X-ray co-crystal of **24b** (magenta) in BACE1 in comparison with **6** (green). Tyr-71 has rotated to a different rotameric conformation, to accommodate the THP ring. A crystallographically observed water is making a hydrogen bond to the oxygen of the THP. A computationally predicted "unstable" water molecule is shown in cyan.

To direct substituents from the fused THP system into the S2' pocket, our synthetic strategy targeted the creation of versatile non–racemic homoallylic alcohols that would ultimately set the remaining stereocenters in the molecule and provide a handle for late-stage modification. This strategy, in combination with the [3+2] cycloaddition approach described above, resulted in the synthesis of chiral, late-stage intermediates required for analog generation in a stereoselective manner (Scheme 4). To prepare the initial analogs, addition of nucleophiles to chiral epoxides or aldehydes was first explored. The first and most versatile R substituent was derived from (*R*)-(−)-glycidyl benzyl ether. Copper-catalyzed addition of vinylmagnesium bromide afforded the desired (*R*)-homoallylic alcohol **25a** (Scheme 5) bearing the versatile hydroxymethyl substituent in a protected form.[24] Alternatively, when desired substituents could not be generated late in the synthetic sequence, these groups were introduced beginning with aldehydes. In the case where R is cyclopropyl, we found that addition of allylmagnesium bromide to cyclopropyl carboxaldehyde was the most efficient approach to this homoallylic substrate, albeit initially in racemic form (**25b**).[25]

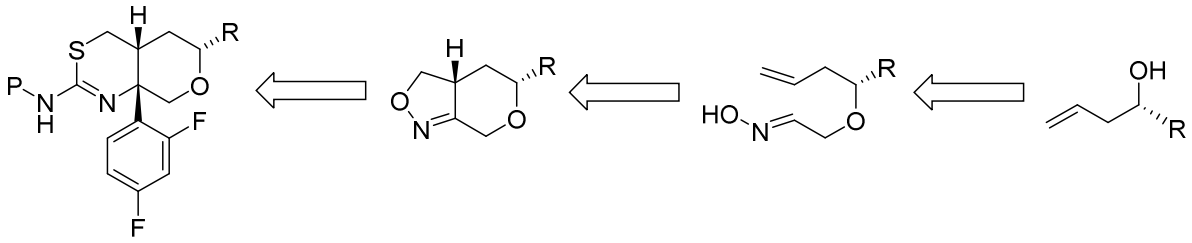


**Scheme 4**. Retrosynthetic analysis for analog generation

The alcohol was elaborated as previously described to afford the oxime intermediate **28a,b** as a direct precursor to a nitrile oxide. Subsequent [3+2] cycloaddition was controlled by establishment of an equatorial R group and proceeded with excellent diastereoselectivity to afford an intermediate in which the benzyloxymethyl group (or cyclopropyl) of **29a,b** was *trans*

to the ring junction of the newly formed fused isoxazoline ring system (confirmed by 2D NMR, see supporting information for details). Introduction of the final chiral center through Lewis acid-catalyzed anion addition occurred with complete selectivity to form a *cis* ring junction in modest to good yields. Thioamidine ring formation was initiated by N-O bond reduction of **30a,b** using zinc in acetic acid to afford **31a,b**. Thiourea formation by reaction with a suitable isothiocyanate was straightforward and was followed by thioamidine cyclization. Two complementary methods were used for this purpose. The free alcohol of thiourea **32a** and the cyclopropyl THP **32b** were each activated with triflic anhydride at -60$^{o}$C followed by spontaneous thioamidine cyclization to **33a,b**. Alternatively **32a'** was transformed with aqueous acid in methanol at elevated temperature to afford the thioamidine **33a'**. Following routine final transformations, this versatile route afforded thioamidines **34**, **35** and **35'** equipped with three chiral centers and versatile protecting groups to accommodate later transformation in the sequence.

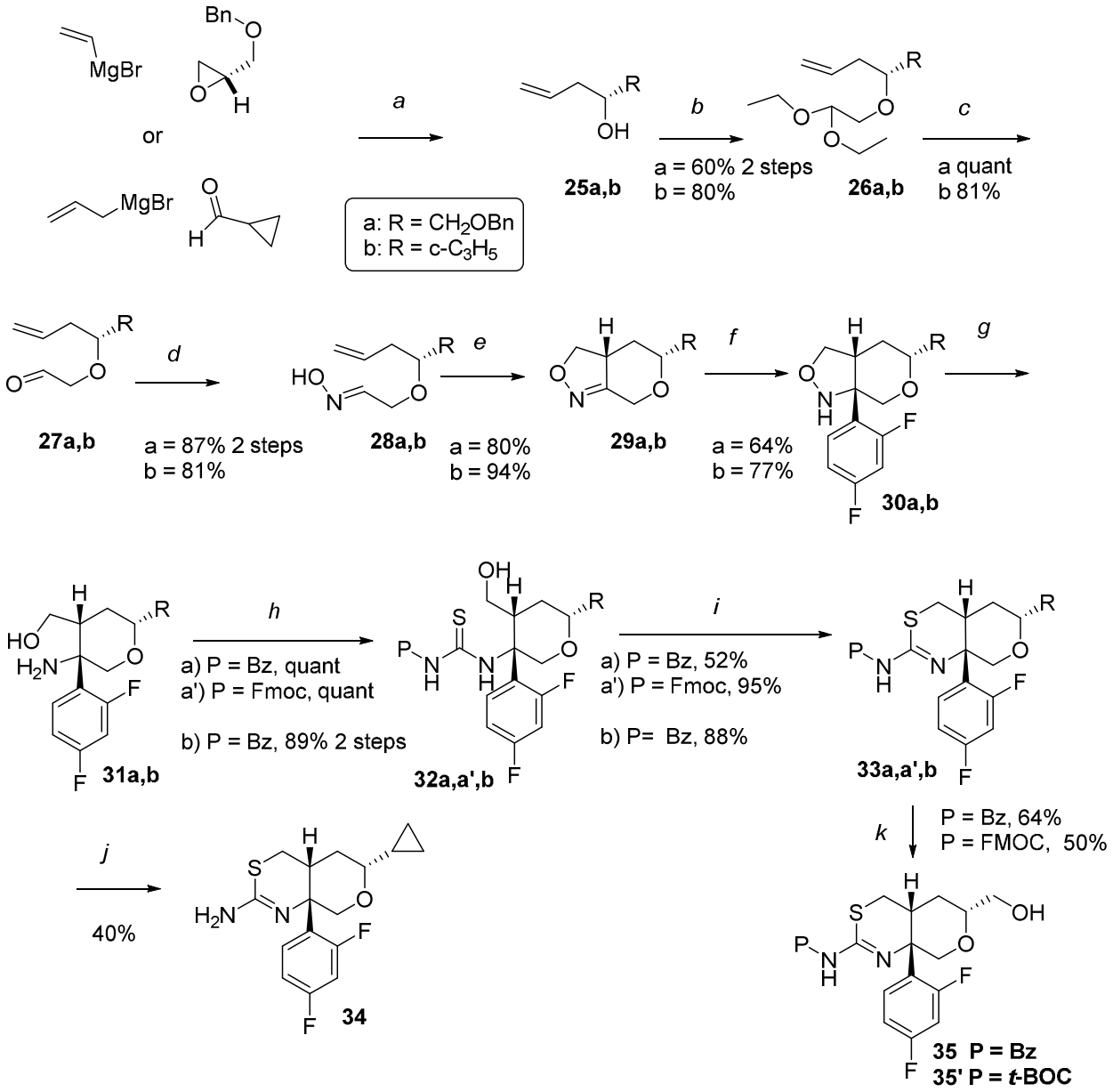


**Scheme 5**. Reagents and conditions: (a) R=$CH_2OBn$: vinylMgBr, CuI-$Et_2O$, THF -78 $^oC$- rt; R = c-$C_3H_5$[24];(b) $BrCH_2CH(OEt)_2$, NaH, THF, 0 $^oC$ then 68 $^oC$; (c) aq HCl, THF, 40-70 $^oC$; (d) $NH_2OH$-HCl, NaOAc, EtOH-$H_2O$, 60 $^oC$; (e) aq NaOCl, $Et_3N$, $CH_2Cl_2$, rt; (f) $BF_3$-$OEt_2$, IPE-tol 1:1, or tol, -78 $^oC$ then 1-bromo-2,4-difluorobenzene, *n*-BuLi, -78 $^oC$-rt; (g) Zn, AcOH, rt; (h) R = $CH_2OBn$: FMOC-NCS, $CH_2Cl_2$, rt or R = $CH_2OBn$: Bz-NCS, $CH_2Cl_2$, rt; R = c-$C_3H_5$: BzNCS, $CH_2Cl_2$, rt; (i) P=FMOC, R = $CH_2OBn$: concd HCl, aq, MeOH, 70 $^oC$; P=Bz, R = $CH_2OBn$: $Tf_2O$, pyr, $CH_2Cl_2$, -60 $^oC$; R = c-$C_3H_5$: $Tf_2O$, pyr, $CH_2Cl_2$, -50 $^oC$; (j) R = c-$C_3H_5$: DBU, MeOH, 60$^oC$, then chiral HPLC; (k) P=FMOC, R = $CH_2OBn$: concd HCl, 120 $^oC$ followed by piperidine, DMF, rt then *t*-BOC)$_2O$, $Et_3N$, THF/MeOH, rt; P=Bz, R = $CH_2OBn$: $NaBrO_3$, EtOAc-$H_2O$, 0 $^oC$.

The versatile intermediate **35** was transformed into a variety of substituents aimed at exploring the S2' binding pocket. The alcohol group was immediately converted to the fluoride (**36**) using (diethylamino)sulfur trifluoride (DAST) or to the methoxy group with methyl iodide (**43**); alternatively, the alcohol can be deoxygenated in two steps via chloride formation followed by Superhydride reduction (**42**). Alcohol **35** can be reliably transformed into the aldehyde, which becomes a precursor for alkyl substituents via a Wittig reaction followed by hydrogenation (**39**,**40)**. The stereochemistry of **39** was confirmed through 2-D NMR studies and the configuration of the three chiral centers of **36** was confirmed by single crystal x-ray (see supplementary material). The aldehyde also underwent difluorination with DAST to provide **38**.

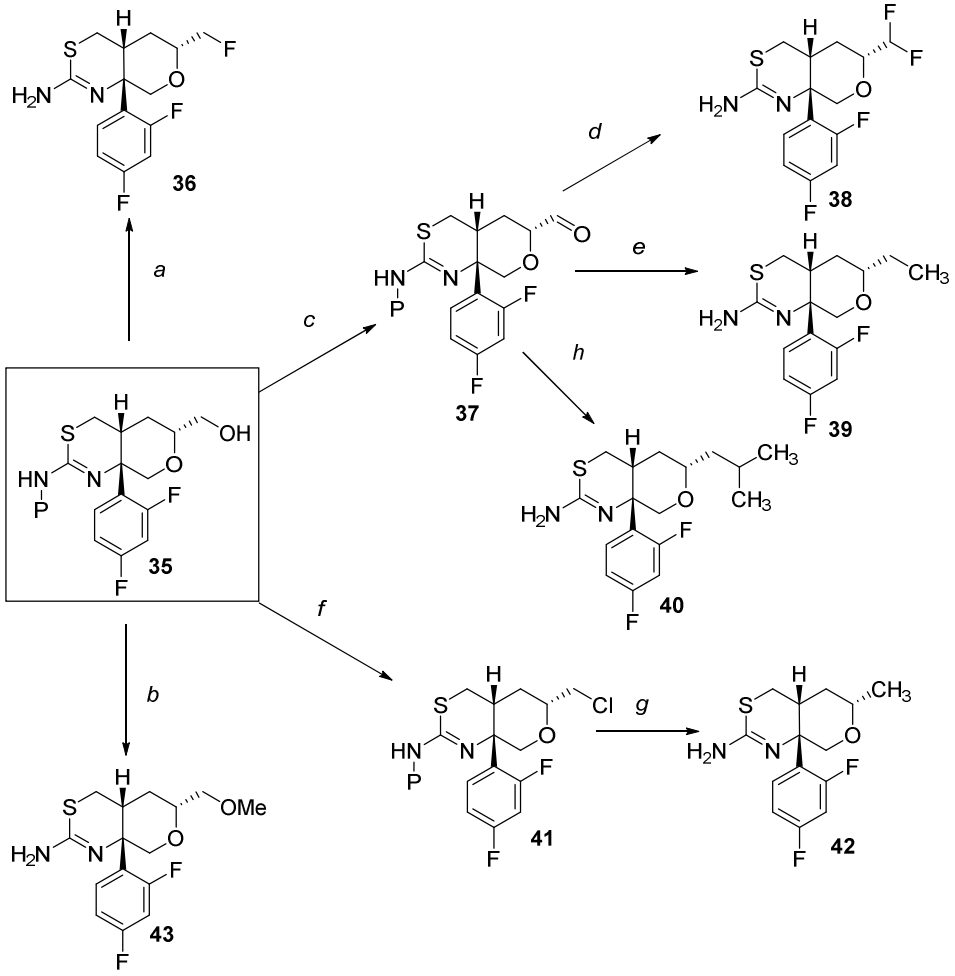


**Scheme 6**. Reagents and conditions: (a) P=*t*-BOC: DAST, pentane-$CH_2Cl_2$ 1:1, rt, 51% then TFA, $CH_2Cl_2$, 0 $^oC$, 74%; (b) P= Bz: MeI, NaH, THF, 40 $^oC$, 69% then DBU, MeOH, 70 $^oC$, 72%; (c) P=Bz: $SO_3$-Pyr, DMSO, $Et_3N$, $CH_2Cl_2$,rt, 71%; (d) DAST, $CH_2Cl_2$, -20 $^oC$, 58% then DBU, MeOH, 60$^oC$, 96%; (e) $Ph_3P^+Me$ $Br^-$, *t*-BuOK, THF, -15$^oC$-rt, 82% then $H_2$, Pd/C, MeOH, rt, 100% then DBU, MeOH, 80$^o$, 58%; (f) $SOCl_2$, tol, 80 $^oC$, 90%; (g) $LiEt_3BH$, THF, 0 $^oC$, 81% then DBU, MeOH, 80$^o$C, 81%; (h) $Ph_3P^+$*i*-Pr $Br^-$, *n*-BuLi, THF, 0$^o$C-rt, 38% then $H_2$, Pd/C, MeOH, rt, 26% then DBU, MeOH, 60$^o$C, 52%.

In all cases, the effect of small substituents on the THP ring improves the desired selectivity over CatD by significantly enhancing BACE1 potency, relative to **24b** (Table 3). The introduction of even a simple methyl group (**42**) improves BACE1 potency 7-fold in both the FP and WCA assays. In addition, **42** maintains the excellent balance of ADME properties,

with low clearance, good permeability and no predicted P-gp efflux. Increasing the bulk of the alkyl group further improves potency in most cases, but begins to impact the balanced profile of these compounds. The methyl ether (**43**) introduces a new site of metabolism, as evidenced by a significant increase in HLM despite a decrease in logD, relative to the ethyl derivative **39 (**HLM $Cl_{,int,app}$ 67 vs <8). Larger alkyl substituents (**40**) tend to improve potency, but a trend of increasing P-gp efflux suggests a potential to encounter lower brain availability in this direction. The cyclopropyl substituted analog (**34**) offers a nice balance of potency, clearance and MDR, but unfortunately suffers from significant inhibition of CYP2D6 ($IC_{50}$, 1.4 μM). It does, however, raise the possibility that modifying the electronics of the substituent could further aid in P-gp efflux liability. Gratifyingly, the fluorine-containing compounds **36** and **38** maintain similar potency and selectivity, at the same time retaining good predicted brain penetration (MDR BA/AB ratio of 0.9 for each). Moreover, all of these compounds exhibit a significant increase in CatD selectivity relative to **1**.

**Table 3**. In Vitro Data for Compounds

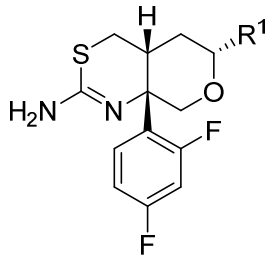


| Cpd | $R^1$ | BACE1 FP $IC_{50}$ (μM)[a] | CatD FP $IC_{50}$ (μM)[b] (fold) | BACE1 WCA $IC_{50}$ (nM)[c] | MDR Er[d] | HLM[e] (mL/min /kg) | LipE | LE |
|---|---|---|---|---|---|---|---|---|
| **24b** | H | 5.1 | >100 (>19.6x) | 265 | 1.3 | <8 | 4.4 | 0.38 |
| **42** | Me | 0.70 | 72.0 (102x) | 39 | 1.2 | <8 | 5.1 | 0.42 |

| | | | | | | | | |
|---|---|---|---|---|---|---|---|---|
| **43** | $CH_2OMe$ | 0.85 | >91.4 (107x) | 30 | 1.6 | 67 | 4.7 | 0.38 |
| **39** | Et | 0.47 | 63 (134x) | 59 | 1.7 | <8 | 4.6 | 0.41 |
| **34** | c-Pr | 0.28 | 45 (161 x) | 24 | 1.4 | <8 | 4.9 | 0.41 |
| **40** | *i*-Bu | 0.15 | 25.1 (167x) | 25 | 2.82 | 19 | 4.4 | 0.41 |
| **38** | $CHF_2$ | 0.67 | 83.1 (124x) | 59 | 0.9 | <8 | 4.6 | 0.38 |
| **36** | $CH_2F$ | 1.07 | >81 (>76x) | 61 | 0.9 | <8 | 4.6 | 0.38 |

[a]$IC_{50}$ values obtained from BACE1 FP Assay. [b]$IC_{50}$ values obtained from CatD FP Assay. [c]$IC_{50}$ values obtained from BACE1 Whole-Cell Assay (WCA). [d]Ratio from the MS-based quantification of apical/basal and basal/apical transfer rates of a test compound at 2 μM across contiguous monolayers from MDR1-transfected MDCK cells. [e]Hepatic clearance predicted from in vitro human microsomal stability study.

The consistent increase in LipE for these compounds relative to the unsubstituted **24b** suggests that productive BACE1-ligand interactions are indeed introduced through exploration of this vector. Moreover, the constant or improved LE through the THP substitution reinforces that relative potency was garnered for the resultant increases in MW. A crystal structure of **36** and BACE1 (Figure 4) confirms that the fluoromethyl substituent is directed toward the lipophilic pocket revealed by the rotation of Tyr-71 and, further, overlays with the unstable water predicted from the structure of **24b**. As expected, the bound compound maintains a low-energy conformation that places the fluoromethyl substituent in a favorable equatorial orientation on the THP ring. Thus, displacement of the calculated, unstable water resulted in a significant (5-7x) improvement in BACE1 potency, as well as improvements in ligand and lipophilic efficiency.

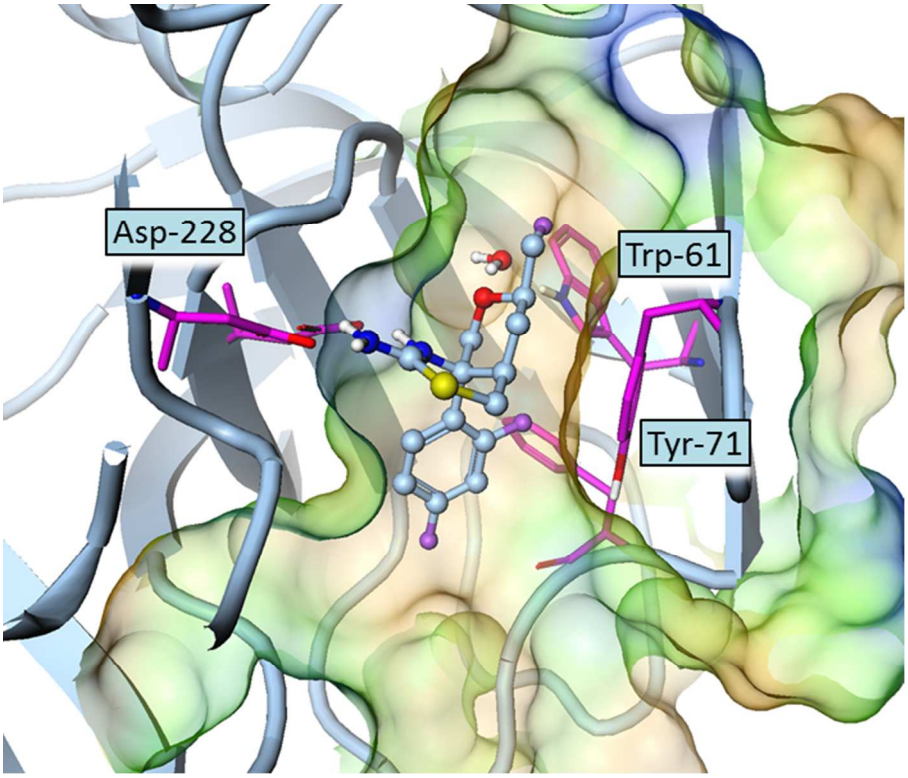


**Figure 4.** Crystal structure of **36** and BACE1. The fluoromethyl substituent is directed toward the lipophilic pocket revealed by the rotation of Tyr-71.

Based on the improved CatD selectivity and balanced ADME profile, the ADME properties of compounds **38, 42** and **36** were examined in more detail. As shown in Table 4, all three compounds exhibit low in vitro clearance in human liver microsomes. Further examination across rodent, dog and non-human primate derived-hepatocytes suggest a low rate of clearance in all species. In addition to high passive permeability (RRCK > 10), all analogs showed excellent CNS penetration ($C_{u,b}/C_{u,p}$ >0.9) in mouse with no predicted P-gp efflux. In addition, **36** was further profiled in a dog neuropharmacokinetic study and showed a similar $C_{u,b}/C_{u,p}$ ratio of 0.78, suggesting confidence in translating the brain availability across multiple species.

**Table 4**. In Vitro and in Vivo PK Properties of Representative Compounds

| PK Properties | 42 | 36 | 38 |
|---|---|---|---|
| In vitro *h*-$Cl_h$ (mL $min^{-1}$ $kg^{-1}$)[a] | <8 | <8 | <8 |
| In vitro *r*-$Cl_h$ (mL $min^{-1}$ $kg^{-1}$)[b] | <14 | <14 | <14 |
| RRCK AB[c] | 17 | 20 | 32 |
| MDR BA/AB[d] | 1.2 | 0.9 | 0.9 |
| B/P (mouse)[e] | 3.90 | 9.2 | 3.51 |
| $F_u$ (plasma)[f] | 0.43 | 0.6 | 0.36 |
| $F_u$ (brain)[f] | 0.10 | 0.18 | 0.11 |
| $C_{u,b}/C_{u,p}$[g] | 0.92 | 1.42 | 1.20 |

[a]Hepatic clearance predicted from in vitro human microsomal stability study. [b]Hepatic clearance predicted from in vitro rat microsomal stability study. [c]RRCK cells with low transporter activity were isolated from Madine-Darby canine kidney cells and were used to estimate intrinsic absorptive permeability; [d]Ratio from the MS-based quantification of apical/basal and basal/apical transfer rates of a test compound at 2 μM across contiguous monolayers from MDR1-transfected MDCK cells. [e]Determined from plasma and brain exposures in mice 60 min post 10 mg/kg subcutaneous dosing; [f]Determined from equilibrium dialysis.[g]As assessed in CD-1 Mice

**In vivo pharmacology**

To assess whether the improved pharmacokinetic properties of this class of thioamidines translate into a pharmacodynamic (PD) response in vivo, acute BACE1 inhibition was examined in male wild-type 129/sve mice following an acute subcutaneous administration of **36** at a dose of 30 and 150 mg/kg. Aβ lowering was measured in brain, cerebrospinal fluid (CSF) and plasma over a time course of 1 to 30 h post dose (Figure 5). The corresponding exposures were also measured in these three compartments in order to delineate the PK/PD relationship for BACE1 inhibition. From a PD perspective, a significant reduction of Aβ was seen in all three compartments. There also appears to be a threshold of maximum inhibition in rodent brain that cannot be breached despite the higher exposures achieved with the 150 mg/kg dose.

Although the time and degree of maximal inhibition was equivalent for the two doses, the decay in inhibition back to baseline was significantly delayed for the 150 mg/kg dose. In brain, a sustained maximum reduction of Aβx-40 and Aβx-42 was observed at 3-5 h post-dose, at 69% and 72% respectively. Efficacy in CSF was more robust with a maximum inhibition of 85%, while the weakest efficacy was observed in plasma, with 54% inhibition. Hysteresis is also clearly demonstrated, with a delay in peak efficacy (3 h) from $C_{max}$ (1 h). Utilization of previously described methods allowed for a $C_{eff}$ determination of 371 nM (free brain).[26]

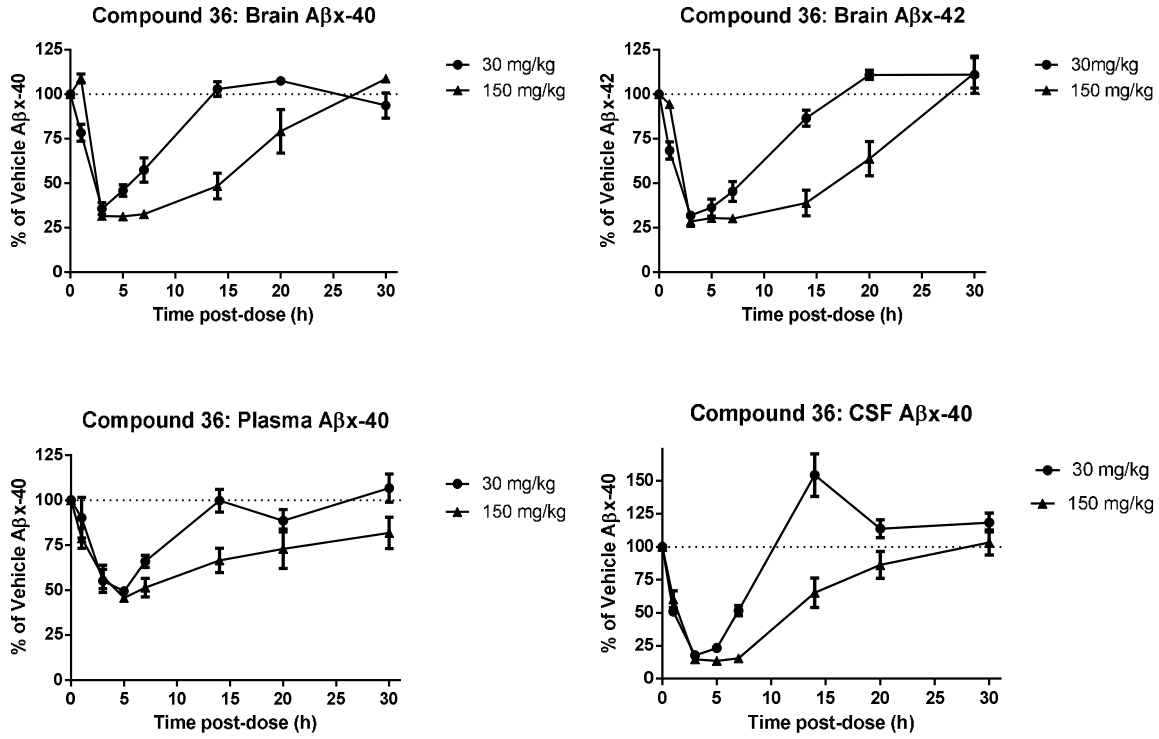


**Figure 5**. Time course effect of **36** on brain, plasma and CSF Aβ following acute administration in mouse. Compound **36** was dosed at 30 or 150 mg/kg sc at time = 0. Data are the mean ± SEM, n=5/group.

In addition to demonstrating brain, plasma, and CSF lowering of Aβ in mice, the efficacy of **36** was also confirmed in biomarker compartments of higher-order species. Using cisterna magna-cannulated beagle dogs, the acute effect of **36** was evaluated in serial CSF and plasma samples collected over a 60 h period (Figure 6). Administration of an 18 mg/kg PO dose of **36** produced a sustained reduction in CSF concentrations of Aβx-40 and Aβx-42, with a maximum decrease of 74% compared to vehicle, but at a $T_{max}$ of 8 h, right-shifted from that seen in mouse. A decrease was also observed in plasma Aβx-40 (45% at $T_{max}$ = 4 h post-dose).

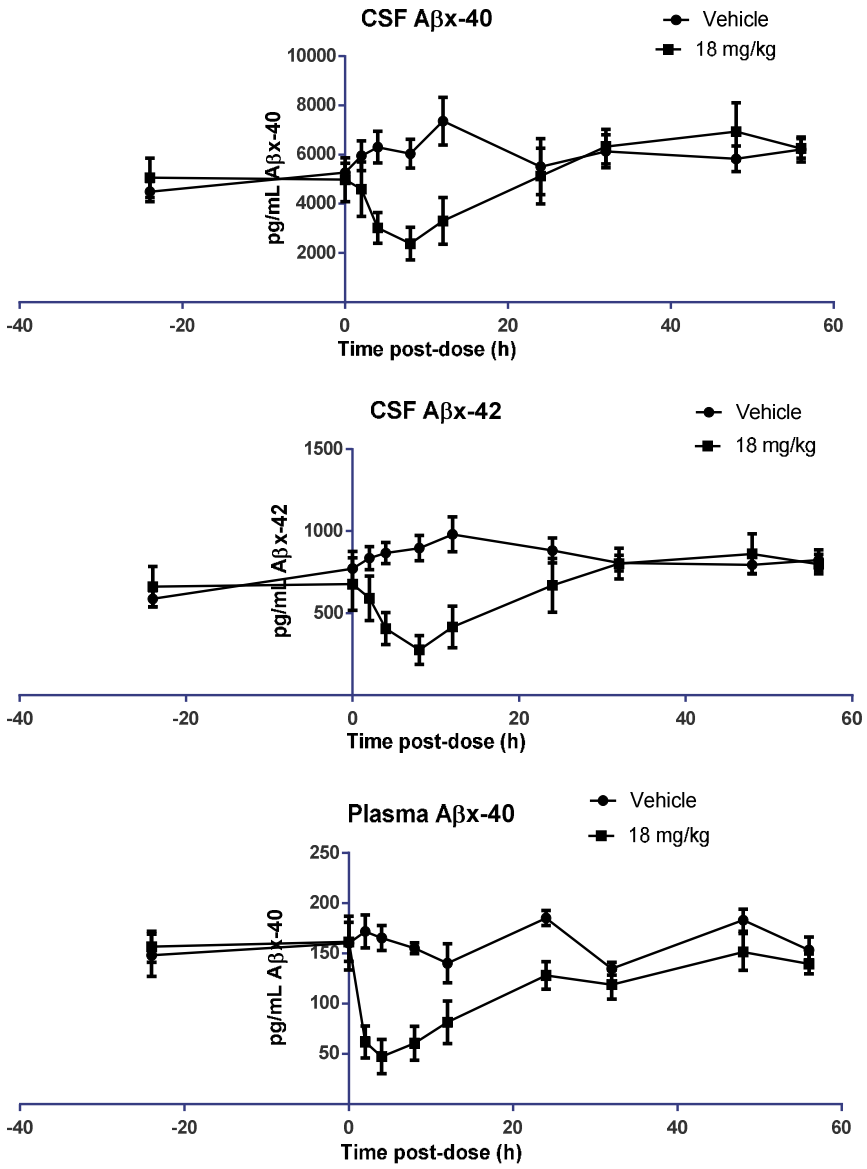


**Figure 6**. Time course of effect of **36** on plasma and CSF Aβ following acute 18 mg/kg p.o. administration in beagle dogs. Compound **36** was dosed at 18 mg/kg PO at time = 0. Data are the mean ± SEM, n=4/group.

Evaluation of the efficacy of **36** in PS1/APP mice with respect to plaque burden modulation was examined following two months of chronic treatment at 100 mg/kg (po) using 2-photon excitation microscopy.[27] Two-photon imaging provides the advantage of being able to

follow changes in individual plaques over time, with each mouse acting as its own control versus prior baseline measurements. Thinned-skull cranial windows were created over the somatosensory cortex of PS1(G384A)APPSWE mice for imaging amyloid plaques by intravital 2-photon microscopy.[28] Images were acquired at baseline and at 1 month and 2 months after initiating compound treatment. The total plaque load in the imaged region was increased by 51±13% over the 2 month period in vehicle-treated animals, suggesting a steady growth of plaques in these mice at the age of 6.5 - 8.5 months. The change rate of individual plaques displayed significant variability, from no detectable difference to a several-fold increase. Surprisingly, two-month treatment with **36** led to a significant regression of total plaque burden, with an average decrease of 26.8% (Figure 7, n=6; $p<0.05$). These results suggest that BACE1 inhibition was effective not only in halting amyloid plaque load increase, but also resulted in regression of plaque burden when administered during the plaque growth phase. Figure 8 illustrates representative images of preexisting parenchymal amyloid plaques and subsequent reductions following two month treatment with **36**.

The demonstration of reduced amyloid deposition in the form of extractable brain Aβ as well as reduction of plaque load and plaque number, following chronic BACE1 inhibitor treatment in amyloid mouse models, has been reported.[29] However, to our knowledge, this is the first definitive evidence that treatment with a BACE1 inhibitor has resulted in inhibition of de novo plaque formation since 2-photon imaging enables the tracking of individual plaque growth in a live mouse with time. This enzymatic inhibition, preventing the formation of Aβ from APP does not rule out the possibility that other mechanisms or processes such as enhanced clearance could be responsible for diminishment of amyloid plaques in this model. One recent report[30] has shown that diminishment of BACE1 activity, either genetically or pharmacologically, enhanced

clearance of axonal and myelin debris, as well as accelerated axonal regeneration following peripheral nerve axotomy in mice, opening up the possibility of BACE1 inhibition as a therapeutic approach for peripheral nerve damage.

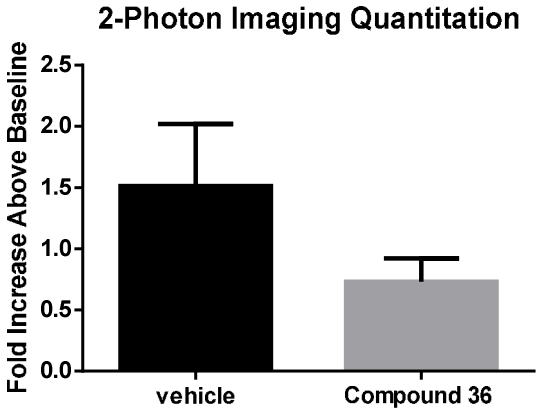


**Figure 7**. Effect of **36** on amyloid plaque-lowering efficacy in 8.5-month-old PS1/APP mice. Fluorescence intensity was quantitated from a defined cortical region (600 μm x 600 μm x 200 μm) at baseline (6.5 months of age) and after 2 months of treatment (8.5 months of age) with vehicle or **36**. Data are the mean ± SEM, n=14; vehicle, n=6; compound **36**.

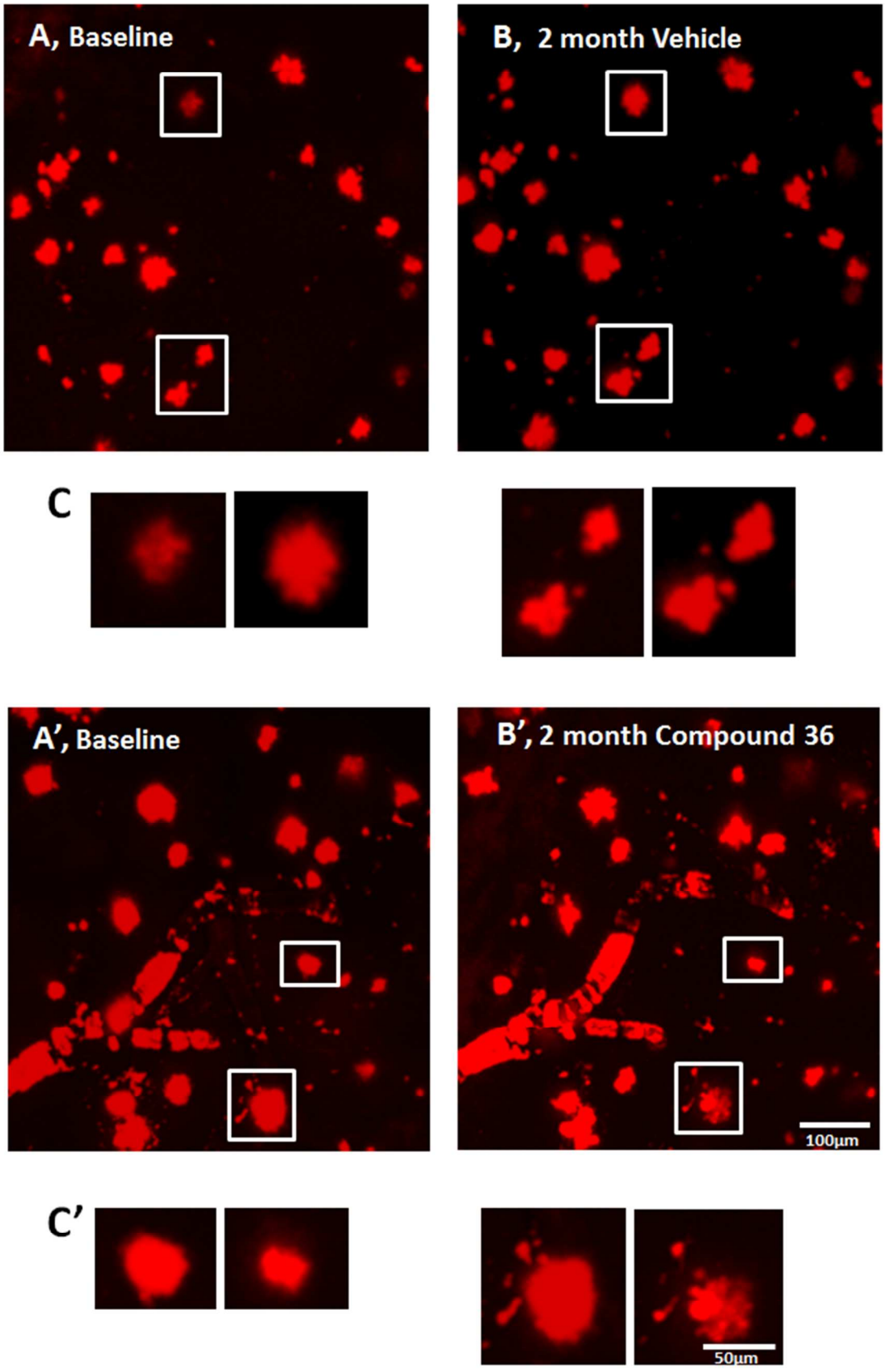
A, Baseline
B, 2 month Vehicle
C
A', Baseline
B', 2 month Compound 36
100µm
C'
50µm

**Figure 8**. Representative 2-photon imaging of preexisting amyloid plaques and subsequent reductions following two months of chronic treatment (PO) with vehicle or compound **36**. A,B) The same cortical region (600 μm x 600 μm x 200 μm) was imaged at baseline (A) and after two-month vehicle treatment (B). C) Examples of plaques which had increased volume with higher magnification (Boxed region in A,B). A',B') A significant percentage of parenchymal plaques showed volume reduction after two-month BACE1 inhibitor (**36**) treatment. C') Examples of plaque regression (Boxed region in A', B').

Additionally, the Aβ-lowering efficacy of **36** in CSF and plasma was examined in 8- to 9-month-old PS1/APP mice following a single subcutaneous dose at 30 mg/kg. The age of the mice was chosen to be in close alignment with the 2-photon imaged animals at the 2-month plaque assessment above. Brain efficacy assessment was not measured acutely since the large Aβ brain load in these mice in the form of amyloid plaques would mask any inhibition that could be obtained following guanidine extraction of the total brain pool of Aβ (data not shown). However, proof that central biomarkers were modulated due to BACE inhibitor treatment can be obtained via Aβ assessment in the CSF compartment. As shown in Figure 9, robust lowering of CSF Aβx-40 and Aβx-42 was observed, with 79% and 72% inhibition, respectively, at $T_{max}$ of 2 hours post-dose. Plasma Aβ inhibition was also robust, with a $T_{max}$ of 2 hours post-dose (Aβx-40: 89% inhibition; Aβx-42: 71% inhibition). The inhibitory effect was sustained, such that 50% inhibition was still evident at 7 hours post-dose.

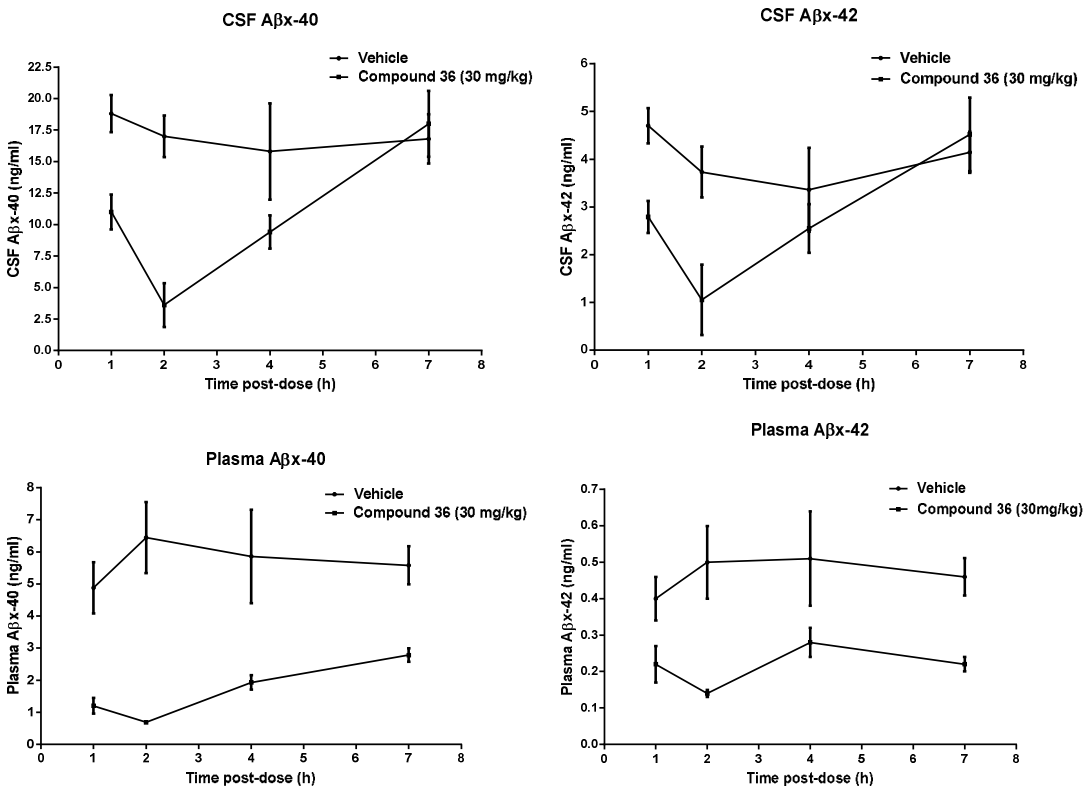


**Figure 9**. Time course data for the acute effect of **36** on CSF and plasma Aβ concentrations in 8- to 9-month-old PS1/APP Mice. Compound **36** was dosed at 30 mg/kg (sc) at time = 0. Data are the mean ± SEM, n=2-5/group.

Taken together, these data demonstrate that **36** is a potent, orally available, brain-permeable BACE1 inhibitor. Compound **36** possesses central efficacy in Aβ lowering in wild-type mouse, PS1/APP mouse, and dog, as well as plaque regression in a mouse model of Alzheimer's disease.

**Toxicology Assessment in Rat**

Having demonstrated a sufficient PK profile and robust efficacy in vivo, **36** was evaluated in a 14-day repeat-dose rat toxicology study. At two doses (75 and 25 mg/kg, respectively) no changes were attributable to **36**, including, most importantly, no accumulation of autofluorescent material in retinal pigment epithelium (RPE), as evaluated microscopically by H&E staining. Thus, at reasonable multiples (up to 12x the AUC-derived $C_{eff}$) for 14 days, no ocular toxicity was observed. In contrast, accumulation of autofluorescent material could be observed after only 7 days with 150 mg/kg of compound **1**.[31] This study thus supports the hypothesis that minimizing CatD liability should mitigate the ocular toxicity previously reported for this series.

## Conclusion

A series of brain-penetrant, orally efficacious thioamidine-derived BACE1 inhibitors are described herein. Truncating older BACE1 inhibitors back to a minimal pharmacophore and rationally building towards the flap by appending a fused THP ring induced a conformational change in the BACE1 active site, revealing a subpocket near S2'. The introduction of small substituents efficiently engaged this pocket, resulting in significant LipE improvements without sacrificing a balanced ADME profile. The reaction sequence effectively created up to three chiral centers and allowed timely exploration of P2' pocket from versatile late stage intermediates. The route was amenable to the synthesis of bulk quantities of material for extended in vivo studies as in the case of **36**. These compounds consistently exhibited good brain penetration and well-behaved pharmacokinetics. Robust efficacy in lowering both peripheral and central Aβ loads was observed in vivo both in mice and dog models. Moreover, chronic dosing of **36** for 2 months revealed that these compounds can lower the plaque load in mice, as assessed by 2-photon analysis. Robust central efficacy led to the selection of **36** for evaluation in

a 2-week rat exploratory toxicology study; there were no ocular findings, supporting the hypothesis that enhanced selectivity for BACE1 over CatD indeed imparts an improved ocular safety profile. Subsequent evolution of this series will require a substantial improvement in potency to lower the efficacious concentration, as well as critical examination of the selectivity over CatD that is required to maintain the clean safety profile described above. These efforts will be described in due course.

## Experimental Section

### Biology

**In Vitro Pharmacology** *sAPPβ Whole-Cell Assay (WCA)*: sAPPβ, the primary cleavage product of BACE1, was determined in H4 human neuroglioma cells over-expressing the wild-type human $APP_{695}$. Cells were treated for 18 h with compound in a final concentration of 1% DMSO. sAPPβ levels were measured by ELISA with a capture APP N-terminal antibody (Affinity BioReagents, OMA1-03132), wild-type sAPPβ-specific reporter antibody p192 (Elan), and tertiary anti-rabbit-HRP (GE Healthcare). The colorimetric reaction was read by an EnVision (PerkinElmer) plate-reader.

*BACE1 Enzyme Cell-Free Assay (FP)*: Beta secretase-1 activity was assessed with soluble BACE1 and the synthetic APP substrate Biotin-GLTNIKTEEISEISYEVEFR-C[oregon green]KK-OH in the presence of compounds in a fluorescence polarization (FP) in vitro assay. Enzyme, substrate and test compounds were incubated in 15 μL of 100 mM sodium acetate pH=4.5 buffer containing 0.001% Tween-20 for 3 hours at 37 $^{o}$C. Following the addition of saturating immunopure streptavidin, fluorescence polarization was measured with a PerkinElmer EnVision plate reader (Ex485 nm/ Em530 nm).

**In Vivo Experiments** All procedures were carried out in compliance with the National Institutes of Health Guide for the Care and Use of Laboratory Animals (1985), under approval of an Institutional Animal Care and Use Committee (IACUC).

*Acute Treatment in Mice*: Male 129/SVE wild-type mice (20–25 g) were in a non-fasted state prior to subcutaneous dosing with vehicle, or 30 or 150 mg/kg **36**, using a dosing volume of 10 mL/kg in 5:5:90 DMSO:Cremophor:saline vehicle. Mice (n = 5 per group) were sacrificed at 1, 3, 5, 7, 14, 20 and 30 h post-dose. Whole blood samples (0.5–1.0 mL) were collected by cardiac puncture into ethylenediaminetetraacetic acid (EDTA)-containing tubes, and plasma was separated by centrifugation (1500 × g for 10 min at 4 °C). The generated plasma was distributed into separate tubes on wet ice for exposure measurements (50 μL) and Aβ analysis (remainder). CSF samples (8–12 μL) were obtained by cisterna magna puncture using a sterile 25 gauge needle and collected with a P-20 Eppendorff pipette. CSF samples were distributed into separate tubes on dry ice for exposure measurements (3 μL) and Aβ analysis (remainder). Whole brain was removed and divided for exposure measurements (cerebellum) and Aβ analysis (left and right hemispheres), weighed, and frozen on dry ice. All samples were stored at –80 °C prior to assay.

*Measurement of Rodent Amyloid-β*: Frozen mouse hemi-brains were homogenized (10% w/v) in 5 M guanidine HCl, using a Qiagen TissueLyser. Each sample was homogenized with a 5 mm stainless steel bead, four times, at a shaking rate of 24 times/s for 90 s, then incubated at 25 °C for 3 h, and ultracentrifuged at 125,000 x g for 1 h at 4 °C. The resulting supernatant was removed and stored in a 96-well polypropylene deep well plate at –80 °C. The Aβ peptides were

further purified through solid-phase extraction using Waters Oasis reversed-phase HLB 96-well column plates (60 mg). Column eluates in ammonium hydroxide from 500-800 μL of original brain supernatant were evaporated to complete dryness and stored at –80 °C until assay. For plasma analysis, 140-175 μL of mouse plasma was treated 1:1 with 5 M guanidine HCl and incubated overnight with rotation at 4 ºC. The entire volume was then purified through solid-phase extraction as indicated above.

Samples were analyzed using a Dissociation-Enhanced Lanthanide Fluorescent Immuno-Assay (DELFIA) platform Enzyme-Linked Immunosorbent Assay (ELISA). Configuration of the antibodies used in determining the level of Aβx-40 and Aβx-42 utilizes a common detect antibody (4G8) in combination with specific C-terminal antibodies for the 40 and 42 cleavage sites. For the Aβx-40 assay, a 384-well black Nunc Maxisorp plate was coated with 15 μL/well (4 μg/mL) capture antibody (Rinat 1219) in 0.1 M sodium bicarbonate coating buffer, pH 8.2. For the Aβx-42 assay, 15 μL/well (8 μg/mL) capture antibody (Rinat 10G3) was used. The plates were sealed and incubated at 4 °C overnight. Plates were washed with phosphate-buffered saline containing 0.05% Tween-20 (PBS-T), and blocked with 75 μL of blocking buffer (1% BSA in PBS-T) for 2 h at 25 °C.

After washing the plates with PBS-T, rodent Aβx-40 (California Peptide) or Aβx-42 (California Peptide) standard was serially diluted in blocking buffer and 15 μL was applied to the plate in quadruplicate. Dried brain samples were reconstituted in 120 μL of blocking buffer, which corresponds to a 4.16- to 6.67-fold concentration. Then 15 μL of undiluted brain sample was

added to the Aβx-42 assay plate in triplicate, or 15 μL of a 1:2 diluted brain sample was added to the Aβx-40 assay plate in triplicate. Dried plasma samples were reconstituted in 40 μL of blocking buffer, which corresponds to a 3.5- to 4.38-fold concentration, and 15 μL was added to the Aβx-40 assay plate in duplicate. CSF samples were diluted 1:8 in blocking buffer, and 15 μL was added to the Aβx-40 assay plate in duplicate. Plates were incubated with sample or standards for 2 h at 25 °C. The plates were washed with PBS-T and 15 μL of detect antibody (4G8-Biotin, Covance), 200 ng/mL in blocking buffer, was added to each well, incubating for 2 h at 25 °C. The plates were then washed with PBS-T, and 15 μL of europium-labeled Streptavidin (PerkinElmer), 50 ng/mL in blocking buffer was added for a 1 h incubation in the dark at 25 °C. The plates were washed with PBS-T, and 15 μL of PerkinElmer Enhancement solution was added to each well with 20 minute incubation at rt. Plates were read on an EnVision plate reader using DELFIA time-resolved fluorimetry (Exc340/Em615), and samples were extrapolated against the standard curve using 4-parameter logistics. Measurement of human amyloid-β in plasma and CSF from PS1/APP mice utilizes the same capture and detect antibodies used for wild-type mice. Vehicle-treated samples from plasma and CSF were serially diluted to optimize sample dilution to the linear phase of an Aβ peptide standard curve. Aβ levels were measured using DELFIA ELISA.

*Acute Treatment in Dog:* Three naïve male beagle dogs (Canis lupus familiaris) were surgically prepared with indwelling cannulae inserted into the cisterna magna and connected to a subcutaneous access port to permit cerebrospinal fluid (CSF) sampling. Animals were allowed a minimum 14-day recovery period during which the catheter was checked for patency. The animals were individually housed in a climate-controlled room with a 12 h light-dark cycle (on 06:00, off 18:00).

For systemic administration, dogs were dosed orally with 20% beta-hydroxypropyl cyclodextrin (vehicle) or 18 mg/kg of **36** dissolved in vehicle. Dose formulations were made the day before each day of dosing, sterile-filtered into a sterile vial, and stored at 2 to 8 ºC. Animals were fasted overnight prior to dosing and were fed approximately 4 h after the start of dosing. Each dog was dosed over a two-week period in a cross-over study design, with each dose condition represented on each day of dosing. All animals were weighed before each day of dosing and each dose was separated by a wash-out period of at least 7 days.

CSF and plasma samples were obtained at -24 (Day -1), 0, 2, 4, 8, 12, 24, 32, 48 and 56 h relative to the start of dose administration on each day of dosing. The -24 and 0 h time points served as pre-dose baseline controls. Whole blood samples of approximately 2 mL were collected from the jugular vein into EDTA-containing tubes, then placed on wet ice. Plasma was separated out by centrifugation at 3000 revolutions/minute for 10 minutes at 4 ºC. The resulting plasma samples, approximately 1 mL each, were then stored at -80 ºC until shipped on dry ice for analysis. CSF samples (6 drops, approximately 0.30 mL) were obtained using a sterile Huber needle inserted into the subcutaneous port. The CSF was not withdrawn through the needle but allowed to flow naturally and was collected as it dripped from the needle hub. A small amount of CSF (2 drops, approximately 0.1 mL of dead volume) was initially collected and discarded prior to each sampling point. The CSF was placed on dry ice upon collection and later stored at -80 ºC until shipped on dry ice for analysis.

*Measurement of Dog Amyloid-β:* Samples were analyzed using a Dissociation-Enhanced Lanthanide Fluorescent Immuno-Assay (DELFIA) platform Enzyme-Linked Immunosorbent Assay (ELISA). For the detection of Aβ, 96-well plates were coated with 50 µL per well of

capture antibody in coating buffer (0.1 M $NaHCO_3$, pH 8.2). The capture antibody for the Aβx-40 assay was Rinat RN1219. The capture antibody for the Aβx-42 assay was Rinat 10G3. The capture antibody for the Aβ total assay was Covance 6E10. Plates with coating antibody were covered with foil seals and incubated overnight at 4 ºC.

Coated plates were washed four times with phosphate buffered saline (PBS) with 0.05% Tween-20 (PBS-T), then 130 µL of blocking buffer [PBS-T, 1% bovine serum albumin (BSA)] was added to each well and incubated for 2 h at rt. Plates were washed four times with PBS-T, and 50 µL of diluted sample or standards were added to the plate in duplicate. For dog plasma analysis of Aβx-40 and Aβ total, 120 µL plasma was added to 120 µL blocking buffer and mixed for a 1:2 dilution. For dog CSF analysis of Aβx-42, 40 µL of CSF was added to 160 µL blocking buffer and mixed for a 1:5 dilution. For CSF analysis of Aβx-40, 80 µL of the 1:5 diluted CSF was added to 80 µL of blocking buffer and mixed for a 1:10 dilution. For CSF analysis of Aβ total, 40 µL of the 1:10 diluted CSF was added to 80 µL of blocking buffer and mixed for a 1:30 dilution. To prepare standard curves, human Aβ1-40 for the Aβx-40 or Aβ total assay (California Peptide) or Aβ1-42 for the Aβ42 assay (American Peptide) was serially diluted in blocking buffer using a 1:2 dilution series from 256 pg/well to 0.25 pg/well, while blocking buffer without peptide addition was used as a 0 pg/well control. Sample or standards were applied to plates at 50 µL/well, and plates were sealed with foil lids before incubation overnight at 4 ºC.

Plates were washed four times with PBS-T and incubated with 50 µL of Covance 4G8-biotin detect antibody (0.2 mg/mL in blocking buffer) for 2 h at rt. Plates were washed an additional four times with PBS-T, and 50 µL of PerkinElmer europium-streptavidin (diluted 1:1000 in blocking buffer to a concentration of 0.1 µg/mL with 20 µM EDTA supplement) was added to the plates and incubated at rt for 1 h. Plates were washed four times with PBS-T, and 50 µL per

well of PerkinElmer Enhancement solution warmed to rt was added to the plates for a 30 min incubation with rocking at rt. Europium counts were read on an EnVision plate reader using DELFIA time-resolved fluorimetry (Exc340/Em615), and samples were extrapolated against the standard curve using 4-parameter logistics.

*Two-photon Imaging Assessment of Mouse Brain Amyloid Plaques:* PS1-APP mice (~6.5 month old at the beginning of the study) were utilized for intravital two-photon imaging studies. Briefly, PS1-APP mice were injected with 10 mg/kg (i.p.) methoxy X-04 to label amyloid plaques 24-48 hours before each imaging view. Mice were deeply anaesthetized (80 mg/kg ketamine and 12 mg/kg xylazine) then the skull over the somatosensory cortex region was thinned to ~20 μm in thickness using a dental drill.[28] The brain vasculature was labeled following IV administration of 10 kDa rhodamine dextran (10 mg/kg) immediately before the animal was secured on the stage of a multi-photon microscope. Utilizing a two-photon laser that was mode-locked at 840 nm, images were captured with a 20X water immersion objective (Olympus, model number: XLUMPLFLN20XW, N/A=1.00). The laser power at the sample was less than 40 mW. A z-stack image series was acquired from the pial surface to a depth of ~200 μm into the cortex. These same regions were imaged once every month. Each stack consisted of one color channel to capture amyloid and one color channel to capture vascular structures. The image acquisition and data quantification were blinded with regard to the animal treatment paradigm. The plaques were quantified by a custom analysis package.[32] Image stacks were first Gaussian filtered, then the volume of each individual plaque was calculated by 3D reconstruction. All images were aligned to the baseline image using rigid body registration.[33] After alignment, individual plaques imaged at each time point were quantified and compared. Vascular plaques were identified based on their proximity to the vasculature defined by unique

characteristics and wrapping morphology. Change in CAA was quantified as the ratio between total vascular plaque loads at different time points. Plaque load was represented as the sum of all the quantified plaques within the imaged area. A plaque was counted as "increased" or "decreased" only when its volume changed by more than 30%. New plaque formation was calculated as $N_{new}/N_{total}$ x100, where $N_{new}$ is the number of new plaques and $N_{total}$ is the total number of plaques captured in the first imaging session.

*Pharmacokinetic Studies in Male Wistar Han Rats:* The in-life and bioanalytical portions of these studies were conducted at BioDuro, Pharmaceutical Product Development Inc. (Beijing, China). Male Wistar Han rats (obtained from Vital River, China, 200–250 g) underwent jugular vein cannulation surgery at BioDuro. Rats received either a 1 mg/kg intravenous (iv) dose or a 5 mg/kg oral (po) dose of compounds **36, 38, 42**. The doses were prepared in 20% (w/v) sulfobutyl ether beta-cyclodextrin and delivered in a volume of 1 mL/kg (iv) or 10 mL/kg (po). Animals were sacrificed in a $CO_2$ chamber. Blood samples were collected in $K_2$EDTA treated tubes at designated times between 2 min and 24 hours via jugular vein cannula. Plasma was isolated after centrifugation. The plasma samples were stored at –80°C prior to analysis.

*Neuropharmacokinetic Studies in Male CD-1 Mice:* The in-life and bioanalytical portions of these studies were conducted at BioDuro, Pharmaceutical Product Development Inc. (Beijing, China). Male CD-1 mice were obtained from PUMC, China. Mice received a 10 mg/kg subcutaneous (sc) dose of compounds **36, 38, 42**. The doses were prepared in 5% DMSO/95% (0.5% methylcellulose) and delivered in a volume of 5 mL/kg. Animals were sacrificed in a $CO_2$ chamber. Blood, brain and CSF samples were collected at 1, 4 and 7 hours post-dosing. Plasma was isolated after centrifugation. The plasma, brain and CSF samples were stored at –80°C prior to analysis.

*Measurement of Fractions Unbound in Brain:* The unbound fraction of each compound was determined in brain tissue homogenate using a 96-well equilibrium dialysis method as described by Kalvass et al.[34] with the following exceptions. Brain homogenates were prepared from freshly harvested rat brains following dilution with a 4-fold volume of phosphate buffer and spiked with 1 μM compound. The homogenates were dialyzed against an equal volume (150 μL) of phosphate buffer at 37 $^{o}$C for 6 h. Following the incubation, equal volumes (50 μL) of brain homogenate and buffer samples were collected and mixed with 50 μL of buffer or control homogenate, respectively, for preparation of mixed matrix samples. All samples were then precipitated with internal standard in acetonitrile (200 μL), vortexed, and centrifuged. Supernatants were analyzed using an LC-MS/MS assay. A dilution factor of 5 was applied to the calculation of brain fraction unbound.

*Generic Liquid Chromatography Tandem Mass Spectrometry (LC-MS/MS) Assay for Exposure Measurements in Plasma, Brain and CSF:* Plasma, brain and CSF were collected as described above and frozen at –80 °C until analysis by LC-MS/MS. Standard curves were prepared in respective matrix via serial dilution at a concentration of 1.0–2000 ng/mL (plasma and CSF) or 0.5–2000 ng/g (brain). For plasma, a 50 mL aliquot of sample was precipitated with 500 mL of MTBE containing an internal standard. Samples were vortexed for 1 min, then centrifuged at 3000 rpm for 10 min. The supernatant was transferred to a 96-well plate. Frozen brain tissue was weighed and an isopropanol:water (60:40) volume equivalent to 4 times the mass was added before homogenization in a bead beater (BioSpec Products Inc., Bartlesville, OK). A 50 mL aliquot of sample was precipitated with 500 mL of MTBE containing an internal standard. Samples were vortexed for 1 min, then centrifuged at 3000 rpm for 10 min. The supernatant was transferred to a 96-well plate. For CSF, a 50 mL aliquot of sample was

precipitated with 500 mL of MTBE containing an internal standard. Samples were vortexed for 1 min, then centrifuged at 3000 rpm for 10 min. The supernatant (300 mL) was transferred to a 96-well plate. LC-MS/MS analysis was carried out using a high-performance liquid chromatography system consisting of tertiary Shimadzu LC20AD pumps (Shimadzu Scientific Instruments, Columbia, MD) with a CTC PAL autosampler (Leap Technologies, Carrboro, NC) interfaced to an API 4000 LC-MS/MS quadrupole tandem mass spectrometer (AB Sciex Inc., Ontario, Canada). The mobile phase consisted of solvent A (water with 0.1% formic acid) and solvent B (acetonitrile with 0.1% formic acid). The gradient was as follows: solvent B was held at 5% for 0.4 min, linearly ramped from 5% to 95% in 0.5 min, held at 90% for 0.6 min and then stepped to 5% over 0.01 min. The mass spectrometer was operated using positive electrospray ionization. All raw data was processed using Analyst Software ver. 1.4.2 (AB Sciex Inc., Ontario, Canada).

*Crystallization of BACE*. Crystals of BACE were prepared as previously described.[35] Compound **24B** was soaked into crystals grown using protein expressed and refolded according to the procedure described in reference 34a, while compounds **6** and **36** were soaked into crystals grown using the procedure described in reference 34b, with several modifications to the protein purification scheme. $Ni^{2+}$-affinity and size exclusion chromatography were used as the initial purification steps yielding homogeneous BACE and eliminating the need for a peptide affinity column. Following removal of the prodomain by furin (0.0375 U/mg BACE), anion exchange chromatography (GE Healthcare 1 mL Q HP) was used as a final purification step. Crystals were soaked at 0.6 mM for 1 hour (compounds **6** and **36**) or 3 mM overnight (compound **24B**). Crystals of **6** and **36** were transferred to a cryoprotectant comprised of 80% mother liquor/20% glycerol, while the specimen containing **24B** was harvested directly from the soaking solution.

Crystals were then flash cooled in liquid nitrogen. X-Ray diffraction data for compounds **6** and **36** were collected at sector 17ID at the Advanced Photon Source (Argonne National Laboratory, Argonne, IL, USA) on a Pilatus 6M detector at -170˚ C. Data for compound 24B was collected in-house on a Rigaku FRE rotating anode x-ray generator equipped with a Rigaku Saturn 944 CCD detector. All data was processed using AUTOPROC[36] and XDS[37] and subsequent data manipulation was performed using the CCP4 suite of programs.[38] Initial structures were determined by rigid body refinement of a reference BACE structure, followed by restrained positional refinement in REFMAC.[39] Ligands were automatically fit to difference maps calculated after refinement in AUTOBUSTER[40], and all further refinement was performed in AUTOBUSTER. Data and refinement statistics are reported in Table 1.

**Molecular dynamics**

In order to refine protein-ligand interactions and to test the stability of the modeling of compound **6** to CatD (PDB ID 1LYA), a molecular dynamics (MD) simulation was performed. The binary complex was first optimized with protein preparation wizard in Maestro V9.1.[41] A default quick relaxation protocol was used to minimize the MD system with the Desmond program.[42] Two rounds of steepest descent minimization were performed with a maximum of 2000 steps with and without restrains (force constant of 50 kcal/mol/Å on all solute atoms) keeping the aspartic acid residues (Asp-32 and Asp-228) in the active site fixed throughout all the calculations. The default protocol within Desmond was applied as the first step of relaxation for the MD simulation. After this step, a total of 15 ns' MD simulation was performed, applying the OPLS 2005 force field[43] at a constant pressure of 1 bar and a temperature of 300 K, using the Nosé-Hoover chain method.[44] The short-range and long-range Coulombic interactions were calculated with a cutoff radius of 9 Å and with the Smooth particle mesh method.[45] Time step

scheduling was used as follows: the multistep RESPA integrator[46] with an inner time step of 2.0 fs for bonded forces and non-bonded near forces within the short range cutoff, and an outer time step of 6.0 fs for non-bonded far forces beyond the cutoff.

**Chemistry**

*General Methods.* Solvents and reagents were of reagent grade and were used as supplied by the manufacturer. All reactions were run under a $N_2$ atmosphere. Organic extracts were routinely dried over anhydrous $Na_2SO_4$. Concentration refers to rotary evaporation under reduced pressure. Chromatography refers to flash chromatography using disposable RediSep $R_f$ 4 to 120 g silica columns or Biotage disposable columns on a CombiFlash Companion or Biotage Horizon automatic purification system. Microwave reactions were carried out in a SmithCreator microwave reactor from Personal Chemistry. Purification by mass-triggered HPLC was carried out using Waters XTerra PrepMS $C_{18}$ columns, 5 μm, 30 x 100 mm. Compounds were pre-salted as TFA salts and diluted with 1 mL dimethyl sulfoxide. Samples were purified by mass-triggered collection using a mobile phase of 0.1% trifluoroacetic acid in water and acetonitrile with a gradient of 100% aqueous to 100% acetonitrile over 10 minutes, at a flow rate of 20 mL/minute. LC-MS analyses were performed on a Waters Acquity UPLC-MS system with a Waters Aquity HSS T3, 1.7 μm C18 column (50 mm x 2.1 mm). UPLC conditions: solvent A = 0.1% formic acid in water (v/v), solvent B = 0.1% formic acid in acetonitrile; flow rate = 1.25 mL/min; compounds were eluted with a gradient of 5% B/A to 95% B/A for 1.1 min. Optical rotations were run on a Jasco Polarimeter P- 2000. Elemental analyses were performed by QTI, Whitehouse, NJ. All target compounds were analyzed using ultra high performance liquid chromatography /ultraviolet/ evaporative light-scattering detection coupled to time-of-flight mass

spectrometry (UHPLC/UV/ELSD/TOFMS). Unless otherwise noted, all tested compounds were found to be >95% pure by this method.

*UHPLC/MS Analysis.* The UHPLC was performed on a Waters ACQUITY UHPLC system (Waters, Milford, MA), which was equipped with a binary solvent delivery manager, column manager, and sample manager coupled to ELSD and UV detectors (Waters, Milford, MA). Detection was performed on a Waters LCT premier XE mass spectrometry (Waters, Milford, MA). The instrument was fitted with an Acquity BEH (Bridged Ethane Hybrid) C18 column (30 mm × 2.1 mm, 1.7 μm particle size, Waters, Milford, MA) operated at 60 °C.

**3-(2,4-Difluorophenyl)but-3-en-1-yl 4-methylbenzenesulfonate (4).**

To an oven-dried, 2 dram vial equipped with a stir bar was added 100 mg (0.328 mmol) 3-bromobut-3-en-1-yl 4-methylbenzenesulfonate followed by 2,4-difluorophenyl boronic acid (104 mg, 0.656 mmol) and anhydrous THF (4 mL) (THF was previously deoxygenated by bubbling $N_2$ gas via a needle for 20 minutes). Cesium fluoride (199 mg, 1.31 mmol) was then added and to that heterogeneous solution was added palladium tetrakis(triphenylphosphine) (38.5 mg, 0.0330 mmol). The vessel was capped and heated to 70 $^{o}$C for 16 h. Analysis by LC/MS revealed product formation ($M+NH_4$ = 356). The reaction mixture was cooled to rt. The cap of the vial was removed and the mixture stirred in air at rt for 1 h. To the solution was added brine (1 mL) followed by vigorous stirring at rt for 5 minutes. The aqueous layer was removed and extracted with $Et_2O$ (2 x 1 mL). The combined organic extract was dried over sodium sulfate, filtered, and concentrated *in vacuo*. The resulting crude material (100 mg, 90% yield) was employed without purification in the next step.

**3-(2,4-Difluorophenyl)but-3-en-1-yl carbamimidothioate (5).**

To a 2 dram vial equipped with a stir bar was introduced 3-(2,4-difluorophenyl)but-3-en-1-yl 4-methylbenzenesulfonate (**4**) (100 mg, 0.30 mmol) and thiourea (45.4 mg , 0.596 mmol) followed by 0.2 mL of acetonitrile. The resulting thick slurry was capped, heated to 75 $^{o}$C and stirred gently for 18 h. The cap of the vial was removed and the slurry was heated to 80 $^{o}$C for 0.5 h to remove most of the acetonitrile. The resulting gum was employed crude in the next step (60 mg, 83% yield).

**4-(2,4-Difluorophenyl)-4-methyl-5,6-dihydro-4*H*-1,3-thiazin-2-amine (6).**

To a 2 dram vial, equipped with a stir bar, containing 3-(2,4-difluorophenyl)but-3-en-1-yl carbamimidothioate (59 mg, 0.24 mmol) was added 0.5 mL 6 N HCl. The resulting slurry was capped and heated to 95 $^{o}$C for 6 h. To the gum was added drop-wise 2 N NaOH until pH ~10 was reached (~1.2 mL). The solution was extracted with EtOAc (2 x 1.5 mL). The combined extracts were dried *in vacuo* to a gum. The resulting crude material was purified by flash chromatography ($SiO_2$, 12 g, 0-100% gradient of (89% $CH_2Cl_2$/10% MeOH/1% $NH_4OH$)/$CH_2Cl_2$). After evaporation the product was isolated as a gum (10 mg, 17% yield). LC-MS *m/z* 243 (M+1). $^1$H NMR (400 MHz, $CD_3OD$) δ 7.27 (dt, *J* = 6.6, 9.4 Hz, 1H), 6.85-6.95 (m, 2H), 3.27 (td, *J* = 1.6, 3.3 Hz, 2H), 2.91 (ddd, *J* = 3.6, 5.7, 12.5 Hz, 1H), 2.46-2.58 (m, 2H), 1.77 (ddd, *J* = 3.7, 11.9, 14.1 Hz, 1H), 1.56 (d, *J* = 1.4 Hz, 3H).

**(S)-N-((2S)-2-(5-bromo-2,4-difluorophenyl)-4-((tert-butyldimethylsilyl)oxy)-3-(methoxymethyl)butan-2-yl)-2-methylpropane-2-sulfinamide (8)**

To a solution of (S)-N-((Z)-4-((tert-butyldimethylsilyl)oxy)-3-(methoxymethyl)butan-2-ylidene)-2-methylpropane-2-sulfinamide (**7**)[47] (26 g, 74.5 mmol) in toluene (250 mL) at -70 $^{o}$C was added 2.0 M $AlMe_3$ in toluene (41 mL, 82 mmol) drop-wise while maintaining the internal temperature at -70 $^{o}$C. In a separate flask, a solution of 1,5-dibromo-2,4-difluorobenzene (30.4 g, 111.75 mmol) in toluene (250 mL) was treated with 2.5 M *n*-BuLi in hexanes (49 mL, 122.92 mmol) in a drop-wise manner while maintaining the internal temperature at -70 $^{o}$C. After the addition, the mixture was stirred at -70 $^{o}$C for 1 h. At this time point, the solution of (S)-N-((Z)-4-((tert-butyldimethylsilyl)oxy)-3-(methoxymethyl)butan-2-ylidene)-2-methylpropane-2-sulfinamide and trimethylaluminum in toluene was added slowly via cannula to the solution of 1-lithio-5-bromo-2,4-difluorobenzene in toluene while maintaining the internal temperature at -70 $^{o}$C. After the addition, the mixture was stirred at -70 $^{o}$C for 1 h and then warmed to 40 $^{o}$C and stirred for 18 h. Analysis by LC-MS showed the reaction was complete. The mixture was quenched with saturated aqueous $NH_4Cl$ solution and then extracted with EtOAc (2 x 200 mL). The organic layer was dried over $Na_2SO_4$ and concentrated *in vacuo*. The residue was purified by column chromatography to give (S)-N-((2S)-2-(5-bromo-2,4-difluorophenyl)-4-((tert-butyldimethylsilyl)oxy)-3-(methoxymethyl)butan-2-yl)-2-methylpropane-2-sulfinamide (**8**) (10 g, 24.7%) as a yellow oil. $^{1}$H NMR (400 MHz, $CDCl_3$) d 8.21-8.32 (m, 1H), 6.83 (dd, *J* = 7.9, 11.4 Hz, 1H), 3.80 (dd, *J* = 2.3, 10.3 Hz, 1H), 3.53-3.65 (m, 2H), 3.33 (s, 3H), 3.23 (s, 1H), 2.17-2.28 (m, 1H), 1.78 (d, *J* = 0.8 Hz, 3H), 1.16-1.32 (m, 9H), 0.76-0.92 (m, 9H), 0.00 (s, 3H), −0.11-−0.03 (m, 3H)

**(3*S*)-3-Amino-3-(5-bromo-2,4-difluorophenyl)-2-(methoxymethyl)butan-1-ol (9).**

A mixture of (S)-N-((2S)-2-(5-bromo-2,4-difluorophenyl)-4-((tert-butyldimethylsilyl)oxy)-3-(methoxymethyl)butan-2-yl)-2-methylpropane-2-sulfinamide (**8**) (10 g, 18.4 mmol) in 4.0 N

HCl/dioxane (100 mL) was stirred at room temperature for 18 h. Analysis by LC-MS showed the reaction was complete. The mixture was concentrated *in vacuo* and $H_2O$ (30 mL) was added. The mixture was basified with solid NaOH until the solution was found to be at pH=8 and then extracted with EtOAc (30 mL). The organic layer was dried over $Na_2SO_4$ and concentrated *in vacuo* to afford crude (3*S*)-3-amino-3-(5-bromo-2,4-difluorophenyl)-2-(methoxymethyl)butan-1-ol (**9**) (4.5 g, 75.5%) which was used in next step without further purification.

**_N_-{[(2*S*)-2-(5-Bromo-2,4-difluorophenyl)-4-hydroxy-3-(methoxymethyl)butan-2-yl]carbamothioyl}benzamide (10).**

To a solution of (3*S*)-3-amino-3-(5-bromo-2,4-difluorophenyl)-2-(methoxymethyl)butan-1-ol (**9**) (4.5 g, 13.88 mmol) in THF (40 mL) was added benzoyl isothiocyanate (3.4 g, 20.82 mmol) in one portion. The mixture was stirred at room temperature for 2 h. Analysis by TLC (EtOAc) showed the reaction was completed. Water (30 mL) was added and the mixture was extracted with EtOAc (2 x 20 mL), the organic layer was dried over $Na_2SO_4$ and concentrated *in vacuo*. The residue was purified by CombiFlash (EtOAc) to give *N*-{[(2*S*)-2-(5-bromo-2,4-difluorophenyl)-4-hydroxy-3-(methoxymethyl)butan-2-yl]carbamothioyl}benzamide (**10**) (5.2 g, 77%) as a white solid. $^1$H NMR (400 MHz, $CDCl_3$): δ 11.65 (s, 1H), 8.77 (s, 1H), 7.88-7.79 (m, 2H), 7.65-7.60 (m, 1H), 7.56-7.51 (m, 3H), 6.88-6.83 (m, 1H), 4.11-4.00 (m, 1H), 3.78-3.70 (m, 2H), 3.43-3.26 (s, 3H), 2.54-2.52 (m, 1H), 2.20 (s, 3H), 2.10-1.97 (m, 1H).

**_N_-[(4*S*)-4-(5-Bromo-2,4-difluorophenyl)-5-(methoxymethyl)-4-methyl-5,6-dihydro-4*H*-1,3-thiazin-2-yl]benzamide (11).**

To a solution of *N*-{[(2*S*)-2-(5-bromo-2,4-difluorophenyl)-4-hydroxy-3-(methoxymethyl)butan-2-yl]carbamothioyl}benzamide (**10**) (5.2 g, 10.67 mmol) in $CH_2Cl_2$ (100 mL) at -20 $^o$C was

added pyridine (2.5 g, 32 mmol), followed by drop-wise addition of triflic anhydride (4.5 g, 16 mmol). After the addition, the mixture was stirred at -10 $^{o}$C for 30 min. Analysis by TLC (EtOAc) showed the reaction was complete. The reaction mixture was treated with $H_2O$ (50 mL) and the mixture was extracted with $CH_2Cl_2$ (2 x 20 mL) and washed with brine. The organic layer was dried over $Na_2SO_4$, and concentrated *in vacuo* to give crude *N*-[(4*S*)-4-(5-bromo-2,4-difluorophenyl)-5-(methoxymethyl)-4-methyl-5,6-dihydro-4*H*-1,3-thiazin-2-yl]benzamide (**11**) (5.5 g, quant) as a light brown oil, which was used in the next step without further purification.

**(4*S*)-4-(5-Bromo-2,4-difluorophenyl)-5-(methoxymethyl)-4-methyl-5,6-dihydro-4*H*-1,3-thiazin-2-amine (12).**

A solution of crude *N*-[(4*S*)-4-(5-bromo-2,4-difluorophenyl)-5-(methoxymethyl)-4-methyl-5,6-dihydro-4*H*-1,3-thiazin-2-yl]benzamide (**11**) (5.5 g, 11.7 mmol) in $CH_3OH$ (150 mL) was treated with DBU (5.3 g, 35.1 mmol), and the mixture was heated under reflux for 5 h. Analysis by TLC (EtOAc) showed the reaction was complete. The mixture was concentrated *in vacuo* and the residue was dissolved in EtOAc (100 mL) and washed with brine; the organic layer was concentrated *in vacuo* to give crude (4*S*)-4-(5-bromo-2,4-difluorophenyl)-5-(methoxymethyl)-4-methyl-5,6-dihydro-4*H*-1,3-thiazin-2-amine (**12**) (9 g) as a brown oil, which was used in the next step without further purification.

***tert*-Butyl [(4*S*,5*S*)-4-(5-bromo-2,4-difluorophenyl)-5-(methoxymethyl)-4-methyl-5,6-dihydro-4*H*-1,3-thiazin-2-yl]carbamate (13a) and *tert*-Butyl [(4*S*,5*R*)-4-(5-bromo-2,4-difluorophenyl)-5-(methoxymethyl)-4-methyl-5,6-dihydro-4*H*-1,3-thiazin-2-yl]carbamate (13b).**

To a solution of crude (4*S*)-4-(5-bromo-2,4-difluorophenyl)-5-(methoxymethyl)-4-methyl-5,6-dihydro-4*H*-1,3-thiazin-2-amine (**12**) (9 g) in THF (50 mL) was added sat. $NaHCO_3$ solution (20 mL) and $BOC_2O$ (21.4 g, 98.3 mmol); after the addition, the mixture was stirred at room temperature overnight. TLC (EtOAc) showed the reaction was complete. The mixture was extracted with EtOAc (2 x 30 mL ), the organic layer was concentrated *in vacuo*, and the residue was purified by column chromatography on silica gel to give *tert*-butyl [(4*S*,5*S*)-4-(5-bromo-2,4-difluorophenyl)-5-(methoxymethyl)-4-methyl-5,6-dihydro-4*H*-1,3-thiazin-2-yl]carbamate (**13a**) (800 mg, 16.2%) as a yellow solid. LCMS *m/z* 466 (M+1); $^1$H NMR (400 MHz, CHLOROFORM-d) d 7.34 (t, *J* = 7.9 Hz, 1H), 6.86 (dd, *J* = 7.8, 11.5 Hz, 1H), 3.49-3.60 (m, *J* = 4.8 Hz, 1H), 3.40-3.49 (m, 1H), 3.31 (s, 3H), 2.92 (dd, *J* = 4.5, 12.8 Hz, 1H), 2.76-2.86 (m, 1H), 2.63 (dd, *J* = 3.4, 12. 7 Hz, 1H), 1.59 (s, 3H), 1.45 (s, 9H)

*tert*-Butyl [(4*S*,5*R*)-4-(5-bromo-2,4-difluorophenyl)-5-(methoxymethyl)-4-methyl-5,6-dihydro-4*H*-1,3-thiazin-2-yl]carbamate (**13b**) (2.1 g, 42.4%) was isolated as a white solid. LCMS *m/z* 466 (M+1); $^1$H NMR (400 MHz, CHLOROFORM-d) d 7.75-7.92 (m, 1H), 6.80 (dd, *J* = 8.2, 11.4 Hz, 1H), 3.23-3.38 (m, *J* = 3.8 Hz, 1H), 2.97-3.17 (m, 5H), 2.58-2.74 (m, 2H), 1.39-1.53 (m, 12H)

**(4*S*,5*S*)-4-(2,4-Difluorophenyl)-5-(methoxymethyl)-4-methyl-5,6-dihydro-4*H*-1,3-thiazin-2-amine (14a).**

A solution of *tert*-butyl [(4*S*,5*S*)-4-(5-bromo-2,4-difluorophenyl)-5-(methoxymethyl)-4-methyl-5,6-dihydro-4*H*-1,3-thiazin-2-yl]carbamate (**13a**) (80 mg, 0.17 mmol) in anhydrous THF (1.7 mL) was cooled to -78 $^o$C. *n*-BuLi (0.18 mL, 0.40 mmol) was added drop-wise and the reaction mixture was stirred for 10 min. The mixture was then poured into aqueous $NH_4Cl$ and separated.

The aqueous layer was extracted with EtOAc (2 x 25 mL). The combined organic layers were washed with brine (25 mL), dried over sodium sulfate, and concentrated to yield *tert*-butyl [(4*S*,5*S*)-4-(2,4-difluorophenyl)-5-(methoxymethyl)-4-methyl-5,6-dihydro-4*H*-1,3-thiazin-2-yl]carbamate as a crude product that was used without purification. Yield: 60 mg, 0.16 mmol, 90%. LC-MS *m/z* 387.5 (M+1).

A solution of *tert*-butyl [(4*S*,5*S*)-4-(2,4-difluorophenyl)-5-(methoxymethyl)-4-methyl-5,6-dihydro-4*H*-1,3-thiazin-2-yl]carbamate (60 mg, 0.16 mmol) in $CH_2Cl_2$ (0.776 mL) was treated with trifluoroacetic acid (0.059 mL, 0.776 mmol). The reaction turned red immediately and was stirred at rt for 45 minutes. The reaction mixture was concentrated, then taken up in EtOAc and aqueous saturated $NaHCO_3$. The aqueous layer was extracted with EtOAc (3x). The organic layers were combined, dried over $Na_2SO_4$ and concentrated *in vacuo* to afford 21 mg (47% yield) of (4*S*,5*S*)-4-(2,4-difluorophenyl)-5-(methoxymethyl)-4-methyl-5,6-dihydro-4*H*-1,3-thiazin-2-amine (**14a**). LC-MS *m/z* 287 (M+1). $^1$H NMR (400 MHz, $CDCl_3$) δ d 7.19 (dt, *J* = 6.2, 9.0 Hz, 1H), 6.78-6.94 (m, 2H), 3.63 (dd, *J* = 4.4, 9.5 Hz, 1H), 3.46 (t, *J* = 9.4 Hz, 1H), 3.39 (s, 3H), 3.13 (dd, *J* = 4.1, 12.3 Hz, 1H), 2.94 (dd, *J* = 4.3, 9.2 Hz, 1H), 2.74 (dd, *J* = 3.5, 12.3 Hz, 1H), 1.70 (s, 3H). $[\alpha]^{27}{}_D$= -201.5 (c 0.32 , MeOH)

**(4*S*,5*R*)-4-(2,4-Difluorophenyl)-5-(methoxymethyl)-4-methyl-5,6-dihydro-4*H*-1,3-thiazin-2-amine (14b).**

A solution of *tert*-butyl [(4*S*,5*R*)-4-(5-bromo-2,4-difluorophenyl)-5-(methoxymethyl)-4-methyl-5,6-dihydro-4*H*-1,3-thiazin-2-yl]carbamate (**13b**) (140 mg, 0.30 mmol) in anhydrous THF (3.0 mL) was cooled to -78 $^o$C. *n*-BuLi (0.26 mL, 0.66 mmol) was added drop-wise and the reaction was stirred for 10 min. The reaction was then poured into aqueous $NH_4Cl$ and separated. The

aqueous layer was extracted with EtOAc (2 x 25 mL). The combined organic layers were washed with brine (25 mL), dried over sodium sulfate, and concentrated to yield *tert*-butyl [(4*S*,5*R*)-4-(2,4-difluorophenyl)-5-(methoxymethyl)-4-methyl-5,6-dihydro-4*H*-1,3-thiazin-2-yl]carbamate as a crude product. Yield: 110 mg, 0.28 mmol, 95%. LC-MS *m/z* 387.5 (M+1).

A solution of *tert*-butyl [(4*S*,5*R*)-4-(2,4-difluorophenyl)-5-(methoxymethyl)-4-methyl-5,6-dihydro-4*H*-1,3-thiazin-2-yl]carbamate (110 mg, 0.285 mmol) in $CH_2Cl_2$ (0.2 M) was treated with trifluoroacetic acid (0.109 mL, 1.42 mmol, 5 equiv). The reaction turned red immediately and was stirred at rt for 45 minutes. The reaction was then concentrated *in vacuo* and the residue partitioned between EtOAc and aqueous saturated $NaHCO_3$. The aqueous layer was extracted with EtOAc (3x). The organic layers were combined and dried over $Na_2SO_4$ to afford 63 mg (77% yield) of (4*S*,5*R*)-4-(2,4-difluorophenyl)-5-(methoxymethyl)-4-methyl-5,6-dihydro-4*H*-1,3-thiazin-2-amine (**14b**). LC-MS *m/z* 287 (M+1). $^1$H NMR (400 MHz, $CDCl_3$) δ 7.78 (dt, *J* = 7.0, 9.1 Hz, 1H), 6.81-6.88 (m, 1H), 6.77 (ddd, *J* = 2.7, 9.0, 12.0 Hz, 1H), 4.30 (br s, 2H), 3.40-3.48 (m, 1H), 3.21-3.29 (m, 1H), 3.09-3.19 (m, 4H), 2.64-2.76 (m, 2H), 1.53 (d, *J* = 1.8 Hz, 3H). $[\alpha]^{26}{}_D$= -7.35 (c 0.26 , MeOH)

**4-(2,2-Diethoxyethoxy)but-1-ene (16b).**

A solution of but-3-en-1-ol (96%, 28.0 mL, 312 mmol) in tetrahydrofuran (150 mL) was added to a suspension of sodium hydride (60% in mineral oil, 59.9 g, 1.50 mol) in tetrahydrofuran (700 mL) at 0 ºC. After the reaction mixture had stirred for 30 min at this temperature, a solution of 2-bromo-1,1-diethoxyethane (97%, 72.6 mL, 468 mmol) in tetrahydrofuran (150 mL) was added at 0 ºC, and the reaction mixture was then heated to 68 ºC for 66 hours. The reaction mixture was cooled to 0 ºC, slowly quenched with water (150 mL), and concentrated *in vacuo*. After

three extractions with EtOAc, the combined organic layers were dried over magnesium sulfate, filtered, and concentrated *in vacuo* to afford 77 g of **16b** as an oil, which was taken directly to the following step. $^1$H NMR (400 MHz, $CDCl_3$), product peaks only: δ 1.23 (t, *J* = 7.0 Hz, 6H), 2.32-2.38 (m, 2H), 3.50 (d, *J* = 5.3 Hz, 2H), 3.53-3.62 (m, 4H), 3.67-3.75 (m, 2H), 4.63 (t, *J* = 5.3 Hz, 1H), 5.02-5.06 (m, 1H), 5.07-5.13 (m, 1H), 5.77-5.88 (m, 1H).

**(But-3-en-1-yloxy)acetaldehyde (17b).**

A solution of **16b** (77 g, 312 mmol) in tetrahydrofuran (515 mL) was treated with aqueous hydrochloric acid (2 M, 105 mL); the reaction mixture was then brought to 70 ºC and maintained at that temperature for 30 min. After cooling to room temperature, removal of solvents *in vacuo* afforded 40 g of the product as an amber oil, which was taken directly to the following step.

**2-(But-3-en-1-yloxy)acetaldehyde oxime (18b).**

(But-3-en-1-yloxy)acetaldehyde (**17b**) (40 g from the preceding step, 312 mmol) was dissolved in a 2:1 mixture of ethanol and water (700 mL). Sodium acetate (128 g, 1560 mmol) was added, and the mixture was stirred for 20 min. Hydroxylamine hydrochloride (98%, 66.4 g, 936 mmol) was then added, and the reaction mixture was heated to 60 ºC for 18 h, at which point it was cooled to room temperature and concentrated under reduced pressure to remove ethanol. The aqueous residue was poured into water (500 mL) and extracted with EtOAc (4x). The combined organic layers were dried over $MgSO_4$, filtered, concentrated *in vacuo*, and purified by flash chromatography ($SiO_2$, 0% to 40% gradient of EtOAc in heptane) to afford 24 g (60% yield) of **18b** as an oil, presumed from the $^1$H NMR spectrum to be a mixture of *E*- and *Z*-oximes. $^1$H NMR (400 MHz, $CDCl_3$) δ [7.51 (t, *J* = 5.6 Hz), and 6.92 (t, *J* = 3.7 Hz) total 1H], 5.89-5.76 (m,

1H), 5.16-5.04 (m, 2H), [4.36 (d, *J* = 3.7 Hz) and 4.11 (d, *J* = 5.7 Hz), total 2H], 3.57-3.51 (m, 2H), 2.41-2.33 (m, 2H).

**(3a*R*)-3,3a,4,5-Tetrahydro-7*H*-pyrano[3,4-*c*][1,2]oxazole (19b).**

To a solution of 2-(but-3-en-1-yloxy)acetaldehyde oxime (**18b**, 10.1 g, 78.2 mmol) in $CH_2Cl_2$ (495 mL) in a water bath at rt was added triethylamine (817 µL, 5.86 mmol). The solution was treated with bleach (95 mL, 6.15% NaOCl, 78.4 mmol) in a drop-wise introduction via an addition funnel. The internal temp of the reaction mixture was monitored and rose from 18-22.4 $^oC$. The reaction mixture was stirred at rt. At the end of the addition, the reaction mixture was diluted with water and extracted with $CH_2Cl_2$ (3x). The organic phase was dried over $MgSO_4$, filtered and concentrated *in vacuo* to provide 8.5 g (85% yield) of ***rac*-19b** as an amber oil. $^1H$ NMR (400 MHz, $CDCl_3$) δ 4.70 (br d, *J* = 13 Hz, 1H), 4.62 (dd, *J* = 10.2, 8.0 Hz, 1H), 4.12 (dd, *J* = 13.5, 1.2 Hz, 1H), 4.09-4.03 (m, 1H), 3.79 (dd, *J* = 11.6, 8.1 Hz, 1H), 3.50 (ddd, *J* = 12.3, 12.1, 2.0 Hz, 1H), 3.45-3.34 (m, 1H), 2.20-2.13 (m, 1H), 1.84-1.73 (m, 1H) .

The enantiomers of 3,3a,4,5-tetrahydro-7*H*-pyrano[3,4-*c*][1,2]oxazole (***rac*-19b**) (4.1 g, 32 mmol) were separated using supercritical fluid chromatography (Column: Chiralpak AS-H, 5 µm; Eluent: 95:5 $CO_2$/2-propanol). The second-eluting enantiomer afforded 1.2 g, 9.4 mmol of **19b** as an oil. LC-MS *m/z* 128.0 (M+1). $^1H$ NMR (400 MHz, $CD_3OD$) δ 4.61-4.52 (m, 2H), 4.16 (dd, *J* = 13.3, 1.2 Hz, 1H), 4.02-3.96 (m, 1H), 3.73 (dd, *J* = 11.5, 8.0 Hz, 1H), 3.54 (ddd, *J* = 12.3, 12.3, 1.9 Hz, 1H), 3.53-3.44 (m, 1H), 2.22-2.15 (m, 1H), 1.75-1.63 (m, 1H).

***rac*-(3a*S*,6a*S*)-6a-(2,4-Difluorophenyl)tetrahydro-1*H*,3*H*-furo[3,4-*c*][1,2]oxazole (20a).**

To a stirred solution of 2,4-difluoro-1-iodobenzene (6.58 g, 27.4 mmol) in toluene (110.0 mL) and tetrahydrofuran (11.0 mL) under $N_2$ at -70 $^oC$ (internal temp) was added boron trifluoride

etherate (3.17 mL, 25.7 mmol) (no exotherm) followed by drop-wise addition of *n*-BuLi in hexane (10.2 mL, 25.5 mmol, 2.5 M). The reaction mixture internal temperature was not allowed to rise above -70 $^{o}$C throughout the addition. Once the *n*-BuLi addition was complete, the resulting dark yellow/amber homogeneous solution was stirred at -75 $^{o}$C (internal temp) for 30 min. To this solution was added 3a,4-dihydro-3*H*,6*H*-furo[3,4-*c*][1,2]oxazole (**19a**, 2.0 g, 18 mmol) in toluene (10.0 mL) and tetrahydrofuran (1.0 mL). The resulting amber solution was stirred at -76 $^{o}$C (internal temp) for 60 min. The reaction mixture was quenched with saturated $NH_4Cl$ (200 mL) and warmed to rt. The resulting organic crude was partitioned between $H_2O$ (100 mL) and EtOAc (300 mL). The resulting organic layer was isolated and washed with brine (100 mL), dried over $Na_2SO_4$, filtered, and concentrated *in vacuo* to yield a dark amber oily residue that was re-dissolved in $CH_2Cl_2$ (10 mL) and adsorbed on silica gel (25 g SNAP). The resulting solid was loaded on CombiFlash $R_f$ for purification (120 g High Performance Redisep Gold column, 0 to 50% of EtOAc in Heptanes, 16CV). Fractions containing the new major spot (~25% EtOAc) were combined and concentrated under reduced pressure to yield a pale yellow waxy solid that was suspended in heptane (~5 mL) then filtered and evaporated *in vacuo* to afford ***rac*-20a** (2.42 g, 60%) as a white solid. $^1$H NMR (400 MHz, $CDCl_3$) δ 7.89-7.81 (m, 1H), 6.95-6.76 (m, 2H), 5.10 (s, 1H), 4.53 (t, *J* = 8.3 Hz, 1H), 4.19-4.07 (m, 1H), 3.98 (d, *J* = 9.4 Hz, 1H), 3.92-3.76 (m, 2H), 3.57 (t, *J* = 7.3 Hz, 1H), 3.37 (q, *J* = 7.6 Hz, 1H)

**(3a*R*,7a*S*)-7a-(2,4-Difluorophenyl)hexahydro-1*H*-pyrano[3,4-*c*][1,2]oxazole (20b).**

*n*-Butyllithium (2.5 M solution in hexanes, 3.95 mL, 9.88 mmol) was added to a solution of 1-bromo-2,4-difluorobenzene (0.558 mL, 4.94 mmol) in a 1:3 mixture of tetrahydrofuran and toluene (25 mL) at -78 ºC, and the reaction mixture was stirred at this temperature for 1 h. In a separate flask, a solution of **19b** (628 mg, 4.94 mmol) in toluene (15 mL) was cooled to -78 ºC

and treated with boron trifluoride diethyl etherate (1.22 mL, 9.88 mmol); this mixture was also allowed to stir at -78 ºC for 1 h, and then added via cannula to the aryllithium solution. The reaction mixture was stirred for 1 h and was then quenched with saturated aqueous ammonium chloride solution. After dilution with EtOAc, the layers were separated, and the organic layer was washed with saturated aqueous sodium chloride solution, dried over magnesium sulfate, filtered, and concentrated *in vacuo*. Purification by flash chromatography ($SiO_2$, EtOAc/heptane gradient 0% to 40%) provided 610 mg (51% yield) of **20b** LC-MS *m/z* 242.0 (M+1). $^1$H NMR (400 MHz, $CD_3OD$) δ 7.92-7.84 (m, 1H), 7.00-6.93 (m, 2H), 4.03 (dd, *J* = 12.5, 1.8 Hz, 1H), 4.02-3.95 (br m, 1H), 3.76-3.53 (m, 4H), 3.10-3.03 (m, 1H), 1.93-1.75 (m, 2H).

**_rac_-[(3*R*,4*S*)-4-Amino-4-(2,4-difluorophenyl)tetrahydrofuran-3-yl]methanol (21a).**

To a stirring solution of ***rac*-20a** (1.2 g, 5.28 mmol) in glacial acetic acid (25.0 mL, c=0.211 M) was added zinc dust (<10 micron, 4.5 g, 68.8 mmol). The resulting gray heterogeneous solution was stirred at rt for 18 h. The reaction was filtered through a small plug of Celite followed by a rinse with EtOAc (60 mL). The filtrate was concentrated *in vacuo* and the resulting oily residue was partitioned between saturated $NaHCO_3$ (50 mL) and EtOAc (100 mL). The lower aqueous layer was washed with additional EtOAc (2 x 50 mL). The combined organic extracts were washed with brine (50 mL), dried over $Na_2SO_4$, filtered, and concentrated to afford ***rac*-21a** (975 mg, solid, 80.5%) as a white solid. This product was used directly in the next step. $^1$H NMR (400 MHz, $CDCl_3$) δ 7.53 (dt, *J* = 6.2, 9.05 Hz, 1H), 6.94-6.79 (m, 2H), 4.13-4.00 (m, 2H), 3.97-3.87 (m, 3H), 3.86-3.77 (m, 1H), 2.89-2.74 (m, 1H).

**[(3*S*,4*R*)-3-Amino-3-(2,4-difluorophenyl)tetrahydro-2*H*-pyran-4-yl]methanol (21b).**

To a mixture of **20b** (1.06 g, 4.39 mmol) in acetic acid (10 mL) was added zinc powder (3.74 g, 57.2 mmol), and the resulting mixture was stirred for 18 h. Insoluble material was removed *via* filtration, and the filtrate was concentrated *in vacuo*. The resulting paste was dissolved in EtOAc and washed with saturated sodium bicarbonate, washed with saturated sodium chloride, and dried over $MgSO_4$. Filtration and concentration *in vacuo* provided 900 mg (84% yield) of the product **21b**. LC-MS *m/z* 244 (M+1). $^1$H NMR (400 MHz, $CD_3OD$) δ 7.71-7.64 (m, 1H), 7.05-6.96 (m, 2H), 4.15-4.09 (m, 1H), 4.01 (dd, *J* = 11.3, 2.0 Hz, 1H), 3.62 (ddd, *J* = 12.7, 11.5, 2.7 Hz, 1H), 3.50 (d, *J* = 11.5 Hz, 1H), 3.40-3.37 (m, 2H), 2.48-2.40 (m, 1H), 2.12-2.00 (m, 1H), 1.71-1.78 (m, 1H).

***rac*-*N*-{[(3*S*,4*R*)-3-(2,4-difluorophenyl)-4-(hydroxymethyl)tetrahydrofuran-3-yl]carbamothioyl}benzamide (22a).**

To a very fine suspension of ***rac*-21a** (950 mg, 4.14 mmol) in $CH_2Cl_2$ (40.0 mL, c=0.104 M) rapidly stirring under an atmosphere of nitrogen was added benzoyl isothiocyanate (649 mg, 3.98 mmol, 0.535 mL) in one portion. The resulting yellow solution was stirred at rt for 1.5 h. The reaction mixture was concentrated under reduced pressure to yield a sticky yellow solid which was purified by flash chromatography ($SiO_2$, 40 g RediSep Gold column, EtOAc/heptane gradient of 0-20% over 16CV) to afford 1.48 g (91%) of ***rac*-22a** as an off-white solid. LC-MS *m/z* 393 (M+1). $^1$H NMR (400 MHz, $CDCl_3$) δ 11.80 (s, 1H), 8.86 (s, 1H), 7.79-7.91 (m, 2H), 7.59-7.76 (m, 2H), 7.47-7.57 (m, 2H), 6.85-6.95 (m, 1H), 6.79 (ddd, *J* = 2.5, 8.8, 11.7 Hz, 1H), 4.67 (d, *J* = 9.8 Hz, 1H), 4.39 (dd, *J* = 1.6, 9.8 Hz, 1H), 4.13 (t, *J* = 8.5 Hz, 1H), 3.97-4.07 (m, 1H), 3.91 (ddd, *J* = 4.4, 7.1, 11.8 Hz, 1H), 3.78 (dd, *J* = 7.0, 9.0 Hz, 1H), 3.08-3.22 (m, 1H), 2.80 (dd, *J* = 4.7, 7.0 Hz, 1H).

**9*H*-Fluoren-9-ylmethyl [(3*S*,4*R*)-3-(2,4-difluorophenyl)-4-(hydroxymethyl)tetrahydro-2*H*-pyran-3-yl]carbamothioyl}carbamate (22b).**

To a solution of **21b** (650 mg, 2.67 mmol) in $CH_2Cl_2$ (10 mL) was added 9*H*-fluoren-9-ylmethyl carbonisothiocyanatidate (FMOC-isothiocyanate) (827 mg, 2.94 mmol) and the reaction mixture was stirred for 4 h at room temperature. The mixture was then concentrated *in vacuo* to provide a paste that was purified by flash chromatography ($SiO_2$, Gradient: MeOH/$CH_2Cl_2$, gradient 0% to 5%) to afford 1.17 g (84% yield) of the product **22b**. LC-MS *m/z* 525.2 (M+1).

***rac*-*N*-[(4a*S*,7a*S*)-7a-(2,4-difluorophenyl)-4a,5,7,7a-tetrahydro-4*H*-furo[3,4-*d*][1,3]thiazin-2-yl]benzamide (23a).**

A rapidly stirred suspension of ***rac*-22a** (492 mg, 1.25 mmol) in toluene (10.0 mL) under an atmosphere of nitrogen was heated to 90 $^{o}$C in an oil bath, during which time it became a homogeneous solution. Ghosez' reagent (0.303 g, 2.27 mmol, 0.300 mL) was added in one portion to the hot solution. The resulting homogeneous solution continued to be heated at 90 $^{o}$C for 15 min. The reaction mixture was cooled, concentrated *in vacuo*, and purified by flash chromatography ($SiO_2$, 24 g High Performance Gold Redisep column, EtOAc/Heptanes, 0-80% gradient over 16CV) to afford 456 mg (97%) of **23a** as a white solid. LC-MS *m/z* 375 (M+1). $^1$H NMR (400 MHz, $CDCl_3$) δ 8.12 (d, *J* = 6.8 Hz, 2H), 7.36-7.57 (m, 4H), 6.84-7.00 (m, 2H), 4.41 (d, *J* = 9.2 Hz, 1H), 4.21 (d, *J* = 7.6 Hz, 2H), 4.01 (d, *J* = 7.8 Hz, 1H), 3.27-3.40 (m, *J* = 4.5 Hz, 1H), 3.18 (dd, *J* = 3.5, 13.5 Hz, 1H), 2.90 (dd, *J* = 5.2, 13.6 Hz, 1H).

**(4a*S*,7a*S*)-7a-(2,4-Difluorophenyl)-4a,5,7,7a-tetrahydro-4*H*-furo[3,4-*d*][1,3]thiazin-2-amine (24a).**

To a solution of **23a** (450.0 mg, 1.20 mmol) in methanol (8.0 mL) was added DBU (101.8 mg, 0.668 mmol, 100.0 µL). The reaction mixture was stirred and heated in a tightly capped 20 mL vial at 60 ºC (external) for 16 h. The solution was then cooled to rt and concentrated *in vacuo*. The residue was partitioned between EtOAc (35 mL) and $H_2O$ (10 mL). After extraction, the organic phase was washed with $H_2O$ (2 x 10 mL). The organic extract was dried over $Na_2SO_4$, filtered, concentrated *in vacuo*, and purified by flash chromatography [$SiO_2$, 12 g RediSepGold column, MeOH/$CH_2Cl_2$ (gradient 0-10%: over 35CV)] to afford 261 mg (80% yield) of ***rac*-24a** as a white solid. LC-MS *m/z* 271 (M+1). Enantiomer separation was carried out using a Lux Cellulose-2 250 mm x 21.2 mm 5 µm column eluting with 70% $CO_2$ and 30% MeOH (isocratic) with 0.2% $NH_4^+$ buffer at a flow rate of 80 mL/min (120 bar backpressure). Detection at 210 nm. The desired enantiomer eluted at 8.40 min (peak 2). LC-MS *m/z* 271 (M+1). $^1$H NMR (400 MHz, $CDCl_3$) δ 7.44 (dt, *J* = 6.6, 9.00 Hz, 1H), 6.76-6.90 (m, 2H), 4.43 (dd, *J* = 1.4, 8.8 Hz, 1H), 4.01-4.16 (m, 2H), 3.79 (dd, *J* = 2.2, 8.8 Hz, 1H), 2.99-3.07 (m, 1H), 2.91-2.99 (m, 1H), 2.79-2.88 (m, 1H). $[\alpha]^{27.39}_D$ = - 2.06 (c = 0.785, MeOH).

**(4a*R*,8a*S*)-8a-(2,4-Difluorophenyl)-4,4a,5,6,8,8a-hexahydropyrano[3,4-*d*][1,3]thiazin-2-amine (24b).**

A suspension of **22b** (1.42 g, 2.70 mmol) in MeOH (20 mL) was treated with concentrated HCl (0.675 mL, 8.10 mmol) and heated to 70 ºC for 2 hours. The reaction mixture was then concentrated *in vacuo*, dissolved in $CH_2Cl_2$ and washed with saturated sodium bicarbonate. The organic layer was dried over $MgSO_4$, filtered, and concentrated *in vacuo*. The residue was dissolved in acetonitrile (20 mL), treated with piperidine (2 mL) and stirred at rt for 18 h, and then concentrated *in vacuo*. Purification by flash chromatography ($SiO_2$, MeOH/$CH_2Cl_2$, gradient 0-7%) provided 281 mg (37%) of **24b** as a white solid. LC-MS *m/z* 285.0 (M+1). $^1$H

NMR (400 MHz, $CD_3OD$) δ 7.35 (ddd, *J* = 9.5, 8.7, 6.7 Hz, 1H), 7.00-6.92 (m, 2H), 4.05-3.99 (m, 2H), 3.70-3.62 (m, 1H), 3.63 (br d, *J* = 10.9 Hz, 1H), 2.90-2.82 (m, 2H), 2.73-2.67 (m, 1H), 2.12-1.99 (m, 1H), 1.52-1.45 (m, 1H).

**(2*R*)-1-(Benzyloxy)pent-4-en-2-ol (25a).**

A mixture of (2*R*)-2-[(benzyloxy)methyl]oxirane (9.8 g, 60 mmol) and copper(I) iodide (648 mg, 3.40 mmol) in diethyl ether (150 mL) was cooled to -78 ºC. Vinylmagnesium chloride (1.6 M in THF, 41.0 mL, 65.6 mmol) was added drop-wise, and the reaction mixture was allowed to warm slowly to rt and stir for 18 h. Ice and saturated aq $NH_4Cl$ were added to the reaction mixture, which was then extracted with EtOAc. The combined organic layers were washed with saturated aq $NH_4Cl$, dried over $MgSO_4$, filtered, and concentrated *in vacuo*. This material was used in the following step without further purification. $^1$H NMR (400 MHz, $CDCl_3$), product peaks only: δ 7.4-7.3 (m, 5H), 5.89-5.78 (m, 1H), 5.16-5.09 (m, 2H), 4.57 (s, 2H), 3.93-3.87 (m, 1H), 3.53 (dd, *J* = 9.5, 3.4 Hz, 1H), 3.39 (dd, *J* = 9.4, 7.4 Hz, 1H), 2.25-2.31 (m, 2H).

**({[(2*R*)-2-(2,2-Diethoxyethoxy)pent-4-en-1-yl]oxy}methyl)benzene (26a).**

A solution of (2*R*)-1-(benzyloxy)pent-4-en-2-ol (**25a**) (material from the previous step, 60 mmol) in THF (50 mL) was added drop-wise to a suspension of sodium hydride (60% in mineral oil, 11.0 g, 275 mmol) in THF (100 mL) at 0 ºC. After the reaction mixture had stirred for 30 minutes at this temperature, a solution of 2-bromo-1,1-diethoxyethane (97%, 13.3 mL, 85.8 mmol) in THF (50 mL) was added at 0 ºC, and the reaction mixture was then heated to reflux for 18 h. Additional 2-bromo-1,1-diethoxyethane (11 mL, 71 mmol) was added, and heating was continued for a further 24 h. The reaction mixture was cooled to 0 ºC, quenched with water, and extracted with EtOAc (3x). The combined organic layers were washed with water, washed with

saturated aq NaCl, dried over $Na_2SO_4$, filtered, and concentrated *in vacuo*. Purification by flash chromatography ($SiO_2$, EtOAc/heptane, Gradient: 0% to 15%) afforded 11.04 g (60% yield over two steps) of **26a** as a colorless oil. $^1$H NMR (400 MHz, $CDCl_3$) δ 7.38-7.27 (m, 5H), 5.90-5.78 (m, 1H), 5.12-5.02 (m, 2H), 4.61 (t, *J* = 5.3 Hz, 1H), 4.55 (s, 2H), 3.74-3.49 (m, 9H), 2.36-2.31 (m, 2H), 1.22 (t, *J* = 7.0 Hz, 3H), 1.21 (t, *J* = 7.1 Hz, 3H).

**[1-(2,2-Diethoxyethoxy)but-3-en-1-yl]cyclopropane (26b).**

1-Cyclopropylbut-3-en-1-ol[24] (**25b**, 92%, 8.1 g, 66 mmol) was added to a suspension of sodium hydride (60% in mineral oil, 8.25 g, 206 mmol) in THF (105 mL) at 0 °C. The cooling bath was removed and the suspension was stirred until the internal temperature reached 21 °C. The reaction mixture was then cooled in an ice bath, and 2-bromo-1,1-diethoxyethane (97%, 18.5 mL, 119 mmol) was added drop-wise at a rate that maintained the internal temperature below 5 °C. After warming to rt, the reaction mixture was heated to 58 °C (internal) for 27 hours. Sodium hydride (60% in mineral oil, 3.3 g, 83 mmol) and 2-bromo-1,1-diethoxyethane (97%, 10 mL, 64 mmol) were added again, and the reaction mixture was heated at mild reflux for 14 h. The reaction mixture was then cooled to 0 °C, slowly quenched with water (100 mL) and extracted with diethyl ether (3 x 200 mL). The combined organic layers were dried over $Na_2SO_4$, filtered, and concentrated *in vacuo*. Purification via flash chromatography ($SiO_2$, EtOAc/heptane, gradient: 0-10%) afforded 12.1 g (80% yield) of **26b** as a colorless oil. $^1$H NMR (400 MHz, $CDCl_3$) δ 5.98-5.87 (m, 1H), 5.11-5.05 (m, 1H), 5.04-5.00 (m, 1H), 4.61 (t, *J* = 5.3 Hz, 1H), 3.75-3.66 (m, 3H), 3.62-3.54 (m, 2H), 3.47 (dd, *J* = 10.3, 5.5 Hz, 1H), 2.70 (dt, *J* = 8.4, 6.0 Hz, 1H), 2.41-2.36 (m, 2H), 1.22 (t, *J* = 7.0 Hz, 3H), 0.90-0.80 (m, 1H), 0.62-0.54 (m, 1H), 0.50-0.35 (m, 2H), 0.14-0.07 (m, 1H).

**{[(2*R*)-1-(Benzyloxy)pent-4-en-2-yl]oxy}acetaldehyde (27a).**

To a solution of **26a** (10.14 g, 32.88 mmol) in THF (110 mL) was added aqueous HCl (2 M, 19.5 mL, 39.0 mmol), and the reaction mixture was then heated to 75 ºC for 1 hour. The reaction was concentrated to approximately half the original volume and then partitioned between EtOAc and water. The aqueous layer was extracted with EtOAc, and the combined organic layers were washed with saturated aq sodium chloride, dried over $Na_2SO_4$, filtered, and concentrated *in vacuo*, to afford 7.76 g (87% yield) of **27a** as a colorless oil, which was used directly in the following step. $^1$H NMR (400 MHz, $CDCl_3$) δ 9.72 (t, $J$ = 1.0 Hz, 1H), 7.39-7.27 (m, 5H), 5.89-5.78 (m, 1H), 5.15-5.06 (m, 2H), 4.53 (br s, 2H), 4.28-4.18 (m, 2H), 3.68-3.62 (m, 1H), 3.57-3.54 (m, 2H), 2.42-2.28 (m, 2H).

**[(1-Cyclopropylbut-3-en-1-yl)oxy]acetaldehyde (27b).**

A mixture of **26b** (2.97 g, 13.0 mmol), aqueous HCl (1 M, 39 mL, 39 mmol) and THF (39 mL) was stirred at rt for 12.5 h, then heated to 40 °C for 3 h. The reaction mixture was cooled to rt and slowly transferred into a stirring biphasic mixture of saturated aqueous sodium bicarbonate (200 mL) and diethyl ether (200 mL). The aqueous layer was extracted with diethyl ether (2 x 100 mL) and the combined organic extracts were dried over $Na_2SO_4$, filtered, and concentrated *in vacuo* (900 mbar, 60 °C) to afford 3.63 g (81% yield) of **27b** as a colorless oil, which contained residual diethyl ether and THF by $^1$H NMR analysis. This material was taken directly into the following step. $^1$H NMR (400 MHz, $CDCl_3$) δ 9.78-9.76 (m, 1H), 5.98-5.86 (m, 1H), 5.15-5.04 (m, 2H), 4.15 (br AB quartet, $J_{AB}$ = 17.8 Hz, $\Delta\nu_{AB}$=22.8 Hz, 2H), 2.71 (dt, $J$ = 8.8, 5.9 Hz, 1H), 2.47-2.41 (m, 2H), 0.91-0.81 (m, 1H), 0.66-0.58 (m, 1H), 0.57-0.49 (m, 1H), 0.38-0.31 (m, 1H), 0.15-0.08 (m, 1H).

**2-{[(2*R*)-1-(Benzyloxy)pent-4-en-2-yl]oxy}-*N*-hydroxyethanimine (28a).**

To a solution of **27a** (7.76 g, 32.9 mmol) in a 2:1 mixture of ethanol and water (127 mL) was added sodium acetate (13.6 g, 166 mmol), and the mixture was stirred for 15 min. Hydroxylamine hydrochloride (98%, 7.05 g, 99.4 mmol) was then added, and the reaction mixture was heated to 60 ºC for 18 h. The reaction mixture was partitioned between EtOAc and water, and the aqueous layer was extracted with EtOAc. The combined organic layers were washed with saturated aqueous NaCl, dried over $Na_2SO_4$, filtered, and concentrated *in vacuo*. Purification by flash chromatography ($SiO_2$, EtOAc/heptane, Gradient: 0 to 30%) afforded 7.12 g (87% yield over 2 steps) of **28a** as a colorless oil, presumed from the $^1$H NMR spectrum to be a mixture of E and Z oximes. $^1$H NMR (400 MHz, $CDCl_3$) δ 7.39-7.27 (m, 5H), 7.55-7.47 and 7.01-6.93 (2 br m, total 1H), 5.87-5.75 (m, 1H), 5.14-5.05 (m, 2H), 4.56 and 4.55 (2 s, total 2H), 4.49-4.45 (br m) and [4.25 (dd, half of ABX pattern, $J$ = 12.9, 5.6 Hz) and 4.20 (dd, half of ABX pattern, $J$ = 12.9, 5.8 Hz)] total 2H}, 3.65-3.47 (m, 3H), 2.37-2.30 (m, 2H).

**2-[(1-Cyclopropylbut-3-en-1-yl)oxy]-*N*-hydroxyethanimine (28b).**

To a solution of **27b** (3.63 g from the previous step, <13.0 mmol) in a 2:1 mixture of ethanol and water (39 mL) was added sodium acetate (5.32 g, 64.9 mmol). After the reaction mixture had been stirred for 15 min, hydroxylamine hydrochloride (98%, 2.76 g, 38.9 mmol) was added, and the reaction mixture was heated to 60 °C for 5 minutes, at which time water (4 x 1 mL) was added until a solution resulted. After the mixture had stirred for 1 h at 60 °C, it was cooled to rt, concentrated *in vacuo* to remove ethanol, and diluted with saturated aqueous NaCl (100 mL). The mixture was extracted with diethyl ether (3 x 100 mL), and the combined organic layers were dried over $Na_2SO_4$, filtered, and concentrated *in vacuo* at 22 °C. Purification by flash

chromatography ($SiO_2$, EtOAc/heptane, 0 to 25%) provided 1.77 g (81%) of **28b** as a thick, opaque oil. By $^1$H NMR analysis, this material consisted of a roughly 1:1 mixture of *E*- and *Z*-oxime isomers. $^1$H NMR (400 MHz, $CDCl_3$) δ [7.50 (dd, *J* = 5.7 and 5.6 Hz) and 6.99-6.92 (m), total 1H], 5.97-5.84 (m, 1H), 5.15-5.03 (m, 2H), [4.53 (dd, half of ABX pattern, *J* = 16.4 and 3.5 Hz) and 4.41 (dd, half of ABX pattern, *J* = 16.4 and 3.6 Hz)] and [4.27 (dd, half of ABX pattern, *J* = 12.9 and 5.5 Hz) and 4.16 (dd, half of ABX pattern, *J* = 12.9 and 5.8 Hz)], total 2H}, 2.74-2.65 (m, 1H), 2.44-2.37 (m, 2H), 0.91-0.81 (m, 1H), 0.68-0.59 (m, 1H), 0.56-0.47 (m, 1H), 0.44-0.35 (m, 1H), 0.15-0.07 (m, 1H).

**(3a*R*,5*R*)-5-[(Benzyloxy)methyl]-3,3a,4,5-tetrahydro-7*H*-pyrano[3,4-*c*][1,2]oxazole (29a).**

A solution of **28a** (7.12 g, 28.6 mmol) in $CH_2Cl_2$ (168 mL) was placed in a rt water bath. Triethylamine (0.299 mL, 2.14 mmol) was added, followed by addition of bleach (aqueous sodium hypochlorite solution, 6.15%, 71 mL, 59 mmol) at a rate slow enough to maintain the internal reaction temperature between 22 ºC and 25.5 ºC. Upon completion of the addition, the reaction mixture was diluted with water and extracted with $CH_2Cl_2$ (3x). The combined organic extracts were washed with saturated aqueous NaCl, dried over $Na_2SO_4$, filtered, and concentrated *in vacuo*. Purification by flash chromatography ($SiO_2$, EtOAc/heptane, 0 to 35%) provided 5.65 g (80% yield) of **29a** as a yellow oil. The indicated relative stereochemistry was assigned based on nuclear Overhauser enhancement studies, which revealed an interaction between the methine protons on carbons 3a and 5. LCMS *m/z* 248.1 (M+1). $^1$H NMR (400 MHz, $CDCl_3$) δ 7.39-7.27 (m, 5H), 4.77 (d, *J* = 13.5 Hz, 1H), 4.65-4.54 (m, 3H), 4.23 (dd, *J* = 13.5 and 1.2 Hz, 1H), 3.79 (dd, *J* = 11.8 and 8.1 Hz, 1H), 3.77-3.68 (m, 1H), 3.57 (dd, half of ABX pattern, *J* = 10.2 and 5.8 Hz, 1H), 3.49 (dd, half of ABX pattern, *J* = 10.2 and 4.2 Hz, 1H), 3.52-3.40 (m, 1H), 2.24-2.17 (m, 1H), 1.63-1.51 (m, 1H).

***rel*-(3a*R*,5*R*)-5-cyclopropyl-3,3a,4,5-tetrahydro-7*H*-pyrano[3,4-*c*][1,2]oxazole (29b).**

An aqueous solution of sodium hypochlorite (6.15% solution, 27.1 mL, 22.4 mmol) was added drop-wise over 24 minutes to a solution of **28b** (1.85 g, 10.9 mmol) and triethylamine (0.114 mL, 0.818 mmol) in $CH_2Cl_2$ (64 mL) that was immersed in a rt water bath. The rate of addition was adjusted to maintain the internal temperature of the reaction between 19.5 °C and 22.8 °C. After completion of the addition, the reaction mixture was diluted with water (50 mL) and the aqueous layer was extracted with $CH_2Cl_2$ (3 x 50 mL). The combined organic layers were washed with saturated aqueous NaCl (50 mL), dried over $Na_2SO_4$, filtered, and concentrated *in vacuo* (300 mbar, 40 °C) to provide 1.73 g (94% yield) of **29b** as a pale yellow oil. The indicated relative stereochemistry was assigned based on nuclear Overhauser enhancement studies, which revealed an interaction between the methine protons on carbons 3a and 5. GC-MS *m/z* 167 [M+]. $^1$H NMR (400 MHz, $CDCl_3$) δ 4.73 (d, *J* = 13.5 Hz, 1H), 4.61 (dd, *J* = 10.2 and 8.0 Hz, 1H), 4.14 (dd, *J* = 13.5 and 1.0 Hz, 1H), 3.80 (dd, *J* = 11.5 and 8.0 Hz, 1H), 3.48-3.36 (m, 1H), 2.83 (ddd, *J* = 11.0, 8.0 and 1.8 Hz, 1H), 2.31 (ddd, *J* = 13.0, 6.5 and 1.5 Hz, 1H), 1.64 (ddd, *J* = 12.8, 11.4, and 1.5 Hz, 1H), 0.98-0.89 (m, 1H), 0.64-0.51 (m, 2H), 0.45-0.38 (m, 1H), 0.28-0.21 (m, 1H).

**(3a*R*,5*R*,7a*S*)-5-[(Benzyloxy)methyl]-7a-(2,4-difluorophenyl)hexahydro-1*H*-pyrano[3,4-*c*][1,2]oxazole (30a).**

Boron trifluoride diethyl etherate (60.1 mL, 226 mmol) was added to a solution of **29a** (50 g, 202 mmol) in a 1:1 mixture of toluene and isopropyl ether (2000 mL total volume) at -78 ºC. An emulsion was formed instantly and it remained through the course of the reaction. The reaction mixture was stirred at this temperature for 30 minutes and then treated with 2,4-difluoro-1-

iodobenzene (27.1 mL, 226 mmol). *n*-Butyllithium (2.5 M in hexanes, 85.7 mL, 214 mmol) was slowly added while maintaining the reaction temperature at -78 to -73 ºC. The resulting yellow emulsion mixture was allowed to stir at -78 $^{o}$C for 1 h 20 min. An aliquot of the reaction mixture was quenched with $NH_4Cl$ (aq, sat'd) and organics were extracted with EtOAc. Analysis by TLC of the organic layer (40:60 / EtOAc:heptanes) showed a minor (only visible when stained in $KMnO_4$) amount of starting material together with the major product spot. The reaction was then quenched with saturated aqueous $NH_4Cl$ and water (1000 mL). The resulting heterogeneous solution was partitioned between $H_2O$ (1000 mL) and EtOAc (750 mL) and the now heterogeneous mixture was allowed to warm up to rt. The organic layer was isolated and the aqueous layer was back-extracted with EtOAc (3 x 250 mL). The combined organics were washed with brine (550 mL), dried over $Na_2SO_4$, filtered and concentrated under reduced pressure to yield a yellow oily residue. The residue was redissolved in EtOAc, adsorbed on silica gel and loaded on CombiFlash 1 (330 g Redisep column, 25CV, 0 to 70% of EtOAc in heptanes) for purification purposes. Fractions that contained the product spot were combined and concentrated under reduced pressure to afford **30a** as a yellow oily residue. Yield: 46.9 g, 64%. LC-MS *m/z* 362.2 (M+1). $^1$H NMR (400 MHz, $CDCl_3$) δ 7.93 (ddd, *J* = 9.1, 9.0 and 6.8 Hz, 1H), 7.40-7.28 (m, 5H), 6.93-6.87 (m, 1H), 6.80 (ddd, *J* = 11.9, 8.6 and 2.5 Hz, 1H), 4.60 (AB quartet, $J_{AB}$ = 12.1 Hz 2H), 4.14 (dd, *J* = 12.7 and 1.8 Hz, 1H), 3.90-3.82 (m, 2H), 3.72 (br d, *J* = 7 Hz, 1H), 3.59-3.53 (m, 2H), 3.50 (dd, half of ABX pattern, *J* = 10.2 and 4.1 Hz, 1H), 3.12-3.04 (m, 1H), 1.90-1.82 (m, 1H), 1.60-1.48 (m, 1H, assumed; partially obscured by water peak).

***rel*-(3a*R*,5*R*,7a*S*)-5-Cyclopropyl-7a-(2,4-difluorophenyl)hexahydro-1*H*-pyrano[3,4-*c*][1,2]oxazole (30b).**

Boron trifluoride diethyl etherate (2.97 mL, 24.1 mmol) was added drop-wise to a solution of **29b** (1.67 g, 9.99 mmol) in toluene (150 mL) at an internal temperature of −72.5 °C. The reaction mixture was stirred at −73 °C to −76 °C for 30 minutes, then treated with 2,4-difluoro-1-iodobenzene (98%, 1.37 mL, 11.2 mmol) in one portion. While the reaction temperature was maintained below −73 °C, *n*-BuLi (2.5 M in hexanes, 4.24 mL, 10.6 mmol) was added in a drop-wise manner over 15 minutes. The reaction mixture was stirred at −73 °C to −75 °C for 1 h, then was quenched with saturated aqueous $NH_4Cl$ (350 mL) at −74 °C and allowed to warm to rt. The resulting mixture was extracted with EtOAc (400 mL), and the aqueous layer was extracted with additional EtOAc (250 mL and 100 mL). The combined organic layers were dried over $Na_2SO_4$, filtered, and concentrated *in vacuo*. Purification by flash chromatography ($SiO_2$, EtOAc/heptane, 0 to 30%) afforded 2.16 g (77% yield) of **30b** as a white solid after azeotroping with $CH_2Cl_2$. GC-MS *m/z* 281 [M+]. $^1$H NMR (400 MHz, $CDCl_3$) δ 7.98-7.88 (m, 1H), 6.93-6.84 (m, 1H), 6.79 (ddd, *J* = 11.9, 8.6 and 2.4 Hz, 1H), 6.34 (br s, 1H), 4.04 (br d, *J* = 12.7 Hz, 1H), 3.83 (d, *J* = 12.5 Hz, 1H), 3.72 (d, *J* = 7.0 Hz, 1H), 3.54 (dd, *J* = 6.8 and 5.1 Hz, 1H), 3.08-2.99 (m, 1H), 2.95-2.86 (m, 1H), 1.99 (br dd, *J* = 13.8 and 6.8 Hz, 1H), 1.68-1.56 (m, 1H), 1.00-0.88 (m, 1H), 0.64-0.51 (m, 2H), 0.47-0.37 (m, 1H), 0.33-0.24 (m, 1H).

**[(2*R*,4*R*,5*S*)-5-Amino-2-[(benzyloxy)methyl]-5-(2,4-difluorophenyl)tetrahydro-2*H*-pyran-4-yl]methanol (31a).**

To a mixture of **30a** (46.9 g, 130 mmol) in acetic acid (430 mL) was added zinc powder (110 g, 1690 mmol), and the reaction mixture was stirred for 18 h. Analysis by TLC (30% EtOAc/heptane) indicated all starting material had been consumed. The insoluble material was removed via filtration, and the solids were washed with EtOAc. The combined filtrates were washed with saturated 1 N KOH, and the aqueous layer was extracted with EtOAc. The

combined organic layers were washed with saturated aqueous NaCl, dried over $Na_2SO_4$, filtered, and concentrated *in vacuo* to afford 49.5 g (quantitative yield) of **31a** as an opaque oil, which was used in the following reaction without additional purification. LC-MS *m/z* 364.4 (M+1). $^1$H NMR (400 MHz, $CDCl_3$) δ 7.79-7.62 (br m, 1H), 7.40-7.27 (m, 5H), 7.05-6.92 (br m, 1H), 6.83 (ddd, $J$ = 12.6, 8.6 and 2.6 Hz, 1H), 4.61 (AB quartet, upfield signals are broadened, $J_{AB}$ = 12.1 Hz, 2H), 4.22 (dd, $J$ = 11.5 and 2.3 Hz, 1H), 3.92-3.82 (br m, 1H), 3.73-3.60 (br m, 1H), 3.60-3.42 (m, 3H), 3.41-3.32 (m, 1H), 2.41-2.24 (br m, 1H), 2.16-1.98 (br m, 1H), 1.65 (ddd, $J$ = 14.0, 4.3 and 2.6 Hz, 1H).

**_rel_-[(2_R_,4_R_,5_S_)-5-Amino-2-cyclopropyl-5-(2,4-difluorophenyl)tetrahydro-2_H_-pyran-4-yl]methanol (31b).**

To a solution of **30b** (1.19 g, 4.23 mmol) in glacial acetic acid (12 mL) stirred at room temperature was added zinc powder (3.51 g, 53.7 mmol) in one portion. During the 15 min after the zinc addition, a gradual internal exotherm from 22 ºC initial to 38 ºC peak was observed. After the exotherm peaked at 38 ºC, it took ~15 min for it to gradually subside back to 29 ºC. After 1 h, the reaction mixture internal temperature was 22 ºC. The reaction mixture was stirred at rt for 18 h. The reaction mixture was filtered through a small plug of Celite, followed by an additional rinse with EtOAc (100 mL). The filtrate was slowly poured over stirring sat aq $NaHCO_3$ (250 mL) and EtOAc (200 mL). The mixture was extracted and separated. The lower aq layer was washed with additional EtOAc (2 x 150 mL). The combined upper extracts were washed with brine (200 mL) then dried over $Na_2SO_4$, filtered and concentrated *in vacuo*, to afford 1.22 g of **31b** as a thick, pale amber gum (1.22 g), which was taken directly to the following step without additional purification. LC-MS *m/z* 284.1 [M+H+]. $^1$H NMR (400 MHz, $CDCl_3$) δ 7.61-7.77 (br m, 1H), 6.90-7.05 (br m, 1H), 6.82 (ddd, $J$ = 12.7, 8.6 and 2.6 Hz, 1H),

4.13 (dd, *J* = 11.5 and 2.5 Hz, 1H), 3.55 (br dd, *J* = 11 and 2 Hz, 1H), 3.49-3.32 (br m, 2H), 2.89 (ddd, *J* = 11.3, 8.2, and 2.5 Hz, 1H), 2.34-2.03 (br m, 2H), 1.81 (ddd, *J* = 14.0, 4.0 and 2.6 Hz, 1H), 1.13-1.01 (br m, 1H), 0.65-0.53 (m, 2H), 0.48-0.41 (m, 1H), 0.32-0.24 (m, 1H).

**_N_-{[(3*S*,4*R*,6*R*)-6-[(Benzyloxy)methyl]-3-(2,4-difluorophenyl)-4-(hydroxymethyl)tetrahydro-2*H*-pyran-3-yl]carbamothioyl}benzamide (32a).**

To a solution of [(2*R*,4*R*,5*S*)-5-amino-2-[(benzyloxy)methyl]-5-(2,4-difluorophenyl)tetrahydro-2*H*-pyran-4-yl]methanol (**31a**) (50.1 g, 138 mmol) in anhydrous $CH_2Cl_2$ (1380 mL) was added benzoyl isothiocyanate (22.3 g, 18.4 mL, 137 mmol) and the reaction mixture was stirred at rt for 18 h. An aliquot of the reaction mixture was analyzed by LC/MS, which showed complete consumption of starting material and major product mass. The reaction mixture was concentrated under reduced pressure to yield 73 g (100%) of an orange oily residue (**32a**). This material was used in the next step without purification.

**_N_-{[(3*S*,4*R*,6*R*)-6-[(Benzyloxy)methyl]-3-(2,4-difluorophenyl)-4-(hydroxymethyl)tetrahydro-2*H*-pyran-3-yl]carbamothioyl}-2-(9*H*-fluoren-9-yl)acetamide (32a').**

A solution of 49.5 g (136 mmol) **31a** in 1.4 L of anhydrous $CH_2Cl_2$ was treated with the 42.2 g (150 mmol) of FMOC isothiocyanate. The reaction mixture was stirred at rt for 18 h. Analysis by TLC (1:1 EtOAc/heptanes) indicated that starting material was consumed and a new less polar spot had appeared. The reaction mixture was concentrated to dryness and the residue was chromatographed (SIM) on an 330 g column eluting with 0-30% EtOAc/heptanes. Some of the early fractions were re-chromatographed on a 330 g column eluting with 0-30% EtOAc/heptanes. After evaporation of the solvent, there was obtained **32a'** as a pink solid. This

material was contaminated with a small amount of less polar cyclized material **33a'**, and a very minor impurity that was highly colored. The material was used directly in the next transformation. Yield, 91.4 g, quant. LC-MS *m/z* 645.2 (M+1).

***rel*-*N*-[(3*S*,4*R*,6*R*)-6-Cyclopropyl-3-(2,4-difluorophenyl)-4-(hydroxymethyl)tetrahydro-2*H*-pyran-3-yl]carbamothioyl}benzamide (32b).**

To a solution of **31b** (1.20 g, 4.23 mmol) in $CH_2Cl_2$ (45 mL) was added benzoyl isothiocyanate (0.540 mL, 4.02 mmol). After the reaction mixture had stirred at rt for 15 h, it was partitioned between aqueous HCl (0.1 M, 20 mL) and $CH_2Cl_2$ (35 mL). The organic layer was washed with saturated aqueous sodium bicarbonate (25 mL) and with saturated aqueous NaCl (25 mL), then dried over $Na_2SO_4$, filtered, and concentrated *in vacuo*. Purification by flash chromatography ($SiO_2$, EtOAc/heptane, 0 to 45%) provided 1.69 g (89% yield) of **32b** as a white solid. LC-MS *m/z* 447.2 [M+1]. $^1$H NMR (400 MHz, CD3CN) δ 11.64 (br s, 1H), 9.28 (br s, 1H), 7.93-7.89 (m, 2H), 7.69-7.64 (m, 1H), 7.58-7.52 (m, 2H), 7.58-7.44 (br m, 1H), 6.99-6.86 (m, 2H), 3.86-3.48 (br m, 2H), 3.47-3.35 (m, 1H), 3.01 (ddd, *J* = 11.3, 7.6 and 2.7 Hz, 1H), 3.0-2.89 (br m, 1H), 2.6-2.3 (br m, 1H), 2.03-1.96 (m, 1H), 1.9-1.7 (br m, 1H), 1.00-0.90 (m, 1H), 0.53-0.44 (m, 2H), 0.40-0.34 (m, 1H), 0.31-0.26 (m, 1H).

***N*-[(4a*R*,6*R*,8a*S*)-6-[(Benzyloxy)methyl]-8a-(2,4-difluorophenyl)-4,4a,5,6,8,8a-hexahydropyrano[3,4-*d*][1,3]thiazin-2-yl]benzamide (33a).**

To a solution of *N*-{[(3*S*,4*R*,6*R*)-6-[(benzyloxy)methyl]-3-(2,4-difluorophenyl)-4-(hydroxymethyl)tetrahydro-2*H*-pyran-3-yl]carbamothioyl}benzamide (**32a**) (5.17 g, 9.82 mmol) in anhydrous $CH_2Cl_2$ (89 mL) was added pyridine (3 mL, 37.3 mmol). The solution was cooled to -60 $^oC$ (dry ice/acetone), then triflic anhydride (3.3 mL, 19.6 mmol) in anhydrous $CH_2Cl_2$ (17 mL) was added drop-wise. The reaction mixture turned from clear to yellow. The reaction was gradually warmed to -5 $^oC$ over 3 h. Water was then added, and the mixture extracted. The aqueous layer was washed once more with $CH_2Cl_2$. The combined organic layers were washed with brine, dried over $Na_2SO_4$, filtered, and concentrated *in vacuo*. Purification by flash chromatography ($SiO_2$, 80 g, EtOAc/heptane, 0 to 30%) afforded 2.58 g (52% yield) of *N*-[(4a*R*,6*R*,8a*S*)-6-[(benzyloxy)methyl]-8a-(2,4-difluorophenyl)-4,4a,5,6,8,8a-hexahydropyrano[3,4-*d*][1,3]thiazin-2-yl]benzamide (**33a**) as a white solid. LC-MS *m/z* 509.2 [M+1]. $^1$H NMR (400 MHz, $CD_3OD$) δ ppm 8.12 (d, *J* = 7.4 Hz, 2H), 7.52 (d, *J* = 7.4 Hz, 1H), 7.39 - 7.49 (m, 3H), 7.27 - 7.34 (m, 2H), 7.16 - 7.27 (m, 3H), 7.00 - 7.11 (m, 2H), 4.50 - 4.63 (m, 2H), 4.13 (m, 1H), 3.89 (m, 2H), 3.54 - 3.66 (m, 2H), 3.13 - 3.24 (m, 1H), 2.93 (m, *J* = 4.1 Hz, 1H), 2.74 (m, *J* = 13.1, 2.9 Hz, 1H), 1.88 - 2.00 (m, 1H), 1.66 - 1.75 (m, 1H).

**_N_-[(4a_R_,6_R_,8a_S_)-6-[(Benzyloxy)methyl]-8a-(2,4-difluorophenyl)-4,4a,5,6,8,8a-hexahydropyrano[3,4-_d_][1,3]thiazin-2-yl]-2-(9_H_-fluoren-9-yl)acetamide (33a').**

The material for this reaction was split in half for the cyclization, but combined for workup: In two 2 L round bottom flasks was dissolved **32a'** (45.7 g, 71.0 mmol ) in MeOH (958 mL). The solution was treated with 18.5 mL of concd HCl and the reaction mixture was heated to 70 °C for 3 hours. Analysis by LCMS and TLC (1:1 EtOAc/heptane indicated starting material was consumed. The reaction mixture was concentrated to a paste. The residues from the two reactions were dissolved in $CH_2Cl_2$ and washed with saturated aqueous $NaHCO_3$. The aqueous phase was

extracted with $CH_2Cl_2$ (2x). The combined $CH_2Cl_2$ extracts were washed with brine and then the organic phase was dried over $Na_2SO_4$, and concentrated *in vacuo*. There was recovered **33a'** as a pale yellow foam. Yield 83.9 g 95%. LC-MS *m/z* 627.1 (M+1). $^1$H NMR (400 MHz, $CDCl_3$) δ 7.76 (d, *J* = 7.6 Hz, 2H), 7.70 (t, *J* = 6.7 Hz, 2H), 7.37 - 7.43 (m, 2H), 7.26 - 7.36 (m, 8H), 6.94 (m, *J* = 6.7, 6.7 Hz, 1H), 6.81 - 6.90 (m, 1H), 4.50 - 4.64 (m, 2H), 4.36 - 4.43 (m, 2H), 4.28 - 4.35 (m, 1H), 4.13 (d, *J* = 12.3 Hz, 1H), 3.84 - 3.95 (m, 1H), 3.75 (br s, 1H), 3.62 (dd, *J* = 10.0, 6.3 Hz, 1H), 3.48 (dd, *J* = 10.0, 4.4 Hz, 1H), 3.09 (br s, 1H) 2.95 (dd, *J* = 12.8, 3.8 Hz, 1H), 2.60 (m, *J* = 11.30 Hz, 1H), 1.90 (m, *J* = 12.90 Hz, 1H), 1.66 (d, *J* = 12.29 Hz, 1H).

***rel*-*N*-[(4a*R*,6*R*,8a*S*)-6-Cyclopropyl-8a-(2,4-difluorophenyl)-4,4a,5,6,8,8a-hexahydropyrano[3,4-*d*][1,3]thiazin-2-yl]benzamide (33b).**

To a magnetically stirred solution of **32b** (1680 mg, 3.76 mmol) and pyridine (1.09 mL, 13.5 mmol) in $CH_2Cl_2$ (67 mL, anhydrous) at -50 ºC (xylenes:dry ice bath, internal temperature) was added trifluoromethanesulfonic anhydride (1.27 mL, 7.52 mmol) in a drop-wise fashion and then the reaction mixture was gradually warmed to 0 ºC over 90 min. The reaction mixture was partitioned between $CH_2Cl_2$ (150 mL) and water (100 mL). The phases were separated and the lower organic layer was washed with water (2 x 75 mL) followed by brine (1 x 75 mL). The organic layer was dried over $Na_2SO_4$, filtered, concentrated *in vacuo* and purified by flash chromatography ($SiO_2$, 80 g RediSep Gold Column, EtOAc/heptane, 0 to 35% over 23CV, 60 mL/min) to afford 1.42 g (88% yield) of **33b** as a solid. LC-MS *m/z* 429.1 [M+1]. $^1$H NMR (400 MHz, $CDCl_3$) δ 11.7-12.5 (v br s, 1H), 8.24 (br d, *J* = 7.6 Hz, 2H), 7.54-7.48 (m, 1H), 7.48-7.38 (m, 3H), 6.97-6.82 (m, 2H), 4.08 (br dd, *J* = 12.4 and 1.3 Hz, 1H), 3.80 (d, *J* = 12.3 Hz, 1H),

3.13-3.05 (m, 1H), 3.04-2.93 (m, 2H), 2.64 (dd, *J* = 12.8 and 2.6 Hz, 1H), 2.18-2.05 (m, 1H), 1.83-1.75 (m, 1H), 1.06-0.96 (m, 1H), 0.62-0.50 (m, 2H), 0.46-0.40 (m, 1H), 0.29-0.22 (m, 1H).

**(4a*R*,6*R*,8a*S*)-6-Cyclopropyl-8a-(2,4-difluorophenyl)-4,4a,5,6,8,8a-hexahydropyrano[3,4-*d*][1,3]thiazin-2-amine (34).**

To a solution of **33b** (480 mg, 1.12 mmol) in methanol (20 mL) was added DBU (95%, 130 μL, 0.83 mmol) and heated to 80 °C for 9 h. The reaction mixture was cooled and concentrated *in vacuo*, then partitioned between $CH_2Cl_2$ (100 mL) and water (40 mL). The organic layer was dried over $Na_2SO_4$, filtered, and concentrated *in vacuo*. The residue was purified via flash chromatography ($SiO_2$, MeOH/$CH_2Cl_2$, 0 to 15%) to provide ***rac*-34**, which was separated into its enantiomers using supercritical fluid chromatography (Column: Phenomenex Lux® Cellulose-4, 5 μm; Eluent: 7:3 carbon dioxide / methanol containing 0.2% isopropylamine). The first-eluting enantiomer provided 147 mg (40% yield) as a pale yellow solid. The indicated absolute stereochemistry was assigned to compound **34** on the basis of this compound's biological activity; its enantiomer proved essentially inactive. Yield: 147 mg, 0.453 mmol, 40%. LCMS *m/z* 325.2 [M+H+]. $^1$H NMR (400 MHz, $CDCl_3$) δ 7.36 (ddd, *J* = 9, 9 and 6.7 Hz, 1H), 6.89-6.82 (m, 1H), 6.78 (ddd, *J* = 12.4, 8.6 and 2.6 Hz, 1H), 4.01 (dd, *J* = 11.0 and 2.4 Hz, 1H), 3.79 (d, *J* = 11.2 Hz, 1H), 2.95 (dd, *J* = 12.2 and 4.2 Hz, 1H), 2.90-2.79 (m, 2H), 2.60 (dd, *J* = 12.3 and 2.7 Hz, 1H), 2.00-1.88 (m, 1H), 1.61 (ddd, *J* = 13.4, 4.1 and 2.2 Hz, 1H), 1.05-0.95 (m, 1H), 0.60-0.48 (m, 2H), 0.46-0.39 (m, 1H), 0.26-0.19 (m, 1H). $[\alpha]^{25.4}{}_D$ = + 19.6 (c = 0.355, MeOH)

***N*-[(4a*R*,6*R*,8a*S*)-8a-(2,4-Difluorophenyl)-6-(hydroxymethyl)-4,4a,5,6,8,8a-hexahydropyrano[3,4-*d*][1,3]thiazin-2-yl]benzamide (35).**

To a solution of *N*-[(4a*R*,6*R*,8a*S*)-6-[(benzyloxy)methyl]-8a-(2,4-difluorophenyl)-4,4a,5,6,8,8a-hexahydropyrano[3,4-*d*][1,3]thiazin-2-yl]benzamide (**33a**) (255 mg, 0.501 mmol) in EtOAc (8 mL) was added sodium bromate (378 mg, 2.5 mmol in 7 mL water). The reaction mixture was cooled to 0 $^{o}$C and was then added drop-wise to a vigorously stirred biphasic mixture of sodium dithionate (436 mg 2.5 mmol) in 12 mL water over 10 minutes. The yellow/orange mixture was removed from the ice bath and stirred at rt for 1.5 h. The mixture was diluted with EtOAc (15 mL) and water (10 mL). The layers were separated and the EtOAc phase washed with saturated aq sodium thiosulfate (10 mL). The color was completely discharged, and then brine (15 mL) was added. The EtOAc phase was dried ($Na_2SO_4$), filtered, and concd *in vacuo*. Purification by flash chromatography ($SiO_2$, 12 g, EtOAc/heptane, 0 to 100%) afforded 134 mg (64%) of **35** as a white solid. LCMS *m/z* 419.3 [M+1H+]. $^1$H NMR (400 MHz, CHLOROFORM-*d*) d ppm 8.20 (d, *J* = 7.4 Hz, 2H) 7.34 - 7.54 (m, 4H) 6.83 - 6.95 (m, 2H) 4.16 (dd, *J* = 12.1, 1.6 Hz, 1H) 3.77 - 3.85 (m, 2H) 3.60 - 3.70 (m, 2H) 3.11 - 3.19 (m, 1H) 3.00 (dd, *J* = 13.0, 4.2 Hz, 1H) 2.63 (dd, *J* = 12.9, 2.7 Hz, 1H) 1.94 - 2.05 (m, 1H) 1.58 (ddd, *J* = 13.5, 4.3, 2.2 Hz, 1H).

***tert*-Butyl [(4a*R*,6*R*,8a*S*)-8a-(2,4-difluorophenyl)-6-(hydroxymethyl)-4,4a,5,6,8,8a-hexahydropyrano[3,4-*d*][1,3]thiazin-2-yl]carbamate (35').**

A mixture of **33a'** (83.9 g, 134 mmol) in concd HCl (1.2 L) was heated to 120 °C for 3 h. The reaction mixture was removed from heat and allowed to cool to rt. Analysis by TLC (1:1 EtOAc/heptane) indicated that two more polar substances were present. The major product was the desired debenzylated substance, together with a minor amount of doubly deprotected material, which all precipitated from the aqueous phase. The aqueous HCl was decanted to afford

a gum. The gum was taken up in EtOAc and carefully basified with sat. aqueous bicarbonate. The aqueous phase was extracted with EtOAc (three times). The combined EtOAc extracts were washed with $H_2O$, brine, and then dried over $Na_2SO_4$. The organic phase was concentrated *in vacuo* to afford a yellow foam, which was used directly in the next step. Yield 65.4 g, 91%. LC-MS *m/z* 537.6 (M+1).

The product (65.4 g 122 mmol) from the previous reaction was taken up in DMF (80 mL), followed by the addition of piperidine (40 mL). The reaction mixture was stirred at rt for 1 hour. Analysis by TLC (1:1 EtOAc/heptane or 10% MeOH/$CH_2Cl_2$) indicated that starting material had been consumed. The mixture was concentrated to a lesser volume and saturated aqueous sodium bicarbonate solution was added, followed by extraction with EtOAc (4x). The EtOAc extracts were combined and washed with $H_2O$ and with brine, followed by drying over $Na_2SO_4$. The organic phase was concentrated to dryness. The residue was triturated in $CH_2Cl_2$ and then filtered, and the product was air-dried. [(4a*R*,6*R*,8a*S*)-2-Amino-8a-(2,4-difluorophenyl)-4,4a,5,6,8,8a-hexahydropyrano[3,4-*d*][1,3]thiazin-6-yl]methanol was recovered as a white solid. Yield: 29.5 g, 77 %. LC-MS *m/z* 315.5 (M+1). $^1$H NMR (400 MHz, $CDCl_3$) δ 7.32 (m, *J* = 8.8, 8.8, 6.9 Hz, 1H), 6.74 - 6.88 (m, 2H), 4.09 (m, 1H), 3.80 (d, *J* = 11.1 Hz, 1H), 3.70 - 3.78 (m, 1H), 3.58 - 3.69 (m, 2H), 2.87 - 2.98 (m, 2H), 2.56 - 2.63 (m, 1H), 1.79 - 1.91 (m, 1H), 1.35 - 1.43 (m, 1H).

To a solution of [(4a*R*,6*R*,8a*S*)-2-amino-8a-(2,4-difluorophenyl)-4,4a,5,6,8,8a-hexahydropyrano[3,4-*d*][1,3]thiazin-6-yl]methanol (29.5 g, 93.8 mmol) in a mixture of THF (295 mL) and MeOH (135 mL) was added triethylamine (21.1 mL, 150 mmol) followed by addition of *t*-BOC anhydride in one portion. The reaction mixture was stirred at rt for 18 h. Analysis by TLC (10% MeOH/$CH_2Cl_2$ or 1:1 EtOAc/hexane) indicated a new less polar spot

which was UV active. The reaction mixture was concentrated *in vacuo* and the residue was taken up in EtOAc, washed with $H_2O$ and saturated brine, and then the solution was dried over $Na_2SO_4$, and concentrated *in vacuo*. The residue was triturated in a minimum volume of $CH_2Cl_2$ and the product was isolated by filtration. The triturated material was still impure, containing a minor amount of less polar material and baseline material. The product was chromatographed (SIM) on a 12 g CombiFlash column eluting with 50-100% EtOAc/heptane gradient. After evaporation of the eluent, **35'** was obtained as a white solid. Yield: 32.3 g, 83%. LC-MS *m/z* 415.2 (M+1). $^1$H NMR (400 MHz, $CD_3OD$) δ 7.30 - 7.38 (m, 1H), 6.98 - 7.06 (m, 2H), 4.05 - 4.11 (m, 1H), 3.79 (d, *J* = 11.9 Hz, 1H), 3.67 - 3.75 (m, 1H), 3.56 (d, *J* = 5.1 Hz, 2H), 3.02 - 3.15 (m, 1H), 2.85 - 2.94 (m, 1H), 2.65 - 2.73 (m, 1H), 1.68 - 1.82 (m, 1H), 1.57 - 1.67 (m, 1H), 1.47-1.50 (m, 9H).

**(4a*R*,6*R*,8a*S*)-8a-(2,4-Difluorophenyl)-6-(fluoromethyl)-4,4a,5,6,8,8a-hexahydropyrano[3,4-*d*][1,3]thiazin-2-amine (36).**

Diethylaminosulfur trifluoride (DAST) (2.39 mL, 18.1 mmol) was dissolved in a mixture of pentane (78 mL) and $CH_2Cl_2$ (49 mL) at room temperature in a 1000 mL round bottomed flask equipped with addition funnel and $N_2$ inlet. The alcohol **35'** (5.0 g, 12 mmol) dissolved in a mixture of pentane (60 mL) and $CH_2Cl_2$ (105 mL) was added drop-wise to the DAST solution. The reaction was stirred at room temperature for 18 h. Analysis by TLC (1:1 EtOAc/heptane) showed a new less polar spot with no starting material evident at this point (however a small amount of starting material was recovered at the end of the workup). The organic reaction mixture was treated with an equal volume of sat. aqueous bicarbonate solution followed by extraction with $CH_2Cl_2$ (three times) and then the organic phase was dried over $Na_2SO_4$, and evaporated *in vacuo*. The crude residue was chromatographed (SIM) on a 330 g gold column

eluting with a 0-25% EtOAc/heptane gradient. Evaporation of the eluent afforded *tert*-butyl [(4a*R*,6*R*,8a*S*)-8a-(2,4-difluorophenyl)-6-(fluoromethyl)-4,4a,5,6,8,8a-hexahydropyrano[3,4-*d*][1,3]thiazin-2-yl]carbamate as a white solid. Yield: 2.54 g, 50.6%. For safety reasons in using DAST, five separate reactions on a 5.0 g scale were run using the preceding conditions and the products were combined to afford additional quantities of *tert*-butyl [(4a*R*,6*R*,8a*S*)-8a-(2,4-difluorophenyl)-6-(fluoromethyl)-4,4a,5,6,8,8a-hexahydropyrano[3,4-*d*][1,3]thiazin-2-yl]carbamate. Yield: 12.7 g, 51%. LC-MS *m/z* 415.4 (M-1). $^1$H NMR (400 MHz, $CDCl_3$), δ 7.36-7.28 (m, 1H), 6.96-6.89 (m, 1H), 6.85 (ddd, *J* = 12.4, 8.4 and 2.4 Hz, 1H), 4.50 (ddd, half of ABXY pattern, *J* = 47.7, 9.9 and 6.4 Hz, 1H), 4.42 (ddd, half of ABXY pattern, *J* = 46.7, 9.9 and 3.6 Hz, 1H), 4.15 (dd, *J* = 11.9 and 1.9 Hz, 1H), 3.91-4.03 (m, 1H), 3.79 (br d, *J* = 12 Hz, 1H), 3.10-3.01 (br m, 1H), 2.93 (dd, *J* = 12.9 and 3.8 Hz, 1H), 2.57 (dd, *J* = 12.9 and 2.8 Hz, 1H), 1.99-1.87 (m, 1H), 1.53 (s, 9H).

A solution of *tert*-butyl [(4a*R*,6*R*,8a*S*)-8a-(2,4-difluorophenyl)-6-(fluoromethyl)-4,4a,5,6,8,8a-hexahydropyrano[3,4-*d*][1,3]thiazin-2-yl]carbamate (24.0 g, 57.6 mmol) in $CH_2Cl_2$ (696 mL) was cooled to 0 $^o$C and was treated with trifluoroacetic acid (TFA) (80 mL, 1100 mmol). The reaction mixture was allowed to warm to rt and was then stirred for 4 hours. Analysis by TLC (1:1 EtOAc/heptane or 10% MeOH/$CH_2Cl_2$) indicated that starting material was consumed. The mixture was diluted with EtOAc and then carefully basified with sat. aqueous bicarbonate solution. It was found that the aqueous bicarbonate solution was not sufficiently basic to neutralize the TFA salt of the thioamidine and thus the aqueous layer was treated with solid NaOH until the aqueous phase pH was above 10. The mixture was separated and the aqueous layer was extracted twice more with EtOAc. The combined EtOAc extracts were washed with $H_2O$, brine and then dried over $Na_2SO_4$. The organic phase was concentrated *in vacuo*. The

product was chromatographed (SIM) on a 330 g gold column eluting with a 0-10% MeOH/$CH_2Cl_2$ gradient. Fractions containing the product were concentrated *in vacuo* to afford **36** as a white solid. Yield: 17.3 g, 95%. LC-MS *m/z* 317.2 (M+1). $^1$H NMR (600 MHz, DMSO-$d_6$) δ 7.41-7.36 (m, 1H), 7.34-7.28 (m, 1H), 7.26-7.21 (m, 1H), 4.57-4.38 (m, 2H), 4.01-3.92 (m, 2H), 3.88 (d, half of AB quartet, $J$ = 12.3 Hz, 1H), 3.21-3.14 (m, 1H), 3.02 (br d, $J$ = 13 Hz, 1H), 2.88 (dd, $J$ = 13.2 and 3.5 Hz, 1H), 1.66-1.72 (m, 1H), 1.56-1.64 (m, 1H). $[\alpha]^{25.4}{}_D$ = -2.20 (c = 0.355, MeOH). The structure of this compound was further confirmed by generating a single-crystal X-ray structure (see Supporting Information).

**_N_-[(4a_R_,6_R_,8a_S_)-8a-(2,4-Difluorophenyl)-6-formyl-4,4a,5,6,8,8a-hexahydropyrano[3,4-_d_][1,3]thiazin-2-yl]benzamide (37).**

To a solution of **35** (19 g, 45 mmol) in $CH_2Cl_2$ (908 mL) in a rt water bath was added triethylamine (75.9 mL, 545 mmol). After 5 minutes, dimethyl sulfoxide (45.2 mL, 636 mmol) was rapidly added, immediately followed by sulfur trioxide pyridine complex (98%, 59.0 g, 363 mmol) in a single portion. The resulting solution was stirred at rt for 4 h, whereupon it was diluted with a 1:1 mixture of saturated aqueous NaCl and water, and stirred for 10 minutes. The aqueous layer was extracted with $CH_2Cl_2$ (2x) and the combined organic layers were washed with water until the pH of the aqueous extract was pH 6 – 7, then were washed with 0.2 N HCl (2x), and once with saturated aqueous NaCl. After being dried over $Na_2SO_4$, the organic layer was filtered and concentrated *in vacuo*. Purification by flash chromatography ($SiO_2$, EtOAc/heptane, 0 to 100%) provided 13.27 g (71% yield) of **37** as a pale yellow solid. $^1$H NMR (400 MHz, $CDCl_3$) δ 9.71 (br s, 1H), 8.24-8.16 (m, 2H), 7.56-7.50 (m, 1H), 7.48-7.36 (m, 3H), 6.98-6.87 (m, 2H), 4.23 (dd, $J$ = 12.2 and 1.6 Hz, 1H), 4.15-4.09 (m, 1H), 3.94 (d, $J$ = 12.1 Hz,

1H), 3.22-3.13 (m, 1H), 3.04 (dd, *J* = 13.1 and 4.0 Hz, 1H), 2.69 (dd, *J* = 13.0 and 2.9 Hz, 1H), 2.15-2.02 (m, 1H), 1.99-1.92 (m, 1H).

**(4a*R*,6*R*,8a*S*)-6-(Difluoromethyl)-8a-(2,4-difluorophenyl)-4,4a,5,6,8,8a-hexahydropyrano[3,4-*d*][1,3]thiazin-2-amine (38).**

To a solution of **37** (previously azeotroped twice with 5 mL of toluene; 3.30 g, 7.92 mmol) in $CH_2Cl_2$ (80 mL) cooled to -20 °C was added (diethylamino)sulfur trifluoride (2.62 mL, 19.8 mmol) drop-wise over 7 minutes and the reaction mixture was allowed to slowly warm to rt. After 5 h at rt, it was cooled to 0 °C, diluted with saturated aqueous sodium bicarbonate (45 mL), and extracted with $CH_2Cl_2$ (3 x 40 mL). The combined organic layers were dried over $Na_2SO_4$, filtered, and concentrated *in vacuo*. Purification by flash chromatography ($SiO_2$, EtOAc/heptane, 0 to 80%) provided 2.03 g (58% yield) of *N*-[(4a*R*,6*R*,8a*S*)-6-(difluoromethyl)-8a-(2,4-difluorophenyl)-4,4a,5,6,8,8a-hexahydropyrano[3,4-*d*][1,3]thiazin-2-yl]benzamide as a white solid. $^1$H NMR (400 MHz, $CD_3OD$) δ 8.12 (br d, *J* = 7 Hz, 2H), 7.58-7.51 (m, 1H), 7.50-7.42 (m, 3H), 7.12-7.02 (m, 2H), 5.83 (td, *J* = 55.4 and 4.3 Hz, 1H), 4.17 (br d, *J* = 12 Hz, 1H), 3.95 (d, *J* = 12.1 Hz, 1H), 4.02-3.91 (m, 1H), 3.26-3.16 (m, 1H), 2.97 (dd, *J* = 13 and 4 Hz, 1H), 2.79 (dd, *J* = 12.9 and 2.7 Hz, 1H), 2.08-1.96 (m, 1H), 1.85-1.77 (m, 1H).

To a solution of *N*-[(4a*R*,6*R*,8a*S*)-6-(difluoromethyl)-8a-(2,4-difluorophenyl)-4,4a,5,6,8,8a-hexahydropyrano[3,4-*d*][1,3]thiazin-2-yl]benzamide (2000 mg, 4.56 mmol) in methanol (20 mL) was added DBU (718 µL, 4.56 mmol). The reaction mixture was heated to 68 ºC for 18 h. The reaction mixture was then cooled slightly and concentrated *in vacuo*. The residue was purified using flash chromatography ($SiO_2$, 40 g gold column, EtOAc/heptanes 15 to 100%) to afford 1.46 g (96% yield) of **38** as a white solid. LC-MS *m/z* 335.1 [M+1]. $^1$H NMR (400 MHz,

$CD_3OD$) δ 7.35 (ddd, *J* = 9, 9 and 7 Hz, 1H), 7.01-6.93 (m, 2H), 5.77 (td, *J* = 55.6 and 3.9 Hz, 1H), 4.11 (dd, *J* = 11.1 and 2.0 Hz, 1H), 3.92-3.81 (m, 1H), 3.73 (d, *J* = 11.0 Hz, 1H), 2.97-2.87 (m, 2H), 2.75-2.69 (m, 1H), 1.99-1.88 (m, 1H), 1.66-1.59 (m, 1H). $[\alpha]^{27}{}_{D}$ = -2.13 (c 0.835 , MeOH)

**(4a*R*,6*S*,8a*S*)-8a-(2,4-Difluorophenyl)-6-ethyl-4,4a,5,6,8,8a-hexahydropyrano[3,4-*d*][1,3]thiazin-2-amine (39).**

To a magnetically stirred suspension of methyltriphenylphosphonium bromide (547 mg, 1.5 mmol) in THF (9 mL, anhydrous) at rt under a nitrogen atmosphere was added *t*-BuOK (1.0 M in THF, 1.5 mL, 1.5 mmol) in a drop-wise fashion. All solids dissolved and then the solution turned deep yellow/pale orange. A precipitate formed immediately thereafter and this mixture was stirred at rt for 1 h and was then cooled to -15 ºC (internal). A solution of **37** (312 mg, 0.75 mmol) in THF (3 mL, anhydrous) was added in a drop-wise fashion over 5 min. The internal temperature never exceeded -12 ºC. One minute after the addition was complete, the cooling bath was removed and the reaction was allowed to warm to rt over 20 min (21 ºC internal). The reaction mixture was stirred at rt for 10 min and then cooled to 0 ºC (external bath temp). The reaction was quenched by addition of saturated aq $NH_4Cl$ (15 mL) and the mixture was then extracted with EtOAc (2 x 25 mL). The combined organic extracts were dried over $Na_2SO_4$, filtered, and concentrated *in vacuo*. The crude residue was purified by flash chromatography ($SiO_2$, 24 g RediSep Gold, EtOAc/heptane, 0 to 25% over 20CV, 35 mL/min) to afford 256 mg (82% yield) of *N*-[(4a*R*,6*R*,8a*S*)-8a-(2,4-difluorophenyl)-6-vinyl-4,4a,5,6,8,8a-hexahydropyrano[3,4-*d*][1,3]thiazin-2-yl]benzamide as a white solid. LC-MS *m/z* 415 (M+1). $^1$H NMR (400 MHz, $CDCl_3$) δ 8.15 (d, *J* = 7.4 Hz, 2H), 7.48-7.29 (m, 4H), 6.90-6.74 (m, 2H), 5.84 (ddd, *J* = 17.3, 10.7 and 5.7 Hz, 1H), 5.33-5.21 (m, 1H), 5.11 (td, *J* = 10.7 and 1.2 Hz, 1H), 4.11

(dd, *J* = 12.1 and 1.8 Hz, 2H), 3.76 (d, *J* = 12.1 Hz, 1H), 3.18-3.05 (m, 1H), 2.95 (dd, *J* = 12.7 and 4.1 Hz, 1H), 2.64-2.50 (m, 1H), 2.08-1.91 (m, 1H), 1.72-1.61 (m, 1H).

A solution of *N*-[(4a*R*,6*R*,8a*S*)-8a-(2,4-difluorophenyl)-6-vinyl-4,4a,5,6,8,8a-hexahydropyrano[3,4-*d*][1,3]thiazin-2-yl]benzamide (50 mg. 0.12 mmol) in MeOH (35 mL) was placed in a 250 mL Parr bottle. The solution was treated with solid palladium on activated carbon (10 wt % dry basis, wet Degussa type E101 NE/W; 50 mg). The vessel was sealed, evacuated and then charged with $H_2$ (25 PSI) and mechanically shaken for 90 min. The reaction vessel was then evacuated and recharged with $N_2$ gas. The mixture was then carefully filtered through Celite and the filter cake washed with MeOH (30 mL). The combined filtrate was concentrated *in vacuo* to afford 50 mg (quantitative yield) of *N*-[(4a*R*,6*S*,8a*S*)-8a-(2,4-difluorophenyl)-6-ethyl-4,4a,5,6,8,8a-hexahydropyrano[3,4-*d*][1,3]thiazin-2-yl]benzamide as an off-white/pale yellow solid. LC-MS *m/z* 417 (M+1). $^1$H NMR (400 MHz, $CDCl_3$) δ 8.22 (d, *J* = 7.0 Hz, 2H), 7.32-7.55 (m, 4H), 6.79-6.97 (m, 2H), 4.10 (d, *J* = 12.1 Hz, 1H), 3.76 (d, *J* = 11.9 Hz, 1H), 3.45-3.58 (m, 1H), 3.04-3.18 (m, *J* = 10.0 Hz, 1H), 2.99 (dd, *J* = 3.8, 13.0 Hz, 1H), 2.62 (d, *J* = 12.5 Hz, 1H), 1.81-1.95 (m, 1H), 1.56-1.72 (m, 2H), 1.45-1.56 (m, 1H), 0.95 (t, *J* = 7.4 Hz, 3H).

To a solution of *N*-[(4a*R*,6*S*,8a*S*)-8a-(2,4-difluorophenyl)-6-ethyl-4,4a,5,6,8,8a-hexahydropyrano[3,4-*d*][1,3]thiazin-2-yl]benzamide (45 mg, 108 μmol) in MeOH (2 mL, anhydrous) was added DBU (13 μL, 82 μmol) in a sealed vial with magnetic stirring and heated to 80 ºC. The mixture soon became a complete solution and the reaction was stirred at 80 ºC for 18 h. The solvent was removed using $N_2$ flow and the residue was partitioned between $CH_2Cl_2$ (12 mL) and water (4 mL). The $CH_2Cl_2$ layer was dried over $Na_2SO_4$, filtered through cotton and purified using flash chromatography ($SiO_2$, 4 g RediSep Gold Column, MeOH/$CH_2Cl_2$, 0 to 15%

over 15 min, 18 mL/min) to afford 20.2 mg (58% yield) of **39** as a white foam (20.2 mg, 58%). LCMS *m/z* 313 (M+1). $^1$H NMR (400 MHz, $CDCl_3$) δ 7.28 (dt, *J* = 9.0 and 6.6 Hz, 1H), 6.83-6.66 (m, 2H), 3.98 (dd, *J* = 11.0 and 2.5 Hz, 1H), 3.70 (d, *J* = 11.2 Hz, 1H), 3.46-3.35 (m, 1H), 2.88 (dd, *J* = 12.2 and 4.2 Hz, 1H), 2.84-2.75 (m, 1H), 2.52 (dd, *J* = 12.1 and 2.7 Hz, 1H), 1.71-1.51 (m, 2H), 1.50-1.37 (m, 2H), 0.96-0.85 (m, 3H).

**(4a*R*,6*S*,8a*S*)-8a-(2,4-Difluorophenyl)-6-(2-methylpropyl)-4,4a,5,6,8,8a-hexahydropyrano[3,4-*d*][1,3]thiazin-2-amine (40).**

To a suspension of triphenyl(propan-2-yl)phosphonium iodide (1.08 g, 2.50 mmol) in THF (10 mL) at 0 °C was added *n*-BuLi (2.5 M in hexanes, 0.90 mL, 2.25 mmol) in a drop-wise fashion. The resulting solution was stirred and allowed to warm to rt over 30 minutes, whereupon it was cooled to 0 °C. A solution of **37** (104 mg, 0.250 mmol) in THF (1 mL) was added, and stirring was continued at 0 °C for 1 h, then at rt for 3 h. The reaction mixture was diluted with EtOAc (20 mL), washed with saturated aqueous sodium bicarbonate (3 x 20 mL), washed with water (20 mL), dried over $Na_2SO_4$, filtered, and concentrated *in vacuo*. Purification by flash chromatography ($SiO_2$, EtOAc/heptane, 0 to 30%) afforded 42 mg (38% yield) of *N*-[(4a*R*,6*R*,8a*S*)-8a-(2,4-difluorophenyl)-6-(2-methylprop-1-en-1-yl)-4,4a,5,6,8,8a-hexahydropyrano[3,4-*d*][1,3]thiazin-2-yl]benzamide as a white solid. LC-MS *m/z* 443.3 [M+1]. $^1$H NMR (400 MHz, $CDCl_3$) δ 11.8 (v br s, 1H), 8.24 (d, *J* = 7.4 Hz, 2H), 7.55-7.38 (m, 4H), 6.97-6.85 (m, 2H), 5.27 (d, *J* = 8 Hz, 1H), 4.40-4.31 (m, 1H), 4.19 (d, *J* = 12.1 Hz, 1H), 3.80 (d, *J* = 12.1 Hz, 1H), 3.22-3.13 (m, 1H), 3.06-2.98 (m, 1H), 2.68-2.59 (m, 1H), 2.13-2.00 (m, 1H), 1.75 (s, 6H), 1.67-1.59 (m, 1H). $[\alpha]^{25.9}{}_D$ = -5.59 (c = 0.340, MeOH).

To a solution of *N*-[(4a*R*,6*R*,8a*S*)-8a-(2,4-difluorophenyl)-6-(2-methylprop-1-en-1-yl)-4,4a,5,6,8,8a-hexahydropyrano[3,4-*d*][1,3]thiazin-2-yl]benzamide (42 mg, 95 μmol) in MeOH (28 mL) in a Parr bottle was added palladium on activated carbon [10% by weight (dry), 50% water, 224 mg, 105 μmol]. The reaction mixture was charged with hydrogen gas (35 PSI) and mechanically shaken for 20 h. The reaction mixture was then filtered through Celite, and the filter pad was rinsed with MeOH (30 mL). The combined filtrates were concentrated *in vacuo* and purified by flash chromatography ($SiO_2$, EtOAc/heptanes, 0 to 30%) to afford 10.9 mg (26% yield) of *N*-[(4a*R*,6*S*,8a*S*)-8a-(2,4-difluorophenyl)-6-(2-methylpropyl)-4,4a,5,6,8,8a-hexahydro-pyrano[3,4-*d*][1,3]thiazin-2-yl]benzamide as an opaque semi-solid. LC-MS *m/z* 445.2 [M+1]. $^1$H NMR (400 MHz, $CDCl_3$) δ 8.24 (br d, *J* = 8 Hz, 2H), 7.54-7.48 (m, 1H), 7.48-7.37 (m, 3H), 6.96-6.84 (m, 2H), 4.11 (dd, *J* = 12.2 and 1.5 Hz, 1H), 3.77 (d, *J* = 12.1 Hz and 1H), 3.72-3.64 (m, 1H), 3.17-3.09 (m, 1H), 3.01 (dd, *J* = 12.7 and 4.1 Hz, 1H), 2.63 (dd, *J* = 12.7 and 2.7 Hz, 1H), 1.97-1.86 (m, 1H), 1.87-1.76 (m, 1H), 1.65-1.55 (m, 2H), 1.31-1.23 (m,1H), 0.93 (d, *J* = 6.5 Hz, 3H), 0.92 (d, *J* = 6.6 Hz, 3H).

To a solution of *N*-[(4a*R*,6*S*,8a*S*)-8a-(2,4-difluorophenyl)-6-(2-methylpropyl)-4,4a,5,6,8,8a-hexahydro-pyrano[3,4-*d*][1,3]thiazin-2-yl]benzamide (10.5 mg, 23.6 μmol) in MeOH (0.4 mL) was added DBU (3.0 μL, 20 μmol) and the reaction mixture was heated to 60 °C for 18 h in a sealed vial. Solvent was removed under a stream of nitrogen, and the residue was partitioned between water (3 mL) and EtOAc (5 mL). The aqueous layer was extracted with EtOAc (5 mL), and the combined organic layers were dried over $Na_2SO_4$, filtered, and concentrated *in vacuo*. Purification by reversed phase high-performance liquid chromatography (Column: Waters XBridge C18, 5 μm; Mobile phase A: 0.03% ammonium hydroxide in water (v/v); Mobile phase B: 0.03% ammonium hydroxide in acetonitrile (v/v); Gradient: 30% to 100% B) afforded 4.2 mg

(51% yield) of **40**. LC-MS *m/z* 341.1 [M+1]. $^1$H NMR (600 MHz, DMSO-d6) δ 7.36-7.31 (m, 1H), 7.20-7.15 (m, 1H), 7.08 (ddd, *J* = 9, 8 and 2 Hz, 1H), 3.86 (dd, *J* = 10.5 and 1.8 Hz, 1H), 3.54 (d, *J* = 10.5 Hz, 1H), 3.56-3.50 (m, 1H), 2.73-2.62 (m, 3H), 1.79-1.71 (m, 1H), 1.60-1.52 (m, 1H), 1.50-1.45 (m, 1H), 1.40 (ddd, *J* = 14, 8, and 6 Hz, 1H), 1.21 (ddd, *J* = 14, 8, and 4.5 Hz, 1H), 0.89 (d, *J* = 6.1 Hz, 3H), 0.88 (d, *J* = 6.6 Hz, 3H).

**_N_-[(4a_R_,6_R_,8a_S_)-6-(Chloromethyl)-8a-(2,4-difluorophenyl)-4,4a,5,6,8,8a-hexahydropyrano[3,4-_d_][1,3]thiazin-2-yl]benzamide (41).**

To a solution of **35** (2.0 g, 4.8 mmol) in toluene (68 mL) was added thionyl chloride (10.4 mL, 143 mmol), and the reaction mixture was heated to 80 °C for 18 h. After cooling to rt, it was concentrated *in vacuo* and azeotroped with $CH_2Cl_2$ (3x). The residue was dissolved in $CH_2Cl_2$, washed with saturated aqueous NaCl, dried over $Na_2SO_4$, filtered, and concentrated *in vacuo*. Purification by flash chromatography ($SiO_2$, EtOAc/heptanes, 0 to 100%) provided 1.88 g (90% yield) of **41** as an off-white solid. LC-MS *m/z* 437.1 [M+H+]. $^1$H NMR (400 MHz, $CD_3OD$) δ 8.12-8.08 (m, 2H), 7.65-7.59 (m, 1H), 7.55-7.46 (m, 3H), 7.17-7.05 (m, 2H), 4.18 (dd, *J* = 12.2 and 1.3 Hz, 1H), 4.01 (d, *J* = 12.3 Hz, 1H), 3.98-3.91 (m, 1H), 3.69-3.61 (m, 2H), 3.3-3.26 (m, 1H, assumed; partially obscured by solvent peak), 3.07 (br dd, *J* = 13.3 and 3.7 Hz, 1H), 2.91 (br dd, *J* = 13.3 and 2.5 Hz, 1H), 1.93-1.86 (m, 2H).

**(4a_R_,6_S_,8a_S_)-8a-(2,4-Difluorophenyl)-6-methyl-4,4a,5,6,8,8a-hexahydropyrano[3,4-_d_][1,3]thiazin-2-amine (42).**

To a solution of **41** (1.88 g, 4.30 mmol) in THF cooled to 0 °C was added lithium triethylborohydride (1 M in tetrahydrofuran, 34.4 mL, 34.4 mmol) in a drop-wise fashion, and the reaction mixture was allowed to warm to rt. After 18 h, the reaction mixture was partitioned

between aqueous sodium bicarbonate solution and EtOAc. The aqueous layer was extracted twice with EtOAc, and the combined organic layers were dried over $Na_2SO_4$, filtered, and concentrated *in vacuo*. Purification using flash chromatography ($SiO_2$, MeOH/$CH_2Cl_2$, 0 to 10%) afforded 1.4 g (81% yield) of *N*-[(4a*R*,6*S*,8a*S*)-8a-(2,4-difluorophenyl)-6-methyl-4,4a,5,6,8,8a-hexahydropyrano[3,4-*d*][1,3]thiazin-2-yl]benzamide as a white solid. LC-MS *m/z* 403.1 [M+1]. $^1$H NMR (400 MHz, $CDCl_3$) δ 12.29 (br s, 1H), 8.30-8.19 (br m, 2H), 7.54-7.48 (m, 1H), 7.48-7.37 (m, 3H), 6.96-6.84 (m, 2H), 4.15 (dd, *J* = 12.2 and 2.0 Hz, 1H), 3.84-3.77 (m, 1H), 3.77 (d, *J* = 12.3 Hz, 1H), 3.19-3.09 (br m, 1H), 3.01 (dd, *J* = 12.9 and 4.1 Hz, 1H), 2.63 (dd, *J* = 12.8 and 2.8 Hz, 1H), 2.00-1.88 (m, 1H), 1.69-1.62 (m, 1H), 1.30 (d, *J* = 6.2 Hz, 3H).

To a suspension of *N*-[(4a*R*,6*S*,8a*S*)-8a-(2,4-difluorophenyl)-6-methyl-4,4a,5,6,8,8a-hexahydropyrano[3,4-*d*][1,3]thiazin-2-yl]benzamide (1.40 g, 3.48 mmol) in MeOH (100 mL) was added DBU (0.5 mL, 3 mmol), and the resulting mixture was heated to 80 °C for 18 h. After concentration *in vacuo*, the residue was partitioned between saturated aqueous sodium bicarbonate and EtOAc, and the aqueous layer was extracted with EtOAc, and the combined organic layers were washed with saturated aqueous NaCl, dried over $Na_2SO_4$, filtered, and concentrated *in vacuo*. Purification via flash chromatography ($SiO_2$, EtOAc) afforded 840 mg (81% yield) of **42** as a white solid. LC-MS *m/z* 299.2 [M+1]. $^1$H NMR (400 MHz, $CD_3OD$) δ 7.38-7.30 (m, 1H), 7.00-6.92 (m, 2H), 4.08 (dd, *J* = 11.1 and 2.2 Hz, 1H), 3.78-3.69 (m, 1H), 3.65 (d, *J* = 11.1 Hz, 1H), 2.93-2.83 (m, 2H), 2.68-2.62 (m, 1H), 1.76-1.65 (m, 1H), 1.54 (ddd, *J* = 13.1, 4.1 and 2.4 Hz, 1H), 1.22 (d, *J* = 6.2 Hz, 3H). $[\alpha]^{27.4}{}_D$ = - 5.25 (c = 0.755, MeOH).

**(4a*R*,6*R*,8a*S*)-8a-(2,4-Difluorophenyl)-6-(methoxymethyl)-4,4a,5,6,8,8a-hexahydropyrano[3,4-*d*][1,3]thiazin-2-amine (43).**

A solution of **35** (300 mg, 0.717 mmol) in THF (2.5 mL) was added to a mixture of sodium hydride (60% in mineral oil, 60.2 mg, 1.51 mmol) in THF (5 mL), and the reaction mixture was stirred at rt for 25 min. To this was added iodomethane (44.7 μL, 0.717 mmol), and the reaction mixture was heated to 41 °C for 6 h, cooled back to rt, and quenched with saturated aqueous $NH_4Cl$ (15 mL). After extraction with EtOAc (3 x 20 mL), the combined organic layers were dried over $Na_2SO_4$, filtered, and concentrated *in vacuo*. Purification by flash chromatography ($SiO_2$, EtOAc/heptane, 0 to 50%) provided 214 mg (69% yield) of *N*-[(4a*R*,6*R*,8a*S*)-8a-(2,4-difluorophenyl)-6-(methoxymethyl)-4,4a,5,6,8,8a-hexahydropyrano[3,4-*d*][1,3]thiazin-2-yl]benzamide as a white solid. LC-MS *m/z* 329.0 (M+1). $^1$H NMR (400 MHz, $CD_3OD$) δ 8.12 (d, *J* = 7.0 Hz, 2H), 7.57-7.50 (m, *J* = 7.4 Hz, 1H), 7.49-7.38 (m, 3H), 7.12-6.99 (m, 2H), 4.16-4.09 (m, 1H), 3.94-3.80 (m, 2H), 3.58-3.40 (m, 2H), 3.37 (s, 3H), 3.23-3.11 (m, 1H), 3.01-2.90 (m, 1H), 2.74 (dd, *J* = 13.1 and 2.7 Hz, 1H), 1.94-1.79 (m, 1H), 1.75-1.64 (m, 1H) .

To a solution of *N*-[(4a*R*,6*R*,8a*S*)-8a-(2,4-difluorophenyl)-6-(methoxymethyl)-4,4a,5,6,8,8a-hexahydropyrano[3,4-*d*][1,3]thiazin-2-yl]benzamide (214 mg, 0.494 mmol) in MeOH (12 mL) was added DBU (95%, 62 μL, 0.396 mmol) and heated to 72 °C for 18 h. The reaction mixture was concentrated *in vacuo* and purified by flash chromatography ($SiO_2$, MeOH/$CH_2Cl_2$, 0% to 10%), to afford 118 mg (72% yield) of **43** as a white solid. LC-MS *m/z* 329.0 [M+H+]. $^1$H NMR (400 MHz, $CD_3OD$) δ 7.34 (ddd, *J* = 9, 9 and 7 Hz, 1H), 7.00-6.93 (m, 2H), 4.08 (dd, *J* = 11.1 and 2.2 Hz, 1H), 3.84-3.77 (m, 1H), 3.69 (d, *J* = 11.1 Hz, 1H), 3.47 (dd, half of ABX pattern, *J* = 10.4 and 6.6 Hz, 1H), 3.41 (dd, half of ABX pattern, *J* = 10.4 and 4.0 Hz, 1H), 3.38 (s, 3H), 2.95-2.85 (m, 2H), 2.70-2.64 (m, 1H), 1.81-1.70 (m, 1H), 1.52 (ddd, *J* = 13.1, 4.1 and 2.4 Hz, 1H). $[\alpha]^{28.1}{}_D$ = -1.08 (c = 0.365, MeOH).

ACKNOWLEDGEMENTS.

The authors thank Subas Sakya and Ming Liu (WuXi AppTec) for synthetic expertise, Brian Samas for x-ray crystallography, David Karanian for toxicology expertise, and Bruce Rogers, Xinjun Hou, Katherine Brighty, and Pat Verhoest for helpful discussion in manuscript preparation. Use of the IMCA-CAT beamline 17-ID at the Advanced Photon Source was supported by the companies of the Industrial Macromolecular Crystallography Association through a contract with Hauptman-Woodward Medical Research Institute. Use of the Advanced Photon Source was supported by the U.S. Department of Energy, Office of Science, Office of Basic Energy Sciences, under Contract No. DE-AC02-06CH11357.

SUPPORTING INFORMATION

Exposure Data for in vivo mouse experiments, data collection and refinement statistics for crystal structures of BACE1 with **6**, **24b,** and **36** and preparation of intermediate compound **7** are available free of charge via the Internet at http://pubs.acs.org. Atomic coordinates and structure factors for the following BACE co-crystal structures have been deposited with the RCSB: compound **6** (PDB ID code 4X2L), compound **24b** (PDB ID code 4WY1) and compound **36** (PDB ID code 4WY6).

CORRESPONDING AUTHOR FOOTNOTE

* To whom correspondence should be addressed. Phone: 617 395 0670. E-mail: christopher.r.butler@pfizer.com

REFERENCES

1. Hardy, J.; Allsop, D. Amyloid Deposition as the Central Event in the Aetiology of Alzheimer's Disease. *Trends Pharmacol. Sci.* **1991,** *12*, 383.

2. Tanzi, R. E.; Bertram, L. Twenty Years of the Alzheimer's Disease Amyloid Hypothesis: A Genetic Perspective. *Cell* **2005,** *120*, 545.

3. De Strooper, B. Proteases and Proteolysis in Alzheimer Disease: A Multifactorial View on the Disease Process. *Physiol. Rev.* **2010,** *90*, 465-494.

4. Vassar, R.; Kovacs, D. M.; Yan, R.; Wong, P. C. The beta-Secretase Enzyme BACE in Health and Alzheimer's Disease: Regulation, Cell Biology, Function, and Therapeutic Potential. *J. Neurosci.* **2009,** *29*, 12787-12794.

5. Marks, N.; Berg, M. J. BACE and gamma-Secretase Characterization and Their Sorting as Therapeutic Targets to Reduce Amyloidogenesis. *Neurochem. Res.* **2010,** *35*, 181-210.

6. Jonsson, T.; Atwal, J. K.; Steinberg, S.; Snaedal, J.; Jonsson, P. V.; Bjornsson, S.; Stefansson, H.; Sulem, P.; Gudbjartsson, D.; Maloney, J.; Hoyte, K.; Gustafson, A.; Liu, Y.; Lu, Y.; Bhangale, T.; Graham, R. R.; Huttenlocher, J.; Bjornsdottir, G.; Andreassen, O. A.; Jonsson, E. G.; Palotie, A.; Behrens, T. W.; Magnusson, O. T.; Kong, A.; Thorsteinsdottir, U.; Watts, R. J.; Stefansson, K. A Mutation in APP Protects Against Alzheimer's Disease and Age-Related Cognitive Decline. *Nature* **2012,** *488* (7409), 96-9.

7. Evin, G.; Hince, C. BACE1 as a Therapeutic Target in Alzheimer's Disease: Rationale and Current Status. *Drugs Aging* **2013,** *30*, 755-764.

8. Yuan, J.; Venkatraman, S.; Zheng, Y.; McKeever, B. M.; Dillard, L. W.; Singh, S. B. Structure-Based Design of β-Site APP Cleaving Enzyme 1 (BACE1) Inhibitors for the Treatment of Alzheimer's Disease. *J. Med. Chem.* **2013,** *56*, 4156-4180.

9. Woltering, T. J.; Wostl, W.; Hilpert, H.; Rogers-Evans, M.; Pinard, E.; Mayweg, A.; Gobel, M.; Banner, D. W.; Benz, J.; Travagli, M.; Pollastrini, M.; Marconi, G.; Gabellieri, E.; Guba, W.; Mauser, H.; Andreini, M.; Jacobsen, H.; Power, E.; Narquizian, R. BACE1 Inhibitors: a Head Group Scan on a Series of Amides. *Bioorg. Med. Chem. Lett.* **2013,** *23*, 4239-43.

10. Brodney, M. A.; Barreiro, G.; Ogilvie, K.; Hajos-Korcsok, E.; Murray, J.; Vajdos, F.; Ambroise, C.; Christoffersen, C.; Fisher, K.; Lanyon, L.; Liu, J.; Nolan, C. E.; Withka, J. M.; Borzilleri, K. A.; Efremov, I.; Oborski, C. E.; Varghese, A.; O'Neill, B. T. Spirocyclic Sulfamides as β-Secretase 1 (BACE-1) Inhibitors for the Treatment of Alzheimer's Disease: Utilization of Structure Based Drug Design, WaterMap, and CNS Penetration Studies to Identify Centrally Efficacious Inhibitors. *J. Med. Chem.* **2012,** *55*, 9224-9239.

11. Johnson, T. W.; Richardson, P. F.; Bailey, S.; Brooun, A.; Burke, B. J.; Collins, M. R.; Cui, J. J.; Deal, J. G.; Deng, Y.-L.; Dinh, D.; Engstrom, L. D.; He, M.; Hoffman, J.; Hoffman, R. L.; Huang, Q.; Kania, R. S.; Kath, J. C.; Lam, H.; Lam, J. L.; Le, P. T.; Lingardo, L.; Liu, W.; McTigue, M.; Palmer, C. L.; Sach, N. W.; Smeal, T.; Smith, G. L.; Stewart, A. E.; Timofeevski, S.; Zhu, H.; Zhu, J.; Zou, H. Y.; Edwards, M. P. Discovery of (10*R*)-7-Amino-12-fluoro-2,10,16-trimethyl-15-oxo-10,15,16,17-tetrahydro-2*H*-8,4-(metheno)pyrazolo[4,3-*h*][2,5,11]-benzoxadiazacyclotetradecine-3-carbonitrile (PF-06463922), a Macrocyclic Inhibitor of Anaplastic Lymphoma Kinase (ALK) and c-ros Oncogene 1 (ROS1) with Preclinical Brain Exposure and Broad-Spectrum Potency against ALK-Resistant Mutations. *J. Med. Chem.* **2014,** *57*, 4720-4744.

12. May, P. C.; Dean, R. A.; Lowe, S. L.; Martenyi, F.; Sheehan, S. M.; Boggs, L. N.; Monk, S. A.; Mathes, B. M.; Mergott, D. J.; Watson, B. M.; Stout, S. L.; Timm, D. E.; Smith LaBell, E.; Gonzales, C. R.; Nakano, M.; Jhee, S. S.; Yen, M.; Ereshefsky, L.; Lindstrom, T. D.; Calligaro,

D. O.; Cocke, P. J.; Hall, D. G.; Friedrich, S.; Citron, M.; Audia, J. E. Robust Central Reduction of Amyloid-beta in Humans with an Orally Available, Non-peptidic beta-Secretase Inhibitor. *J. Neurosci.* **2011,** *31*, 16507-16.

13. (a) Müller, S.; Dennemärker, J.; Reinheckel, T. Specific Functions of Lysosomal Proteases in Endocytic and Autophagic Pathways. *Biochim. Biophys. Acta, Proteins Proteomics* **2012,** *1824* (1), 34-43; (b) Steinfeld, R.; Reinhardt, K.; Schreiber, K.; Hillebrand, M.; Kraetzner, R.; Brück, W.; Saftig, P.; Gärtner, J. Cathepsin D Deficiency Is Associated with a Human Neurodegenerative Disorder. *Am. J. Hum. Genet.* **2006,** *78*, 988-998.

14. (a) Tamura, Y.; Suzuki, S.; Tada, Y.; Yonezawa, S.; Fujikoshi, C.; Matsumoto, S.; Kooriyama, Y.; Ueno, T. Aminodihydrothiazine Derivatives Substituted with a Cyclic Group. U.S. Patent Application 2010/0075957 A1, March 25, 2010; (b) Oehlrich, D.; Prokopcova, H.; Gijsen, H. J. The Evolution of Amidine-Based Brain Penetrant BACE1 Inhibitors. *Bioorg. Med. Chem. Lett.* **2014,** *24*, 2033-45.

15. Hitchcock, S. A. Structural Modifications that Alter the P-glycoprotein Efflux Properties of Compounds. *J. Med. Chem.* **2012,** *55*, 4877-95.

16. (a) Wager, T. T.; Hou, X.; Verhoest, P. R.; Villalobos, A. Moving Beyond Rules: the Development of a Central Nervous System Multiparameter Optimization (CNS MPO) Approach to Enable Alignment of Druglike Properties. *ACS Chem. Neurosci.* **2010,** *1*, 435-49; (b) Wager, T. T.; Chandrasekaran, R. Y.; Hou, X.; Troutman, M. D.; Verhoest, P. R.; Villalobos, A.; Will, Y. Defining Desirable Central Nervous System Drug Space through the Alignment of Molecular Properties, in Vitro ADME, and Safety Attributes. *ACS Chem. Neurosci.* **2010,** *1*, 420-434.

17. A similar fragment was identified by the authors of reference 12 that lacked the fluoro groups on the aryl group.

18. Hori, A. Y., Shuji; Fujikoshi, Chiaki; Matumoto, Sae; Kooriyama, Yuuji; Ueno, Tatsuhiko; Kato, Terukazu U.S. Patent Application 2014/08637504 A1, April 15, 2014.

19. Robak, M. T.; Herbage, M. A.; Ellman, J. A. Synthesis and Applications of *tert*-Butanesulfinamide. *Chem. Rev. (Washington, DC, U.S.)* **2010,** *110*, 3600-3740.

20. Motoki, T.; Takeda, K.; Kita, Y.; Takaishi, M.; Suzuki, Y.; Ishida, T. Novel Fused Aminodihydrothiazine Derivative. U.S. Patent Application 2010/0093999 A1, April 15, 2010.

21. Ghosez, L. α-Chloroenamines: New Reagents for Organic Synthesis. *Angew. Chem., Int. Ed. Engl.* **1972,** *11*, 852-853.

22. Castro-Pineiro, J. L. H.; A.; Madin, A.; Vo, N.-T. Fused Aminodihydropyrimidone Derivatives, WO2011009897A1, January 27, 2011.

23. Zhu, H. Water's Role in Compound Design for Drug Discovery. In *CCG UGM & Conference*, Montreal, Canada, 2013.

24. (a) Hashimura, K.; Tomita, S.; Hiroya, K.; Ogasawara, K. A Stereocontrolled Route to Both Enantiomers of the Necine Base Dihydroxyheliotridane via Intramolecular 1,3-Dipolar Addition Using the Same Chiral Precursor. *J. Chem. Soc., Chem. Commun.,* **1995,** *229,* 1. (b) Alam, M.; Wise, C.; Baxter, C. A.; Cleator, E.; Walkinshaw, A. Development of a Robust Procedure for the Copper-catalyzed Ring-Opening of Epoxides with Grignard Reagents *Org. ProcessRes. Dev.* **2012**, *16*, 435−441.

25. Tahtaoui, C.; Demailly, A.; Guidemann, C.; Joyeux, C.; Schneider, P. Enantioselective Synthesis of Iclaprim Enantiomers - A Versatile Approach to 2-Substituted Chiral Chromenes. *J. Org. Chem.* **2010,** *75*, 3781-3785.

26. Lu, Y.; Riddell, D.; Hajos-Korcsok, E.; Bales, K.; Wood, K. M.; Nolan, C. E.; Robshaw, A. E.; Zhang, L.; Leung, L.; Becker, S. L.; Tseng, E.; Barricklow, J.; Miller, E. H.; Osgood, S.;

O'Neill, B. T.; Brodney, M. A.; Johnson, D. S.; Pettersson, M. Cerebrospinal Fluid Amyloid-β (Aβ) as an Effect Biomarker for Brain Aβ Lowering Verified by Quantitative Preclinical Analyses. *J. Pharmacol. Exp. Ther.* **2012,** *342*, 366-375.

27. Svoboda, K.; Yasuda, R. Principles of Two-Photon Excitation Microscopy and Its Applications to Neuroscience. *Neuron* **2006,** *50*, 823-839.

28. Pan, F.; Gan, W.-B. Two-Photon Imaging of Dendritic Spine Development in the Mouse Cortex. *Dev. Neurobiol.* **2008,** *68*, 771-778.

29. (a) Eketjäll, S.; Janson, J.; Jeppsson, F.; Svanhagen, A.; Kolmodin, K.; Gustavsson, S.; Radesäter, A-C; Elison, K.; Briem, S.; Appelkvist, P.; Niva, C.; Berg, A-L; Karlström, S.; Swahn B-M.; Fälting, J. AZ-4217: A High Potency BACE Inhibitor Displaying Acute Central Efficacy in Different In Vivo Models and Reduced Amyloid Deposition in Tg2576 Mice. *J Neurosci,* **2013,** 33, 10075-10084. (b) Jacobsen, H.; Ozmen, L.; Caruso, A.; Narquizian, R.; Hilpert, H.; Jacobsen, B.; Terwel, D.; Tanghe, A.; Bohrmann, B. Combined Treatment with a BACE Inhibitor and Anti-Aβ Antibody Gantenerumab Enhances Amyloid Reduction in APPLondon Mice. *J Neurosci,* **2014,** *34*, 11621-11630.

30. Farah, M. H.; Pan, B. H.; Hoffman, P. N.; Ferraris, D.; Tsukamoto, T.; Nguyen, T.; Wong, P. C.; Price, D. L.; Slusher, B. S.; Griffin, J. W. Reduced BACE1 activity enhances clearance of myelin debris and regeneration of axons in the injured peripheral nervous system. *J Neurosci* **2011,** *31*, 5744-5754.

31. There does remain a possibilty that increases in dose or study duration could result in ocular toxicity, but relative to the shorter study with **1** that implicated that accumulation of autofluoresent material in the RPE could be observed with 1 week of dosing. Thus, a two week assessment would be reasonable at this juncture.

32. Otsu, N. A. Threshold Selection Method from Gray-Level Histograms. *IEEE Transactions on Systems, Man and Cybernetics,* **1979,** *9*, 62-66.

33. Maintz, J. B. A.; Viergever, M. A. A Survey of Medical Image Registration. *Med. Image Anal.* **1998,** *2*, 1-36.

34. Kalvass, J. C.; Maurer, T. S. Influence of Nonspecific Brain and Plasma Binding on CNS Exposure: Implications for Rational Drug Discovery. *Biopharm. Drug Dispos.* **2002,** *23*, 327.

35. (a) Tomasselli, A. G.; Paddock, D. J.; Emmons, T. L.; Mildner, A. M.; Leone, J. W.; Lull, J. M.; Cialdella, J. I.; Prince, D. B.; Fischer, H. D.; Heinrikson, R. L.; Benson, T. E. High Yield Expression of Human BACE Constructs in *Eschericia coli* for Refolding, Purification, and High Resolution Diffracting Crystal Forms. *Protein Pept. Lett.* **2008,** *15*, 131; (b) Patel, S.; Vuillard, L.; Cleasby, A.; Murray, C. W.; Yon, J. Apo and Inhibitor Complex Structures of BACE (beta-Secretase). *J. Mol. Biol.* **2004,** *343*, 407-416.

36. Vonrhein, C.; Flensburg, C.; Keller, P.; Sharff, A.; Smart, O.; Paciorek, W.; Womack, T.; Bricogne, G. Data Processing and Analysis with the *AutoPROC* Tool Box. *Acta Crystallogr., Sect. D: Biol. Crystallogr.* **2011,** *67*, 293-302.

37. Kabsch, W. XDS. *Acta Crystallogr., Sect. D: Biol. Crystallogr.* **2010,** *66*, 125-132.

38. (a) French, S.; Wilson, K. On The Treatment of Negative Intensity Observations. *Acta Crystallogr.* **1978,** *A34*, 517-525; (b) Collaborative Computational Project, Number 4. The *CCP4* Suite: Programs for Protein Crystallography. *Acta Crystallogr., Sect. D: Biol. Crystallogr.* **1994,** *50*, 760-763.

39. Murshudov, G. N.; Vagin, A. A.; Dodson, E. J. Refinement of Macromolecular Structures by the Maximum-Likelihood Method. *Acta Crystallogr.* **1997,** *D53*, 240.

40. Bricogne, G.; Blanc, E.; Brandl, M.; Flensburg, C.; Keller, P.; Paciorek, W.; Roversi, P.; Smart, O. S.; Vonrhein, C.; Womack, T. O. *BUSTER*, Global Phasing Ltd: Cambridge, UK, 2011.

41. *Maestro*, 9.7; Schrodinger: New York, NY, 2014.

42. (a) *Desmond Molecular Dynamics System*, 3.7; D.E. Shaw Research: New York, 2014; (b) *Maestro-Desmond Interoperability Tools*, 3.7; Schrodinger: New York, 2014.

43. Banks, J. L.; Beard, H. S.; Cao, Y.; Cho, A. E.; Damm, W.; Farid, R.; Felts, A. K.; Halgren, T. A.; Mainz, D. T.; Maple, J. R.; Murphy, R.; Philipp, D. M.; Repasky, M. P.; Zhang, L. Y.; Berne, B. J.; Friesner, R. A.; Gallicchio, E.; Levy, R. M. Integrated Modeling Program, Applied Chemical Theory (IMPACT). *J. Comput. Chem.* **2005,** *26*, 1752-1780.

44. Martyna, G. J.; Klein, M. L.; Tuckerman, M. Nosé–Hoover Chains: The Canonical Ensemble via Continuous Dynamics. *J. Chem. Phys.* **1992,** *97*, 2635-2643.

45. Essmann, U.; Perera, L.; Berkowitz, M. L.; Darden, T.; Lee, H.; Pedersen, L. G. A Smooth Particle Mesh Ewald Method. *J. Chem. Phys.* **1995,** *103*, 8577-8593.

46. Humphreys, D. D.; Friesner, R. A.; Berne, B. J. A Multiple-Time-Step Molecular Dynamics Algorithm for Macromolecules. *J. Phys. Chem.* **1994,** *98*, 6885-6892.

47. The preparation of intermediate **7** is described in detail in the Supporting Information

**Table of Contents Graphic**

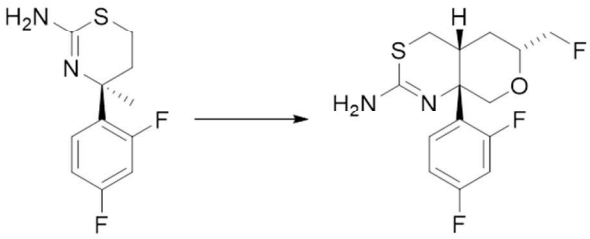


Compound **36**
BACE FP $IC_{50}$ = 1.07 μM
LE = 0.38
CatD FP $IC_{50}$ > 81 μM
BACE WCA $IC_{50}$ = 61 nM
MDR Er = 0.9
$C_{u,b}/C_{u,p}$ = 1.42

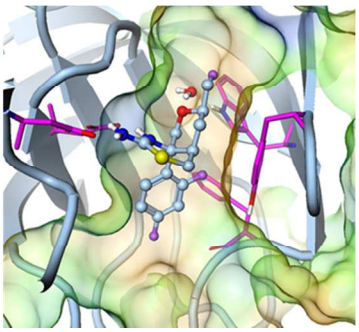

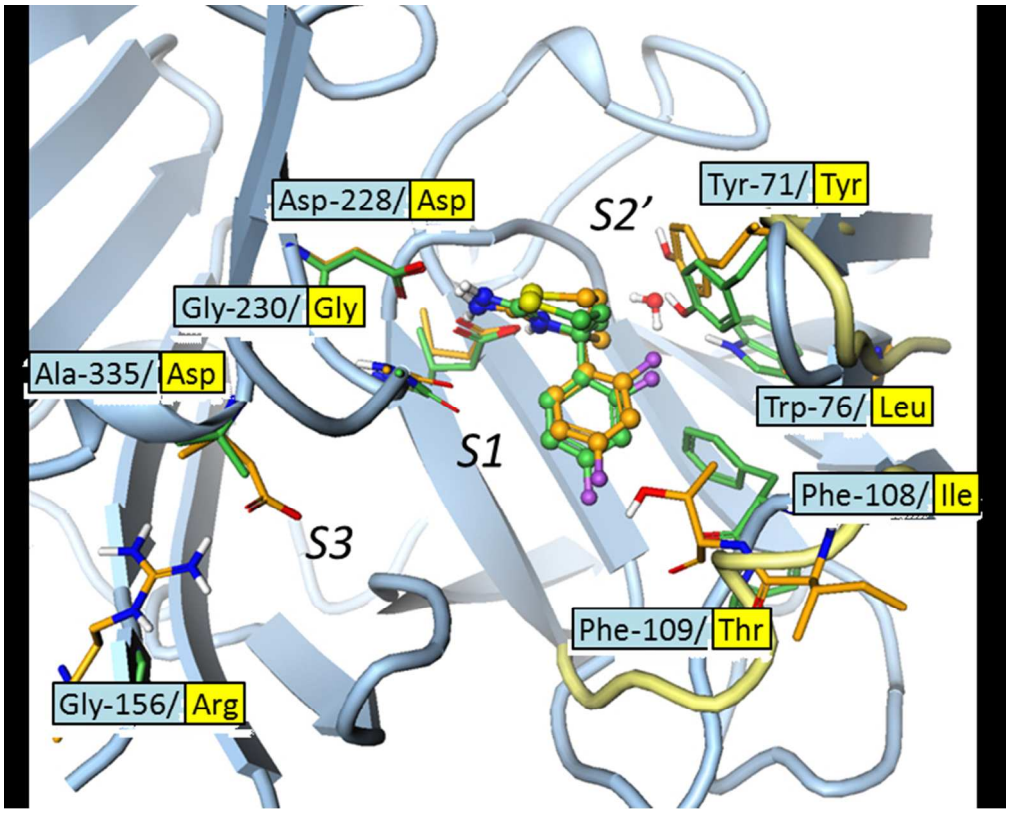


125x101mm (150 x 150 DPI)

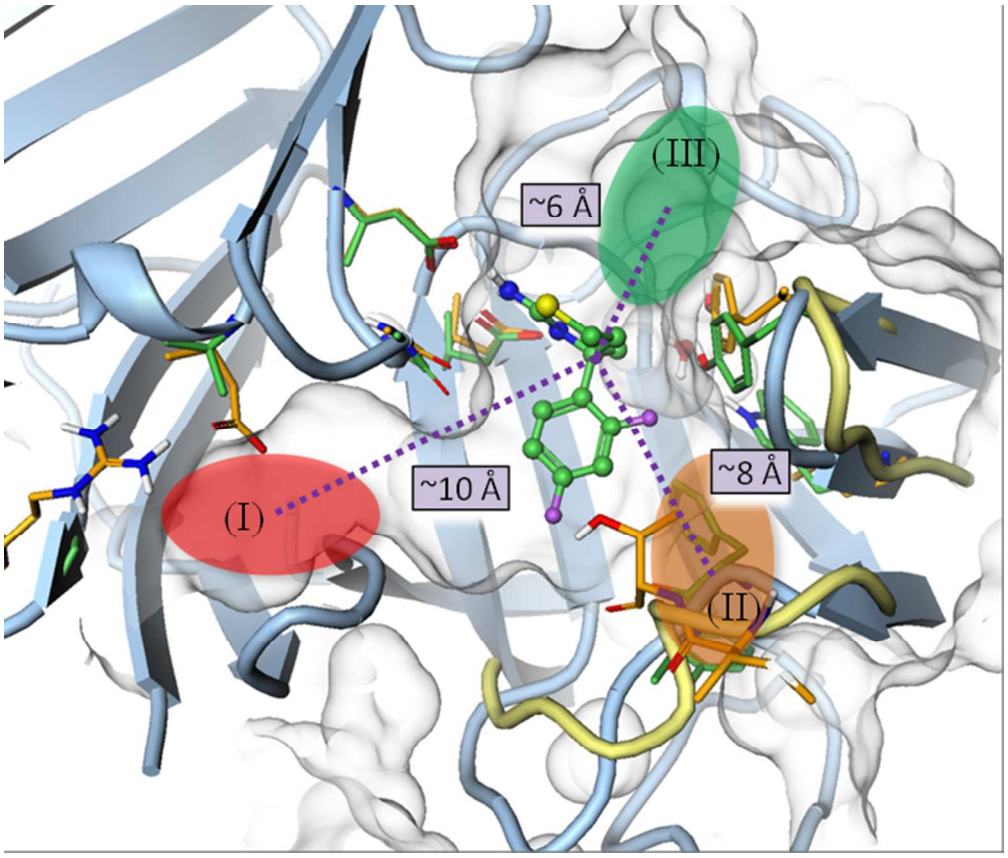


119x101mm (150 x 150 DPI)

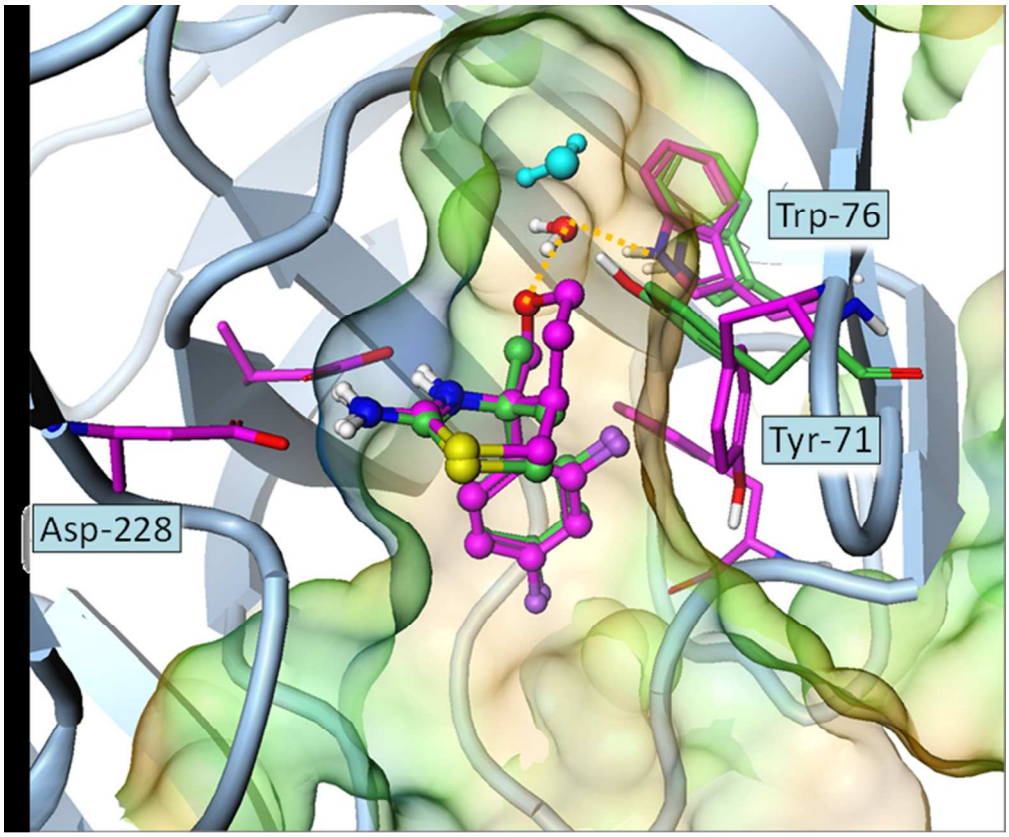


122x101mm (150 x 150 DPI)

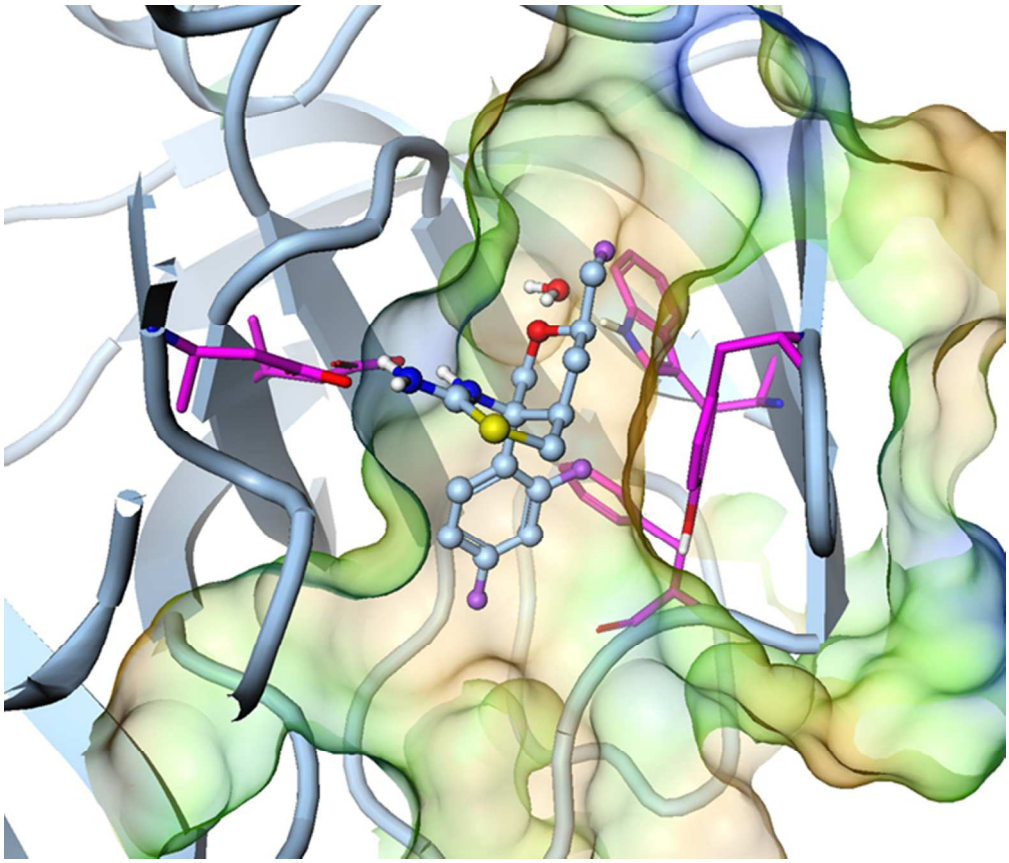

119x101mm (150 x 150 DPI)

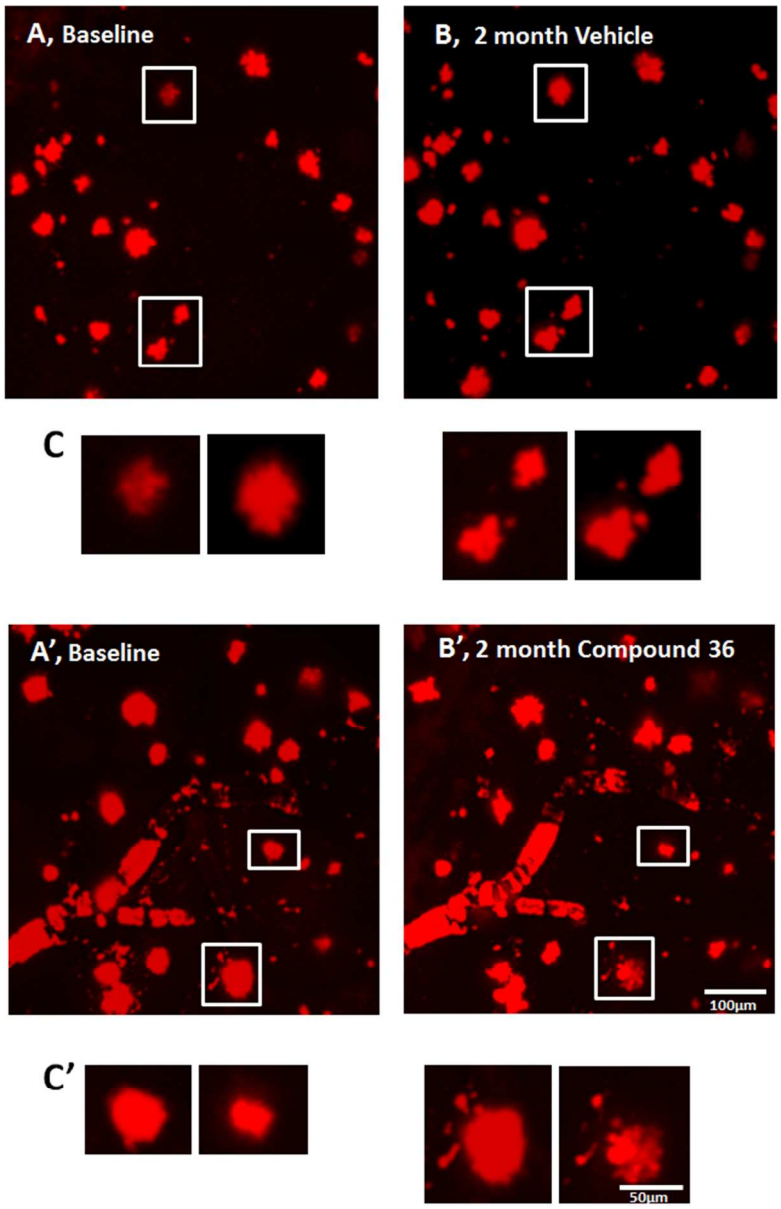


258x349mm (72 x 72 DPI)